Norwegian University of Life Sciences

Master's Thesis 2022 60 ECTS
Faculty of Chemistry, Biotechnology and Food Science

Characterization of a Glycoside hydrolase family 50 member *Pa*GH50A from *Pseudomonas aeruginosa* and exploring the enzyme's potential in modulating biofilm formation

Hibaq Ahmed Farah
Master of science, Biotechnology

Characterization of a Glycoside hydrolase family 50 member *Pa*GH50A from *Pseudomonas aeruginosa* and exploring the enzyme's potential in modulating biofilm formation

Master's Thesis

By

Hibaq Ahmed Farah

Protein Engineering and Proteomics Group

Faculty of Chemistry, Biotechnology and Food science

Norwegian University of Life Sciences

Ås

Acknowledgments

The thesis project was carried out at the Faculty of Chemistry, Biotechnology, and Food Science at the Norwegian University of Life Sciences form August 2021 to June 2022. The project was supervised by Professor Gustav Vaaje-Kolstad and co-supervisor Per Kristian Thorén Edvardsen.

I am extremely grateful for my main supervisor professor Gustav Vaaje-Kolstad for giving me the opportunity to write my thesis project in the Protein Engineering and Proteomics group. Additionally, I am thankful for excellent guidance, ideas, help, and support thought the research year. I would also like to express gratitude to my co-supervisor Per Kristian Thorén Edvardsen whom have provided indispensable advice, guidance, and practical support during all my experimental design and analysis work.

I would like to thank all members of the Protein Engineering and Proteomics group for offering a great working environment. Lastly, I have deep gratitude for my fellow master students for productive discussions, help and good company.

Ås, June 2022

Hibaq Ahmed Farah

Abstract

Pseudomonas aeruginosa is an opportunistic human pathogen that causes acute and chronic lung infections in individuals with compromised immune systems. The bacterium is wide spread in the environment and especially persistent in clinical settings due to its ability to produce complex biofilms which contributes to its virulence.

An important constituent of some *P. aeruginosa* biofilm variants is an exopolysaccharide called PsI. This exopolysaccharide consists of glucose, mannose and rhamnose moieties coupled by α/β-1,3-glycosidic linkages and is regularly branched with mannose attached by α-1,2 linkage.

The main objective of this thesis was to provide a biochemical characterization of a putatively secreted family 50 glycoside hydrolase found in *P. aeruginosa* PA14. The enzyme which was named *Pa*GH50A had previously been shown to have endo-1,3-β-glucanase activity and it was therefore of great interest to investigate its possible activity towards Psl. The secondary aim was to investigate the effect of *Pa*GH50A on biofilms of *P. aeruginosa* strains PAO1 and its mutants PAO1 ΔWspF, PAO1 ΔWspF ΔPsl and PAO1 ΔWspF ΔPel, all biofilm overproducers.

The gene encoding *Pa*GH50A, called *PA14_50830* was cloned into a pNIC-CH vector, containing a hexa-histidine tag for convenient purification, that was subsequently transformed into *E.coli* strain BL21 for protein expression. Expression of enzymatically active protein was successful, and the protein yield obtained after incubation in a shaker incubator was 0.663 mg pure protein/ L and 0.945 mg pure protein/L after cultivation in a Lex-48 bioreactor.

Enzyme activity assays showed that *Pa*GH50A could hydrolyze curdlan, lichenan and most interestingly the psl exopolysaccharide which had not been shown before. Analysis of degradation products by MALDI-TOF MS showed that *Pa*GH50A generated long chain oligomers. *Pa*GH50A was shown to influence the biofilm development of *P. aeruginosa* PAO1 wild type and mutant variants and the effect depended on the when the enzyme was added during the biofilm formation process. The reasons and the mechanism for this phenomenon are unknown, however it can be hypothesized that the presence of *Pa*GH50A leads to up or down regulations of genes involved in biofilm formation. This study represents a step forward in the understanding of *Pa*GH50A, however the biological role of *Pa*GH50A in *P. aeruginosa* biofilms remains unknown. Therefore, further proteomics analysis and employing mutant variants of *Pa*GH50A must be done in order to further the knowledge of *Pa*GH50A and the biofilm formation process.

Sammendrag

Pseudomonas aeruginosa er et opportunistisk humant patogen som forårsaker akutte og kroniske lungeinfeksjoner hos personer med nedsatt immunsystem. Bakterien er vidt spredt i miljøet og er spesielt persistent i kliniske omgivelser på grunn av dens evne til å danne komplekse biofilmer som bidrar til dens virulens.

En viktig bestanddel av noen *P. aeruginosa* biofilmvarianter er et eksopolysakkarid kalt Psl. Dette eksopolysakkaridet består av glukose-, mannose- og rhamnose koblet via α/β-1,3-glykosidbindinger og er regelmessig forgrenet med mannose koblet via α-1,2-kobling.

Hovedmålet med denne oppgaven var å gi en biokjemisk karakterisering av et utskilt familie 50 glykosidhydrolase funnet i *P. aeruginosa* PA14. Enzymet som ble kalt *Pa*GH50A har tidligere blitt vist seg å ha endo-1,3-β-glukanase aktivitet og det var derfor av stor interesse å undersøke dets mulige aktivitet mot Psl. Det sekundære målet var å undersøke effekten av *Pa*GH50A på biofilmer produsert av *P. aeruginosa*-stammer PAO1 og mutanter PAO1 ΔWspF, PAO1 ΔWspF ΔPsl og PAO1 ΔWspF ΔPel, alle biofilmoverprodusenter.

Genet som koder for *Pa*GH50A, kalt PA14_50830, ble klonet inn i en pNIC-CH-vektor, som ble transformert inn i *E.coli*-stammen BL21 for proteinekspresjon. Ekspresjon av enzymatisk aktivt protein var vellykket, og proteinutbyttet etter inkubering i en shakerinkubator var 0,663 mg rent protein/L og 0,945 mg rent protein/L etter dyrking i en Lex-48 bioreaktor.

Enzymaktivitetsanalyser viste at *Pa*GH50A kunne hydrolysere kurdlan, lichenan og mest interessant psl-eksopolysakkaridet som ikke er vist tidligere. Analyse av nedbrytningsprodukter av MALDI-TOF MS viste at *Pa*GH50A genererte langkjedede oligomerer.

PaGH50A ble vist å påvirke biofilmutviklingen av *P. aeruginosa* PAO1 villtype- og mutantvarianter, og effekten var avhengig av når enzymet ble tilsatt under biofilmdannelsesprosessen. Årsakene og mekanismen for dette fenomenet er ukjent, men det kan antas at tilstedeværelsen av *Pa*GH50A fører til opp- eller nedreguleringer av gener involvert i biofilmdannelse. Denne studien representerer et skritt fremover i forståelsen av *Pa*GH50A, men den biologiske rollen til *Pa*GH50A i *P. aeruginosa* biofilmer er fortsatt ukjent. Derfor må ytterligere proteomikkanalyse og bruk av mutant varianter av *Pa*GH50A gjøres for å fremme videre forståelse av *Pa*GH50A og biofilmdannelsesprosessen.

.

Abbreviations

P. aeruginosa	*Pseudomonas aeruginosa*
E. coli	*Escherichia coli*
S. aureus	*Staphylococcus aureus*
GH50	Glycoside hydrolase 50
TLRs	Toll-like receptors
NF_kB	Nuclear Factor-$_k$B
AJ	Adherence junction
TJ	Tight junctions
T3SS	Type 3 secretion system
T2SS	Type 2 secretion system
T1SS	Type 1 secretion system
GAP	GTPase activating proteins
AP	Alkaline proteases
QS	Quorum sensing
AIs	Autoinducers
CF	Cystic fibrosis
CFTR	Cystic fibrosis transmembrane conductance regulator
ER	Endoplasmic reticulum
RND	Resistance nodulation division
EPS	Extracellular polymeric substances
eDNA	Extracellular DNA
ECM	Extracellular matrix
c-di-GMP	Bis-(3′-5′)-cyclic dimeric guanosine monophosphate
GH50	Glycoside hydrolase of family 50
ddH_2O	Double distilled water
LB medium	Lysogeny broth medium
TB medium	Terrific broth medium
BHI medium	Brain heart infusion medium
M9 medium	Minimal medium
IPTG	Isopropyl β-D-1-thiogalactopyranoside
UV	Ultraviolet

SDS-PAGE	Sodium dodecyl sulphate polyacrylamide gel electrophoresis
PCR	Polymerase chain reaction
dNTP	Deoxyribonucleotide triphosphate
IMAC	Immobilized metal affinity chromatography
MWCO	Molecular weight cut off
DNSA	3,5-dinitrosalicylic acid
MBTH	3-methyl-2-benzothiazolinone hydrazone
MALDI-TOF MS	Matrix-assisted laser desorption-ionization time of flight mass spectrometry
HPLC	High performance liquid chromatography
RI	Refractive index
PGC	Porous graphitic carbon
CAD	Charged Aerosol Detector
MS	Mass spectrometry
ESI	Electrospray ionization
OD_{540}/ OD_{620}/ OD_{595}	Optical density
v/v	Volume per volume
CAZy	Carbohydrate active enzyme database
SP	Signal peptide
Da	Dalton
Bp	Base pairs
Tm	Melting Temperature
Rpm	Revolutions per minute
g	Relative centrifugal force

Table of contents

1. Introduction

1.1 Pseudomonas aeruginosa

Pseudomonas aeruginosa was discovered by pharmacologist Carle Gessard and first described in the research paper "*On the blue and green coloration of bandages*" in 1882. In the article, Gessard characterized a novel microorganism based on the blue-green coloration on linin bandages when subjected to ultraviolet light (Gessard, 1882). The cause for the blue-green coloration that Gessard observed was due to the production of two water-soluble pigments; pyocyanin which gave a distinctive blue color and pyoverdin that is a yellow-green, fluorescent pigment resulting in colonies exhibiting a blue-green pigment (Moore & Flaws, Introduction: Pseudomonas aeruginosa, 2011).

P. aeruginosa is a Gram-negative rod-shaped bacterium measuring at 1-5 um long and 0-5-1.0 um wide. It is motile and generates movement through a single polar flagellum. The bacterium is facultative aerobic and produces ATP under aerobic and anaerobic conditions by using nitrate as a terminal electron acceptor or by metabolizing arginine. *P. aeruginosa* is a prototrophic microorganism that has the capabilities to synthesize its nutrients from inorganic materials. It has minimal nutritional requirements and can proliferate with a single carbon source. In addition, it can utilize over 100 types of organic compounds as its source of carbon (Diggle & Whiteley, 2020). The optimum temperature for growth is 37 ^{o}C however the bacterium has a broad range of growth temperatures ranging from 4 to 42 ^{o}C (LaBauve & Wargo, 2021). pH range spans from 4.5 to 9.5 (Klein, et al., 2008) and with a doubling time of 100 to 200 minutes (Yang, et al., 2007).

P. aeruginosa is an ubiquitous pathogen with an extensive span of reservoirs ranging from natural habitats to healthcare facilities. Most commonly the bacterium is found in water and soil, however it does regularly appear on the surfaces of plants and occasionally animals (Silby, Winstanley, Godfrey, Levy, & Jackson, 2011). An increasing emergence of *P. aeruginosa* in clinical environments combined with its antibiotic resistance has led to an increasing focus on healthcare research. The pathogen is responsible for 10 to 20 % of all infection occurring in hospitals (Lahiri, 1998). Its extraordinary metabolic and physiologic versatility enables the bacterium to thrive in diverse environmental niches.

1.1.1 P. *aeruginosa* classification

Taxonomical classification of *P. aeruginosa* is based on phylogenetic analysis of its 16S rRNA sequences. The analysis have revealed that the bacterium belongs to the order of pseudomonadales, family of Pseudomonadaceae and genus of *pseudomonas* (Gomila, Pena, Mulet, Lalucat, & Garcia-Valdes, 2015) (Schoch CL, et al. , 2020).

P. aeruginosa PAO1 was the first strain whose genome was sequenced. It was originally isolated from an infected wound in the 1950s (Diggle & Whiteley, 2020). At 6.3 Mbp *P. aeruginosa* genome encodes up to 5.316 predicted genes (Valot, et al., 2015). With one of the notably larger genomes in comparison to other sequenced bacterial genomes *P. aeruginosa* genome also contain proportionally higher predicted regulatory genes (Rocha, et al., 2019).

1.1.2 Pathogenicity

P. aeruginosa infections are invasive and toxicogenic and consist of three distinct stages: adherence and colonization of epithelial cells, followed by localized invasion of epithelial cells and then in the end systemic infection throughout the body. The infection can halt at multiple points depending on the patient's health status (Moore & Flaws, Epidemiology and Pathogenesis of Pseudomonas aeruginosa Infections, 2011)

1.1.2.1 *Host defenses against P. aeruginosa* invasion

Microorganisms can inter the human body through various ways such as intake of contaminated food, physical injuries or through the respiratory tract (James, 2017). Healthy humans breath more than 10 000 L air/ per day and Inhaled air contains an assortment of microorganisms and particulates. Despite this, lungs of non-immune compromised individuals are inclined to remain free of infections due to the efficiency of the innate immune system. Various cell types are involved in defense against pathogens such as physical barriers, phagocytic and other innate and adaptive immune cells (**Figure 1-1**). The respiratory epithelium is the first line of defense against pathogens. The airways are typically coated in a layer of viscous mucus inhospitable to

inhaled microorganisms that actively moves the microorganisms and particulates unidirectional out of the lungs (Huffnagle, Dickson, & Lukacs, 2016).

The innate immune system is activated through recognition of lipopolysaccharides (LPS) on the cell surface. LPS are glycolipids consisting of three domains lipid A, core oligosaccharide and O-antigen and is an integral component of the outer membrane. LPS functions as an activator of innate immune response by inducing activation of signal transduction cascades, leading to production of proinflammatory cytokines. The cytokines stimulate, recruit, and proliferate immune cells the aide in the immune response (Huszcynski, Lam, & Khursigara, 2019).

The adaptive immune system is initiated when contact between *P. aeruginosa* type IV pili and Toll-like receptors (TLRs) is made (Gellatly & Hancock, 2013). The type IV pili-TLRs interaction activates the Nuclear Factor-$_k$B (NF_kB) signaling pathway which induces expression of pro-inflammatory genes and is critical for activation and differentiation of innate immune cells such as macrophages and neutrophils (Liu, Zhang, Joo, & Sun, 2017). Further inflammatory response incorporates dendritic cells that link the innate and adaptive immune system by presenting antigens to T lymphocytes leading to further differentiation and activation of T and B lymphocytes (Gaudino & Kumar, 2019).

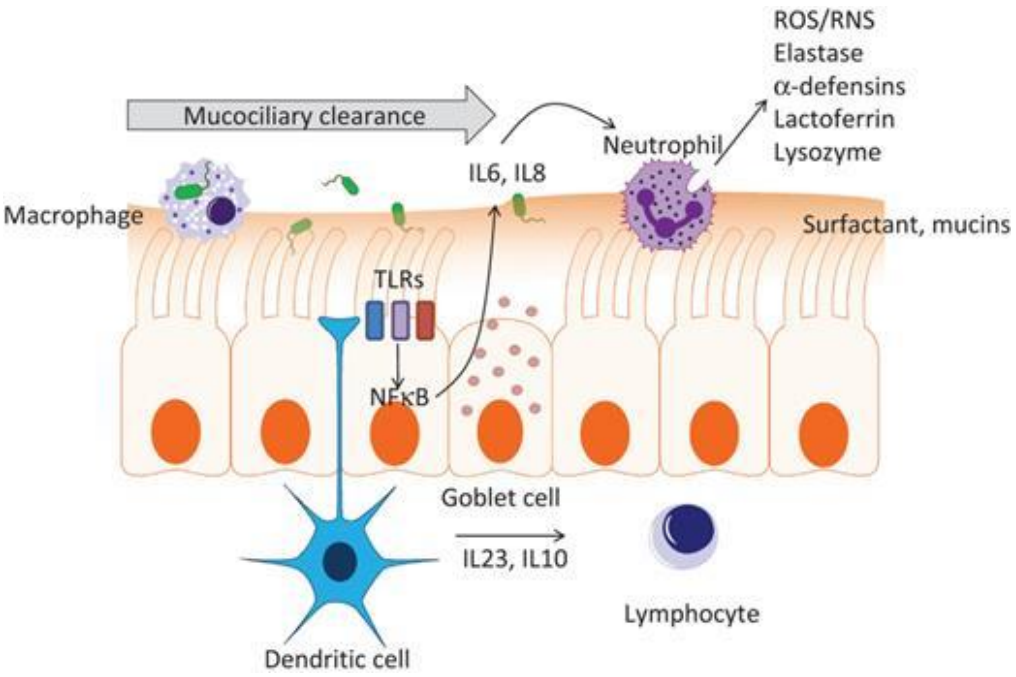

Figure 1-1. Summary of host defenses against microorganisms. Human lungs are typically inhospitable environment for pathogens where the first line of defense is entrapment in the mucus and subsequently removal by cilia. P. aeruginosa causes an inflammatory response in the airways and activates various components of the immune system such as macrophages, dendritic cells, and lymphocytes. Adapted from (Gellatly & Hancock, 2013) with permission from Oxford University Press.

1.1.2.2 *P. aeruginosa* respiratory infection

After entering the airways *P. aeruginosa* reaches the colonization site utilizing a single polar flagellum. The flagellum allows for the bacterium to move through viscous mucus and rapidly scan for cell surfaces that allow for successful transmigration (Golovkine, Reboud, & Huber, 2019). *P. aeruginosa* adheres to the tracheal epithelial cells utilizing type IV pili located at the cell poles. Type IV pilis facilitate movement through an extension-retraction motion, dragging the cell along the semi-solid epithelium in a process called twitching motility. The bacterium then adheres to the colonization site via binding of flagellum and type IV pili to glycolipid asialoGM1. In addition, LPS also participated in bacterial adhesion to epithelial cells (Kipnis, Sawa, & Wiener-Kronish, 2006). Adherence of *P. aeruginosa* allows for the formation of bacterial aggregates embedded in a biofilm like matrix comprised mostly of alginate at this stage. The bacterial aggregates alter the colonized apical cell surface into an environment with a composition similar to a basolateral domain. Adherence junction (AJ) proteins such as E-cadherin, β-caternin and afadin are recruited to the colonization site to insure cell-cell adhesion. Transmigration often occurs at the cell-cell junctions however it has been shown that not all cell junctions permit for transmigration of *P. aeruginosa*. An alternative theory is therefore that *P. aeruginosa* takes advantages of breaches in the cell-cell junctions occurring during epithelial cell division or during excision of senescent cells. Under these circumstances a loss of E-cadherin occurs which permits for entry, followed by other pathogens being attracted to the site due to secreted chemotaxis at the colonization site. At this point *P. aeruginosa* exploits, the junctional weaking and injects exotoxins into the host cell cytoplasm via type 3 secretion system (T3SS) and subsequent bacterial internalization (Golovkine, Reboud, & Huber, Pseudomonas aeruginosa Takes a Multi-Target Approach to Achieve Junction Breach, 2019).

Upon contact with the host epithelial cell type 3 secretion system (T3SS) is activated. Exotoxins – ExoY, ExoS, ExoT and ExoU are expressed in varying degrees in different strains but are translocated into the host cell cytoplasm through a pore in the basolateral domain. Almost all of *P. aeruginosa* strains produces either exotoxin ExoU or ExoS in addition to ExoY and ExoT which have minor roles during colonization (Gellatly & Hancock, 2013). ExoY has nuclotidyl cyclase activity which results in structural alterations of microtubules and actin fibers in the host cell. Noninvasive strains possess ExoU, a phospholipase that induces disruption in the plasma membrane and necrotic cell death. While invasive strains produce ExoS, a bifunction effector protein with two active domains. At the C-terminal an ADP-ribosyltransferase that

disrupts the cytoskeletal organization and a Rho GTPase activating proteins (GAP) domain at the N-terminal (Kipnis, Sawa, & Wiener-Kronish, 2006). ExoS and ExoT are GAP proteins that target members of the Rho GTPase family. GAP proteins remove the terminal phosphate from GTP bound to active G-protein and modifies it to GDP (Golovkine, et al., 2014). Inactivation of G-proteins induces dephosphorylation of Lim kinase and subsequently of cofilin. Cofilin is active in its dephosphorylated state and depolymerizes actin cytoskeleton. This results in a lack of essential components for creating adhesion of cell-cell junctions leading to further colonization (Golovkine, Reboud, & Huber, 2019). *P. aeruginosa* produce a variety of virulence factors during invasion that work in synergy to damage the epithelial cells and hinder immune response (**Figure 1-2**). Extracellular proteases that are associated with successful invasion are elastase and alkaline proteases. Elastases LasA and LasB hydrolyze elastin, collagen type III and IV, IgA and IgG. LasB in particular is secreted into the extracellular matrix utilizing the type 2 secretion system (T2SS) system and is important for disruption of tight junctions (TJ) by inducing downregulation of several genes important for maintaining cell-cell junction integrity (Golovkine, et al., 2014).While alkaline proteases are secreted by type 1 secretion system (T1SS) and degrade components of the complement system as well as host fibronectin to expose distinct basolateral domain receptors for bacterial attachment (Gellatly & Hancock, 2013). Other virulence factors that are secreted are pyocyanin and pyoverdine. Pyocyanin is a blue green metabolite that gives *P. aeruginosa* its distinct color (Gellatly & Hancock, 2013). The metabolite is responsible for causing oxidative stress, inactivating catalase, and disrupting the electron transport chain, which results in apoptosis of neutrophils, inhibition of phagocytose by macrophages and suppression of acute inflammatory response (Allen, et al., 2005). Pyoverdine, a siderophore that sequester iron from inorganic sources and can remove iron from transferrin and other ferroproteins. Once pyoverdine acquires iron it can act as a signaling molecule and regulate production of exotoxins (Kang, et al., 2019).

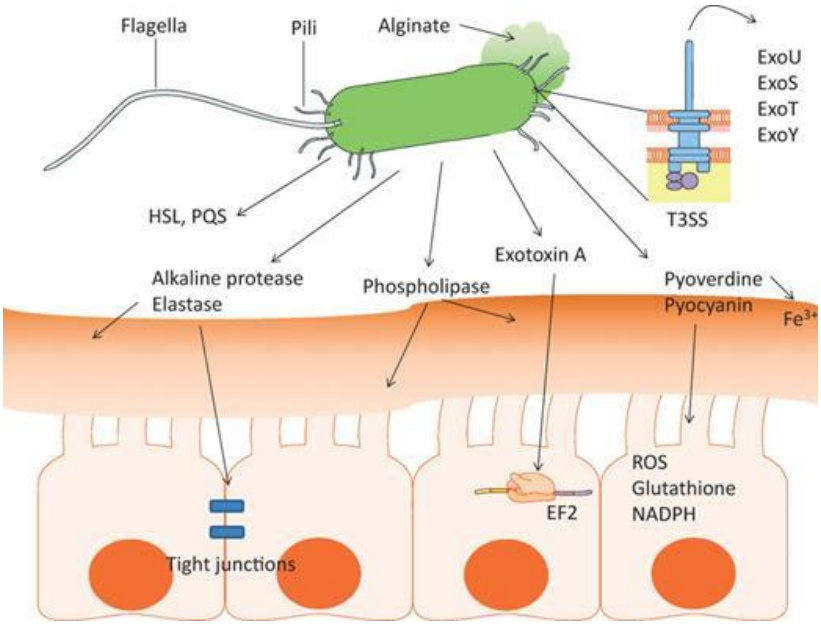

Figure 1-2. A summary of virulence factors produced by P. aeruginosa and how they target the epithelial cells. Flagella and pili are used for adhesion and movement. Invasion of epithelial cell leads to activation of Type 3 Secretion System and secretion of virulence factors. Adapted from (Gellatly & Hancock, 2013) with permission from Oxford University Press.

Proliferation of *P. aeruginosa* in the body is a poorly understood process. Systemic infection is thought to be mediated by the same systems and extracellular proteins and molecules that are responsible for localized infection (Bachta, Allen, Cheung, Chiu, & Hauser, 2020).

1.1.2.2.1 Qurom sensing for regulation of virulence factors

Expression of proteases, toxins and other compounds are regulated by Quorum sensing (QS). QS is a communication mechanism that allows for bacterial population to sense cell density and environmental conditions. It involves the production, secretion, and accumulation of autoinducers (AI). AIs are signal molecules that acts as cofactors for transcriptional regulators and mediates the adaptation of *P. aeruginosa* to novel environments (Rutherford & Bassier, 2012).

Initially when *P. aeruginosa* colonize a new environment there will be a low density of cells, which causes the AIs to have a minimal effect on QS controlled virulence genes. Once a cell density threshold has been reached a coordinated activation of genes that express a variety of QS products is initiated (Thi, Wibowo, & Rehm, 2020). The QS system is hierarchical and is

comprised of LasI, RhlI, PqsABCDH and AmbBCDE pathways (**Figure 1-3**). The LasI system produces AI, *N*-3-oxo-dodecanoyl homoserine lactone (3-O-C_{12}-HSL) which the LasR transcription factor responds to while the RhlI system produces AI, *N*-butyryl-L-homoserine lactone (C_4-HSL) that RhlR transcription factor responds to. LasR-LasI system is the first system in the cascade and regulates the RhIR-RhlI system by inducing the expression of *RhlR* and *RhlI* genes. The QS products of LasI and RhlI pathways are alkaline proteases, phospholipases, lasA and lasB, rhamnolipids, pyocyanin, pyoverdine, etc. The products are secreted to alter group behavior for survival and pathogenicity (Tuon, Dantas, Suss, & Riberiro, 2022)

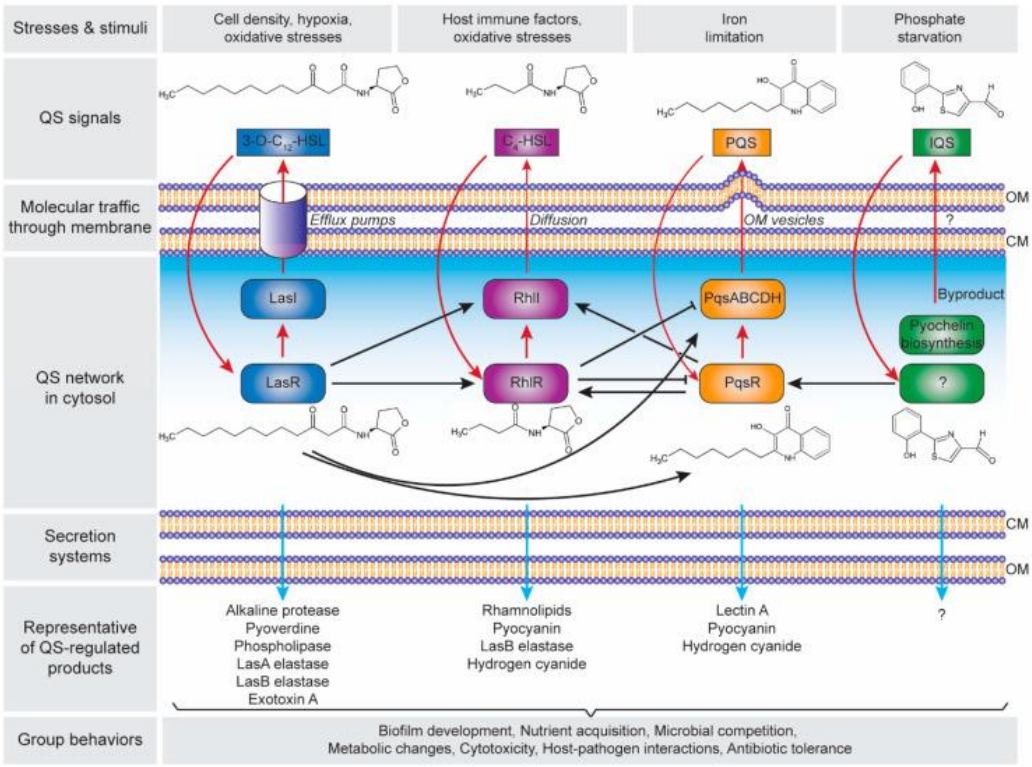

Figure 1-3. Quorum sensing (QS) network in P. aeruginosa. There are four pathways in the QS system which are activated in response to cell density and environmental stresses. The pathways are in a hierarchical pattern and produces products essential for adapting to new environments. Adapted from (Thi, Wibowo, & Rehm, 2020) with permission from MDPI.

1.2 Cystic Fibrosis

Evidence have revealed that a proportion of ecological *P. aeruginosa* strains may in fact not cause disease in humans due to specific phenotypes being required for becoming a human pathogen. Evolutionary steps outside of human tissues have enabled *P. aeruginosa* to

selectively adapt to niches that simulate conditions in human tissues e.g., by mutations of genes in the genome or by acquisition of genes via horizontal gene transfer. *P. aeruginosa* strains that are associated with chronic infections have acquired additional aptitudes from inhospitable heterogenous environments or by a constant migration rate of microorganisms. Environmental adaptions of *P. aeruginosa* that occur during a cystic fibrosis (CF) infection may be loss of unnecessary virulence factors, selection of biofilm with mucoid phenotype and increase synthesis of multidrug efflux pumps, etc. (Qiu, Kulasekara, & Lory, 2009).

P. aeruginosa is classified as an opportunistic pathogen affecting primarily people with compromised immune systems. The pathogen is the leading cause of morbidity and mortality in CF patients (Moradali, Ghods, & Rehm, 2017). CF manifests as a clinical syndrome characterized by chronic pulmonary infection (Lyczak, Cannon, & Pier, 2002). CF, a genetic disease caused by a mutation of the cystic fibrosis transmembrane conductance regulator gene (CFTR) on chromosome 7. The genetic defect is represented as ΔF508 and accounts for 70 % of mutant CFTR cases world wide (Kerem, et al., 1990). The ΔF508 mutation results in impaired post translation processing causing the CFTR protein to be misfolded and thus incapable of departing the endoplasmic reticulum. The main function of CFTR, a cAMP-depended chloride channel is to transport Cl^- across the epithelial cell membrane (Lukacs & Verkman, 2012). The inability to transport Cl^- out of the cell causes the intracellular levels of Cl^- to increase. This is followed by an influx of Na^+ via ENaC channels. The lack of chloride outflow causes the secreted mucus to not attract water resulting in dehydrated and highly viscous mucus which obstructs the lining of organs and tissues leading to functional abnormalities (Shei, Peabody, Kaza, & Rowe, 2018). In certain CF cases effective lung colonization is due to inhibition of HCO_3^- secretion. CFTR in addition to being a chloride channel also drives cAMP depended luminal secretion of HCO_3^-. The amount of water secreted into the lumen is relative to the amount of HCO_3^- and Cl^-. Inhibition of HCO_3^- and Cl^- results in less movement of water by osmose across the membrane and into the lumen causing a viscous mucus to form (Kunzelmann, Schreiber, & Hadorn, 2017).

During CF lung infection the secreted mucus becomes extremely viscous causing the cilia to be immobile and thus preventing removal of microbes from the airways. This subsequently leads to repeated colonization resulting in chronic inflammation and infection (Allen, Borick, & Borick , 2020). As a response to the repeated infections goblet cells produce more mucus leading to the development of bronchiectasis. Bronchiectasis destroys the lungs making the gas

exchange process unable to take place leading to respiratory insufficiency (Schafer, Griese, Chandrasekaran, Chotirmall, & Harti, 2018).

1.3 Intrinsic, acquired, and adaptive resistance mechanisms of *P. aeruginosa*

The eradication of *P. aeruginosa* infection is difficult as it does inadequately respond to antimicrobial agents and the immune system often leaving CF patients with bronchiectasis. The cause of antibiotic resistance in *P. aeruginosa* is due to *P. aeruginosa* intrinsic, acquired and adaptive resistance mechanisms. Intrinsic resistance to antibiotics referring to the inability of the drug to influence *P. aeruginosa*, acquired resistance requires the bacterium to alter its physiology to resist antibiotics while adaptive resistance increases survivability of *P. aeruginosa* by altering gene expression patterns in response to environmental stimulus. Mechanisms that provide *P. aeruginosa* with intrinsic resistance is synthesizing antibiotic inhibiting enzymes, restricting outer membrane permeability, and developing efflux pump systems. Mechanisms for acquired resistance include gaining drug resistance through mutations or acquisition of resistance genes via horizontal gene transfer. Mechanism for adaptive resistance involve the formation of biofilm that makes the bacterial aggregates impervious to therapeutic concentrations of antimicrobial agents (Pang, Raudonis, Glick, Lin, & Cheng, 2019).

P. aeruginosa is a multi-drug resistant Gram-negative pathogen and a major cause for this is efflux pumps which exports noxious compounds out of the cell. MexAB oprM, a resistance nodulation division (RND) efflux transporter that spans across both inner and outer membrane mediates the transport of antimicrobial agents out of the cell (Pesingi, et al., 2019). The MexAB oprM transporter is powered by a proton gradient in which the electrochemical potential difference between the periplasm and the cytoplasm drives protons into the more negatively charged cytoplasm. The proton movement into the cytoplasm is coupled with extrudability of substance from the cytoplasm and outside the cell (Verchere, Dezi, Adrien, Broutin, & Picard, 2015).

1.4 *P. aeruginosa* biofilms

P. aeruginosa can be free living in fluids as planktonic cells or adhered to surfaces as sessile cells (Jefferson, 2004). The transition from a planktonic to a sessile state occurs as a response to the environment followed by cells being subjected to physiological, metabolic, and phenotypic alterations for optimal adaption (Rollet, Gal, & Guzzo, 2009). Biofilms are complex aggregates of sessile microorganisms encased in a self-generated viscoelastic matrix comprised of extracellular polymeric substances (EPS), extracellular DNA (eDNA), proteins and lipids. The extracellular matrix (ECM) represents 90 % of the biofilm biomass. It functions as a scaffold for adhesion to biotic and abiotic surfaces, a defense mechanism against harsh environmental conditions, provides a reservoir for essential nutrients, enzymes, and cytosolic proteins. In addition, the ECM facilitates cell communication and coordination (Maurice, Bedi, & Sadikot, 2018).

1.4.1 Biofilm composition

EPS such as Psl, Pel and alginate are critical for surface adhesion, formation, and stability of the biofilm architecture. The exopolysaccharides differ in chemical structure and biosynthetic mechanisms. In the literature characterization of biosynthetic pathway for Psl, Pel and alginate is limited, with alginate biosynthetic pathway being best characterized due to being associated with chronic pulmonary infection. Only a subset of *P. aeruginosa* strains secrete alginate while most *P. aeruginosa* strains isolated from environmental and clinical sites produce either Psl or Pel. More recent studies indicate that Pel biosynthesis share certain features such as biosynthetic proteins with alginate biosynthesis. On the contrary, Psl biosynthesis have resemblance with EPS/CPS capsular biosynthesis pathway in *Escherichia coli (E. coli)*. In which the pentameric subunits of Psl are assembled in association with an isoprenoid lipid carrier. *P. aeruginosa* genomes encodes for alginate, Psl and Pel biosynthetic operons, yet it is common for the bacteria to predominately produce one of the exopolysaccharides (Franklin , Nivens, Weadge, & Howell, 2011). A hypothesis for this occurrence is that the different exopolysaccharides are induced as a response to a specific environment. *P. aeruginosa* strains isolated from the lungs of CF patients are often initially derived from the environmental reservoirs thus these strains have a significant likelihood of secreting either Psl or Pel. However in chronically infected CF

patients, the ECM mature with an alternative phenotype of mucoidy associated with alginate (Colvin, et al., 2011).The transition to a mucoid phenotype contributes to its virulence and persistence in the lungs (Lamppa & Griswold, 2013).

Psl is composed of a repeating pentamer with a main chain consisting of D-mannose, L-rhamnose and D-glucose moieties coupled by α/β-1,3-glycosidic linkages and a D-mannose sidechain linked by a α-1,2 glycosidic linkage (**Figure 1-4**) (Byrd, et al., 2009). Psl is important for irreversible adhesion of sessile cells to surfaces and cell coordination during the initial stage of biofilm formation for non-mucoid and mucoid strains. Psl functions as a signaling molecule in planktonic cells to stimulate production of diguanylate cyclase, SiAD and SasC which further activates intracellular secondary messenger bis-(3′-5′)-cyclic dimeric guanosine monophosphate (c-di-GMP) leading to an increase in synthesis of Psl and other ECM components. This reinforces the integrity of the biofilm, making it thicker and more robust (Irie, et al., 2012). In mature biofilm Psl is located in the peripheries of the biofilm structure where it maintains the structural integrity of the biofilm. Additionally, it shields *P. aeruginosa* from antimicrobial agents and phagocytosis (Thi, Wibowo, & Rehm, 2020).

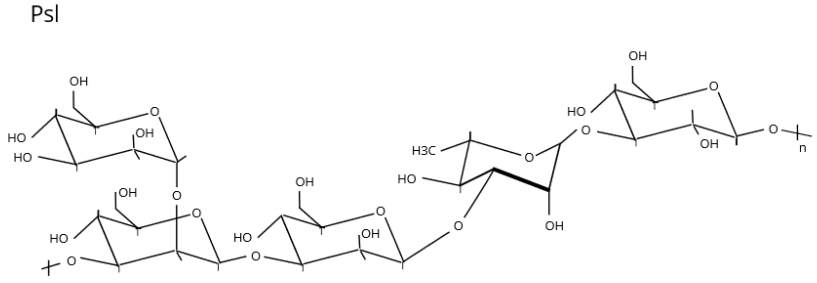

Figure 1-4. Structure of exopolysaccharides Psl. Psl is comprised of a repeating pentamer with the main chain consisting of D-mannose, L-rhamnose and D-glucose moieties coupled by Ŭß-1,3-glycosidic linkages and a D-mannose sidechain linked by a -1Ŭ2 glycosidic linkages.

Pel is thought to be a cationic exopolysaccharide comprised of partially acetylated *N*-Acetylgalactosamine and *N*-Acetulglucosamine linked by 1,4 glycosidic linkages, however an accurate structure for Pel has yet to be established (Jennings, Storek, Ledvina, Coulon, & et. al, 2015). Pel similar to Psl is involved in early biofilm formation and structural maintenance. The regulatory pathway for Pel expression also resembles Psl in that c-di-GMP activates transcription of the *pel* operon (Valentini & Filloux, 2016). Production of Psl or Pel is strain

specific and can be switched as a response to surrounding environment (Jennings, Storek, Ledvina, Coulon, & et. al, 2015).

Alginate is the predominate exopolysaccharide in the biofilm of mucoid *P. aeruginosa* strains. The mucoid phenotype is mostly isolated from CF patients with chronic infections and is due to a mutation in *mucA*, known as *mucA22* (Nivens, Ohman, Williams, & Franklin, 2001). Alginate is an anionic acetylated polymer composed of mostly D-mannuronic acid residues interspersed with L-guiluronic acid and linked by β-1,4-glycosidic linkages (Franklin , Nivens, Weadge, & Howell, 2011). Alginate provides the *P. aeruginosa* cells with increased resistance to opsonization, phagocytosis, protection from toxic oxygen radical and decreased diffusion of antimicrobial agents through the biofilm (Nivens, Ohman, Williams, & Franklin, 2001) . Alginate does not contribute to adhesion of biofilm to surfaces, however the alginate structure effects the viscoelastic properties of biofilms (Thi, Wibowo, & Rehm, 2020).

Cell lysis is a common mechanism by which eDNA and other cellular components is released into the matrix at the initial stage of biofilm formation (Campoccia, Montanaro, & Arciola, 2021). During autolysis, *P. aeruginosa* rapidly transitions from a rod shaped to a round shaped structure. This results in the release of eDNA, cytosolic proteins and RNA which subsequently are encased by membrane vesicles derived from membrane fragments. Following autolysis the pH levels fall, and viscosity increases leading to the biofilm permeability to decrease. eDNA in biofilm acts as a nutrient source, a structural component and as a cation chelator interacting with divalent cations on the outer cell membrane resulting in the activation of type VI secretion system. eDNA in mature biofilm is located on the biofilm surface and stalk and interacts with Pel via cationic-anionic interactions to support biofilm integrity (Thi, Wibowo, & Rehm, 2020).

1.4.2 Biofilm formation

Biofilm formation is a cyclic process, and the development of biofilm occurs sequentially in six stages (**Figure 1-5**). Stage one is the initial reversable attachment of planktonic cells to biotic or abiotic surfaces by means of flagella and type IV pili. Stage two is irreversible attachment where planktonic cells transition to sessile cells and cell division occurs. To overcome surface repulsion FleQ transcription regulator is inhibited by increasing levels of intracellular signaling molecule c-di-GMP resulting in repression of flagellar mobility. In addition, it promotes biosynthesis of EPS required for surface adhesion (Armbruster &

Matthew, 2018). Initially the ECM is mostly compromised of eDNA but develop into being dominated by exopolysaccharides in the later stages. In stage three cells continue to proliferate and microcolonies are formed resulting in a more structured biofilm architecture. Additionally, cells develop coordinated communication via QS to produce products such as rhamnolipids, pyoverdine, pyocyanin, lectins, etc. essential for furthering the biofilm formation. In stage four maturation of microcolonies into a three-dimensional mushroom shaped structure occurs. The biofilm at this stage is heterogeneous with channels for transportation of nutrients and oxygen to the cells within the biofilm (Donlan, 2001). The cells can sequester iron from the environment via pyoverdine. Pyocyanin induces cell lysis and binds eDNA, increasing solution viscosity and cellular aggregation. Lectins become localized in the biofilm's outer membrane facilitating surface adhesion and cell and exopolysaccharide retention (Thi, Wibowo, & Rehm, 2020). In stage five a matrix cavity is formed in the center of the biofilm due to autolysis. Sessile cells transition to planktonic mode which allows for the liberated cells to colonize new environments. Biofilm associated cells have a lower growth rate than planktonic cells due to the low concentrations of essential nutrients and oxygen. This results in an increase in virulence once the cells become liberated from the biofilm (Donlan, 2001). The formation of biofilms is associated with chronic infections while acute infections are associated with planktonic cells (Valentini & Filloux, 2016).

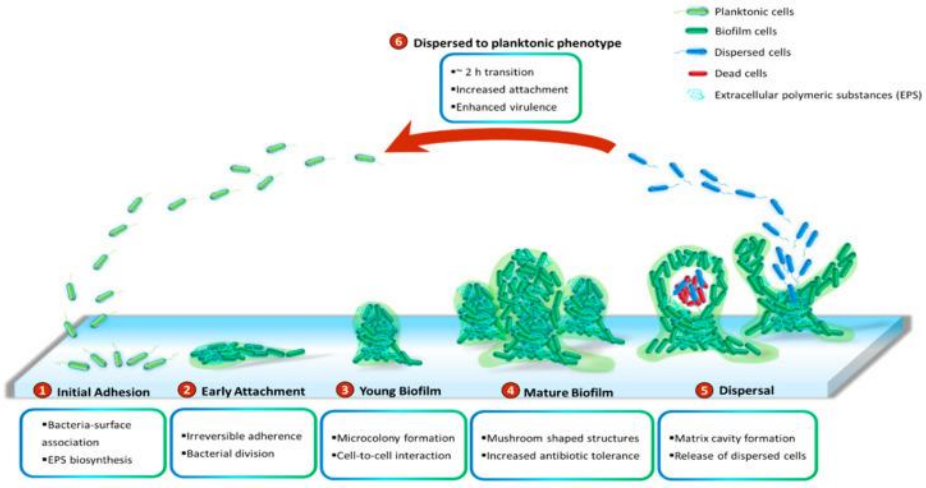

Figure 1-5. Biofilm formation cycle. The biofilm cycle consists of six stages: Initial adhesion, early attachment, young biofilm, mature biofilm, and dispersal. Biofilms are comprised of cell aggregates entrapped in a self-generated matrix consisting of exopolysaccharides, eDNA and lipids. Adapted from (Thi, Wibowo, & Rehm, 2020) with permission from MDPI.

In nature biofilms consist of multiple species of bacteria and is considered the default mode of growth and persistence (Elias & Banin, 2012). *P. aeruginosa* is often a co-colonizer along with other microorganisms such as *Staphylococcus aureus* (*S. aureus*). During a co-infection cell lysis of Gram-positive *S. aureus* allows for *P. aeruginosa* to sequester iron and nutrients. The presence of peptidoglycan and N-acetylglucosamine derived from *S. aureus* induces pyocyanin which reduce the viability of *S. aureus* (Hotterbeekx, Kumar-Singh, Goossens, & Malhotra-Kumar, 2017). *P. aeruginosa* outcompetes *S. aureus* by secreting diguanylate cyclase SiaD which is activated by Psl during the early stages of biofilm development. *P. aeruginosa* remains the dominant pathogen in mixed species biofilms through the production of antimicrobial substances modulating the growth rate of other microorganisms, however it can also be inhibited by organisms like oral streptococci strains that produce hydrogen peroxide or *S. parasanguinis* that can exploit alginate to further its biofilm formation (Thi, Wibowo, & Rehm, 2020).

1.4.3 Biofilm disruption

An adaptive mechanism such as biofilm formation is a key virulence factor for survival and initialing chronic infections. Biofilm formation and dispersal is regulated by QS, EPS and c-di-GMP. Therefore, strategies for biofilm disruption often target regulatory constituents of *P. aeruginosa* cells or the ECM. Anti-biofilm strategies involve inhibiting QS, inducing cell dispersal, targeting exopolysaccharides and iron metabolism with antibiotics, ECM degrading enzymes, QS inhibitor and iron chelators (Thi, Wibowo, & Rehm, 2020).

Complete eradication of biofilm associated infections is difficult despite antimicrobial therapies. *P. aeruginosa* circumvents antimicrobial therapies through resistance and tolerance. Resistance development within biofilms is typically associated with horizontal gene transfer facilitated by proximity of cells within the biofilm (Maurice, Bedi, & Sadikot, 2018). While tolerance is defined as survivability despite bactericidal treatment. *P. aeruginosa* proliferation in the presence of antimicrobial agents promotes mutations resulting in emergence of drug resistant strains (Ferriol-Gonzalez & Domingo-Calep, 2020). Strategies for improving drug penetration and biofilm disruption involve using antibiotics in combination with polymer-degrading enzymes such as alginate lyases, glycoside hydrolases, deoxyribonucleases, etc. (Kovach, Fleming, Wells, Rumbaugh, & Gordon, 2020).

1.5 β-glucans

In nature carbohydrates are the most abundant and structurally diverse class of biological compounds. Initially, carbohydrates were recognized as structural and energy storage molecules. but as the science developed it has been shown that carbohydrates partake in a variety of biological processes such as inflammation, cell-to-cell communication and so forth. Carbohydrates are found in many forms from simple monomers to more complex polysaccharides with multiple branching within their structure. Further complexity is supplement by monomers being coupled by glycosidic linkages in either an α- or β- anomeric configuration (Cerquerira, Bras, Ramos, & Fernandes, 2011).

β-glucans are polysaccharides composed of D-glucose monomers coupled by β-1,3, β-1,4 or β-1,6 glycosidic linkages. It is a naturally occurring substance found in the outer membrane of bacteria, fungi, algae, and certain crops. The biological and physiochemical properties of β-glucans vary greatly depending on the original source of isolation (Bashir & Choi, 2017). Examples of β-glucans are curdlan and lichenin (**Figure 1-6**). Curdlan is a bacterial β-glucan isolated from *Alcaligenes* spp., *Agrobacterium* spp and others. It is a linear 1,3-β-glucan homopolymer and unbranched (Chaudhari, et al., 2021). Lichenin is a complex β-glucan found in *Cetraria islandica*, an islandic moss species. It is composed of D-glucopyranose subunits coupled in a linear manner by β-1,3 and β-1,4 glycosidic linkages (Perlin & Suzuki, 1961).

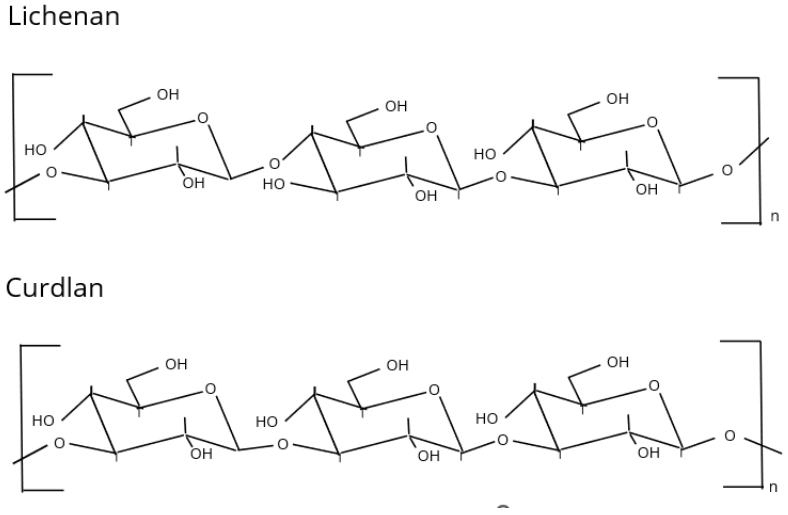

Figure 1-6. structure of lichenin and curdlan. Lichenin is a linear glucan composed of D-glucopyranose subunits coupled by β-1,3 and 1,4 glycosidic linkages while curdlan is a glucose polymer linked by β-1,3 glycosidic linkages.

1.6 Glycoside hydrolases

Glycoside hydrolases (GH) are a major class of biocatalysts for degradation of poly- and oligosaccharides by catalyzing the hydrolysis of O-, N- and S-linked glycosides. They cleave the glycosidic linkages in polysaccharides or polysaccharides coupled to non-polysaccharide moieties with the addition of one H_2O molecule (Ati, Lafite, & Daniellou, 2017). GH belonging to the same family are characterized by having common ancestry, similar 3D structure and identical catalytic mechanisms (Cerquerira, Bras, Ramos, & Fernandes, 2011).

Catalytic mechanisms of action are by inverting or retaining of glycoside residue configuration (**Figure 1-7**). Inverting catalytic mechanism utilizes two enzyme residues, an acid, and a base in a single step S_N2 displacement. This results in an inversion of the anomeric carbon. On the contrary, retaining catalytic mechanism results in the anomeric carbon retaining its configuration by undergoing a double step S_N2 displacement mechanism. In the S_N2 displacement one enzyme residue acts a nucleophile while the other acts as an acid or a base. In the first step the nucleophile attacks the anomeric carbon which leads to the formation of a covalent glycosyl-enzyme intermediate with assistance from the acidic residue. In the following step the deprotonated acidic residue assists the nucleophilic H_2O molecule in hydrolyzing the glycosyl-enzyme intermediate to the final product (Yuan, et al., 2012).

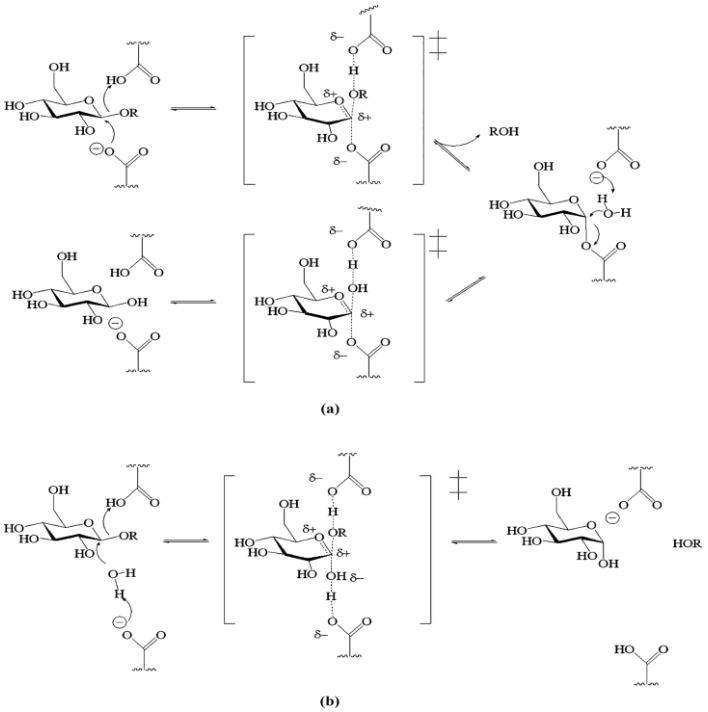

Figure 1-7. Inverting and retaining catalytic mechanism of glycoside hydrolases. a) represents the inverting mechanism which leads to the anomeric carbon inverting its configuration by undergoing a single step S_N2 displacement. b) represents the

retaining mechanism wihich leads to the anomeric carbon retaining its configuration by undergoing a double step S_N2 displacement. Adapted from (Rempel & Withers, 2008) with permission from Oxford University Press.

1.6.1 Glycoside hydrolase family 50

To date the characterized glycoside hydrolases of family 50 (GH50) are β-agarases that hydrolyze the cleavage of β-1,4-glycosidic linkages in agarose. The GH50 enzymes are suspected to utilize a retention mechanism for hydrolyzing polysaccharides. Though the catalytic residues are unknown they are believed to be two glutamic acid residues. It is also suggested that the 3D structure contain $(\beta/\alpha)_8$ barrel fold (Drula, et al., 2022).

The first GH50 protein with β-1,3-glucanase activity was partially characterized by Yi, et al. and was shown to hydrolyse β-1,3-glycosidic linkages in β-glucans such as curdlan and lichenan (Yi, yan, Jiang, & Wang, 2018). This enzyme found in *P. aeruginosa* CAU 342A was shown through sequence analysis to be part of the GH50 family and was named PaBglu50A by the authors. An orthologous enzyme found in *P. aeruginosa* PA14 named *Pa*GH50A was characterized in this study.

1.7 Aim of the study

The aim of this study was to characterize putatively secreted family 50 glycoside hydrolase found in *P. aeruginosa* PA14 with an endo-1,3-β-glucanase activity. The gene *Pa14_50830* was cloned into a pNIC-CH vector containing a hexa-histidine tag that was subsequently transformed into *E. coli* BL21 for protein expression. The secondary objective was to determine possible activity of *Pa*GH50A towards Psl and biofilms of *P. aeruginosa* strain PAO1 and its mutants PAO1 ΔWspF, PAO1 ΔWspF ΔPsl and PAO1 ΔWspF ΔPel.

2. Materials

2.1 Laboratory equipment

Table 2-1. List of laboratory equipment used during the thesis project with corresponding supplier

Category	Equipment	Supplier
Instruments	Äkta Pure	GE Healthcare
	BioPhotometer D30	Eppendorf
	Cell density meter, Ultrospec 10	Biochrom
	HPLC, Dionex Ultimate 3000 RS system with CAD detector and Velos Pro MS	Thermo Scientific/ Corona Ultra
	HPLC, Dionex Ultimate 3000	Thermo Scientific
	Plate reader, VarioSkan Lux	Therno Scientific
	qPCR StepOnePlus™	Applied Biosystems
	Thermocycler, SimpliAMP	Thermo Scientific
	ThermoMixer™ C	Eppendorf
	Ultraflextreme MALDI-TOF MS	Bruker
Equipment		
	µCuvette®	Eppendorf
	Autoclave	Certoclav
	Benchtop UV transilluminator	UVP
	Boiling water bath, SBB Aqua 5 plus	Grant
	Finnpipette™,0.5-10 µL, 10-100 µL, 100-1000 µL	Themo scientific
	Gel Doc™ EZ imager	Bio-Rad Laboratories
	Hair dryer	Solis
	Incubator, static	Termaks
	Incubator, New Brunswick™ Scientific Innova 44	Eppendorf
	Incubator, shaker	Infors HT
	Lex-48 bioreactor	Epiphyte3
	Magnet stirrer, RCT Basic	IKA
	Microcentrifuge, Ministar	VWR

	Microwave oven, MD142	Whirlpool
	Mill-Q® Direct water purification system, Direct 16	Merck
	Mini-PROTEAN® Tetra cell	Bio-Rad Laboratories
	Mini-sub GT cell	Bio-Rad Laboratories
	Membrane dry vacuum pump/ compressor, VCP 80	VWR
	MTP 384 ground steel BC MALDI-TOF MS target plate	Bruker
	MTP Target Frame III	Bruker
	NanoDrop™ One	Thermo Scientific
	Orbital shaker	VWR
	Plate centrifuge, Plate spin II	Kubota
	pH 913	Metrohm
	PowerPac™ Basic 300 V Power supply	Bio-Rad Laboratories
	Scale	Entris Satorious
	Vibra cell	Sonics
	Vortex MS 2 minishaker	IKA®
	Water bath	Thermo Scientific
Centrifuges		
	Centrifuge Avanti J25-S	Beckmann Coulter
	Centrifuge, Sorvall lynx 4000	Thermo Scientific
	Benchtop centrifuge, Allegra X-30R	Beckmann Coulter
	Benchtop centrifuge, 5418R	Eppendorf
	Centrifugation bottles, 50 mL and 1 L	Thermo Scientific
Columns		
	HisTrap™ HP 5 mL column	GE Healthcare
	PGC column, 150 x 2.1 mm	Thermo Scientific
	Rezex™ LC column, 300 x 7.8 mm	Phenomenex
Disposables		
	Assortment of glass ware	-
	Aluminum foil and saran wrap	-
	Cellestar® tubes, 15 and 50 mL	Greiner Bio-One
	Cryogenic tubes, 2 mL	Sarstedt
	Culture tubes, 13 mL	Sarstedt

	Eurofins Genomics barcodes	Eurofins Genomics
	Eppendorf tubes, 1.5 and 2.0 mL	Axygen
	Inoculation loops and needles	Thermo Scientific
	Lens tissue paper	Kimtech Science
	Micro cuvettes	Eppendorf
	MicroAmp™ Adhesive optical cover	Applied Biosystems
	MicroAmp™ optical 96-well reaction plate	Applied Biosystems
	Mini-PROTEAN® TGX Stain Free gels	Bio-Rad Laboratories
	Multiscreen®HTS 96-Well Plates, 0.45 µm Durapore®	Merck Millipore
	96-Well Polystyrene Microwell plate (Sarstedt)	Sarstedt
	PCR tubes, 0.2 mL	Axygen
	Petri dishes, 9 cm	Heger
	Pipette tips	VWR
	Scalpels	Swann Moton
	Semi-Micro Cuvette	Brand
	Serological pipettes, 5 mL, 10 mL and 25 mL	VWR
	Snap Ring Micro-Vials with Snap Ring Caps, 0.3 mL	VWR
	Steritop® Vacuum Driven Disposable 0.22 µm Filtration System	Merck Millipore
	Syringes, 1 mL, 5 mL, 60 mL	BD Plastipak

2.2 Chemicals

Table 2-2. List of laboratory chemicals used during the thesis project with corresponding supplier.

Chemicals	Supplier
1000x SYPRO orange dye	Thermo Scientific
50x TAE Electrophoresis Buffer	Thermo Scientific
10x Tris-Glycine-SDS buffer	Bio-Rad Laboratories
4x NuPAGE LDS Sample buffer	Novex
85 % Glycerol	Merck Millipore
37 % Hydrochloric acid, HCl	Merck Millipore
2.5-Dihydroxybenzoic acid, DHB	Sigma-Aldrich
3,5-Dinotrosalicylic acid	Sigma-Aldrich
3-methyl-2- benzothiazolinone hydrazone hydrochloride, MBTH	Sigma-Aldrich
Acetonitrile	Honeywell
Agar powder	VWR
Ammonium acetate, NH_4Ac	VWR
Ammonium iron (III) sulfate, $FeNH_4(SO_4)_2 \cdot 12H_2O$	Sigma-Aldrich
Antifoam 204	Invitrogen
Avicel Cellulose	Sigma-Aldrich
Bacto tryptone	BD
Bacto yeast extract	BD
BenchMark™ Protein Ladder	Invitrogen
Bio Rad protein assay	Bio Rad Laboratories
Bis-Tris	VWR
Brain Heart Infusion	Oxoid
Calf intestinal alkaline phosphatase, CIP	New England biolabs®
Calcium chloride, $CaCl_2$	Sigma-Aldrich
Casamino acids	SDS
Citric acid, $C_6H_8O_7$	VWR
Complete™ Mini EDTA free protease inhibitor cocktail tablets	Roche
Curdlan	Megazyme
Cutsmart® buffer 10x	New England biolabs®

Disodium EDTA·$2H_2O$	VWR
Dithiothreitol, DTT	Sigma-Aldrich
Dnase 1	NEB
Ethanol, 96 %	VWR
D-Glucose	VWR
Imidazole	PanReac AppliChem
Isopropyl β-D-1-thiogalactopyranoside, IPTG	Sigma-Aldrich
Kanamycin monosulfate	Gibco
Lichenin	Megazyme
Lysozyme	Sigma-Aldrich
Magnesium sulfate, $MgSO_4$	Sigma-Aldrich
Minimal (M9) medium (2x) salts solution	Gibco
PBS	Gibco
PeqGREEN DNA/RNA Dye	Peqlab
Phenylmethylsulphonyl fluoride, PMSF	Sigma-Aldrich
Potassium phosphate dibasic, K_2HPO_4	Sigma-Aldrich
Potassium phosphate monobasic, KH_2PO_4	Sigma-Aldrich
Proteinase K	NEB
Q5® High-fidelity 2X master mix	NEB
Quick-Load 1 kbp	NEB
Restriction enzyme: Aflii	New England biolabs®
Restriction enzyme: PstI-HF	New England biolabs®
SeaKem LE Agarose	Lonza
Sodium chloride, NaCl	VWR
Sodium citrate dihydrate, $C_6H_9Na_3O_9$	Sigma-Aldrich
Sodium hydroxide, NaOH	VWR
Sodium phosphate dibasic dihydrate, $Na_2HPO_4 \cdot 2H_2O$	VWR
Sodium potassium tartrate, $KNaC_4H_4O_6 \cdot 4H_2O$)	Sigma-Aldrich
Sulfamic acid, H_3NSO_3	Sigma-Aldrich
Sulfuric acid, H_2SO_4,	Honeywell
Sucrose	VWR
Triton X-100	Sigma-Aldrich
Tris base	Fisher Bioreagents

Ultrapure™ distilled water	Invitrogen
Zink Chloride, $ZnCl_2$	VWR

2.3 Kits

Table 2-3. Overview of Laboratory kits utilized during the thesis project with corresponding supplier

Kits	Supplier
In-Fusion® HD cloning kit	Takara Bio
NucleoSpin® Gel and PCR Clean-up	Machrey-Nagel
NucleoSpin® Plasmid/ Plasmid (NoLid)	Machrey-Nagel
ONE SHOT™ BL21 (DE3) chemically competent *E. coli*	Invitrogen
ONE SHOT™ TOP 10 chemically competent *E. coli*	Invitrogen

2.4 Primers and plasmids

Table 2-4. Overview of plasmid and primers utilized during the thesis project. Name, sequence and purpose is described. Provided by main-supervisor Gustav Vaaje Kolstad and Co-supervisor Per Kristian Thorén Edvardsen.

Name	Sequence 5'-3'	Comment
pCCI plasmid with *Pa14_50830*	-	Plasmid with *Pa14_50830* from *P. aeruginosa* PA14. Used to prepare DNA construct for cloning.
PA14_GH50_conf_seq_Forward	TCGGCATGGGGTTTCAAC	Primer for cloning of *Pa14_50830*
PA14_GH50_conf_seq_Reverse	GTTGAAACCCCATGCCGA	Primer for cloning of *Pa14_50830*
pNIC-CH Plasmid_Forward	TGTGAGCGGATAACAATTCC	Primer for High copy pNIC-CH plasmid
pNIC-CH Plasmid_Reverse	AGCAGCCAACTCAGCTTCC	Primer for High copy pNIC-CH plasmid

2.5 Enzymes

Table2-5. Overview of enzymes used during thesis project. plasmid information, production organism and supplier and purpose are described.

Protein name	Gene	Plasmid	Antibiotic resistance	Production organism	Supplier	Comment
*Pa*GH50A	*PA14_50830*	pNIC-CH	Kanamycin monosulfate	*E. coli* strain BL21	-	Full length enzyme with hexa His-tag at the C-terminal
Celluclast®	-	-	-	-	Novozymes	Mixture of multiple cellulase enzymes. Used as a positive control.

2.6 Bacteria species and strains

Table2-6. Overview of bacteria species and related mutants used during the thesis project. Name and description of each strain.

E. coli	
Name	Comment
E. coli strain Top 10	Chemically competent *E. coli* cells used during cloning.
E. coli strain Bl21	Chemically competent *E. coli* cells used for recombinant protein expression.
P. aeruginosa	

Name	Comment
P. aeruginosa strain PAO1	Wilde type of *P. aeruginosa*. PAO1 is a commonly used laboratory strain for research on biofilm. The strain produces normal amounts of exopolysaccharide Alginate, Psl and Pel. Kindly provided by Professor Victor Nizet.
P. aeruginosa strain PAO1 ΔWspF	A *P. aeruginosa* mutant that overproduces and secretes exopolysaccharides Alginate, Psl and Pel into the ECM. Kindly provided as a gift from Professor Matthew R. Parsek.
P. aeruginosa strain PAO1 ΔWspF ΔPsl	A *P. aeruginosa* mutant that overproduces and secretes exopolysaccharide Pel into the ECM. Pel is the dominant exopolysaccharide in the matrix. Kindly provided as a gift from Professor Matthew R. Parsek.
P. aeruginosa strain PAO1 ΔWspF ΔPel	A *P. aeruginosa* mutant that overproduces and secretes exopolysaccharide Psl into the ECM. Psl is the dominant exopolysaccharide in the matrix. Kindly provided as a gift from Professor Matthew R. Parsek.

3. Methods

3.1 Preparation of growth media, buffers, and stock solutions

3.1.1 Growth media

Table3-1. Overviewof growth mediumspreparedduring the thesis project

LB medium	¶ 5 g of Bacto tryptone ¶ 2.50 g of Bacto yeast extract ¶ 5 g of NaCl The individual compounds for preparation of lysogeny broth (LB) medium were weighed out and transferred to a 500 mL Beaker. To the same beaker approximately 400 mL ddH_2O was added and the solution was homogenized utilizing a magnet stirrer. Once the compounds were dissolved the pH was checked using pH meter 913 to see whether the pH was between 6.8-7.0 and if it was pH adjusting was not necessary. The medium was transferred to a 500 mL volumetric flask and the volume was adjusted to the mark, so that the final volume equaled 500 mL. LB medium was then transferred to a non-sterile 500 mL GL-45 glass bottle and autoclaved for 15 minutes at 121 ^oC.
LB agar medium supplemented with 50 µg/ mL kanamycin monosulfate	¶ 5g of Tryptone ¶ 5 g of NaCl ¶ 2.50 g of Yeast extract: ¶ 7.5 of Agar powder ¶ 500 µL of 50 mg/mL Kanamycin monosulfate The compounds except for kanamycin monosulfate were weight out and transferred to a non-sterile 500 mL GL-45 glass bottle. 400 mL ddH_2O was added to the bottle and the solution was mixed

	using a magnet stirrer. Once compounds other than agar had dissolved, the volume was adjusted to 500 mL. LB agar medium was manually autoclaved for 15 minutes at 121 ^{o}C. Following sterilization, the medium was transferred to a static incubator for approximately 20 minutes at 50 ^{o}C. When the agar medium temperature had fallen to approximately 50 ^{o}C the medium was transferred to a LAF bench and 500 µL of 50 mg/mL kanamycin monosulfate was added. The medium was mixed, and then poured into petri dishes just enough to cover the bottom of the dish. 500 mL LB agar medium provided approximately 23 LB agar plates. The LB agar plates were slightly covered with the lid and let to hardened and then stored in a plastic sleeve in a cool room.
TB medium	¶ 12 g of Bacto tryptone ¶ 24 g of Bacto yeast extract ¶ 4 mL of 85 % Glycerol ¶ 50 mL of 0.72 M K_2HPO_4 solution ¶ 50 mL of 0.17 M KH_2PO_4 solution Compounds for Terrific broth (TB) medium were weighed out and transferred to a 1 L beaker and dissolved in 800 mL ddH_2O utilizing a magnet stirrer. Once dissolved 4 mL of 85 % glycerol was added using a 5 mL serological pipette. The medium was transferred to a non-sterile 1 L GL-45 glass bottle and the volume was adjusted to 900 mL with ddH_2O. TB medium was autoclaved for 15 minutes at 121 ^{o}C. During the day of use 50 mL of 0.72 M K_2HPO_4 and 50 mL of 0.17 M KH_2PO_4 solution was added to the 900 mL sterile TB medium in a LAF bench such that the finale volume was 1 L.
BHI medium	¶ 37 g of Brain Heart Infusion

	Brain heart infusion (BHI) compound was weighed out and transferred to 1 L beaker and dissolved in 800 mL of ddH_2O utilizing a magnet stirrer. The pH was measured and given to be 7.0 using pH meter 913. The medium was transferred to a 1 L volumetric flask and the finale volume was adjusted to be 1 L. BHI medium was transferred to a non-sterile 1 L GL-45 glass bottle and autoclaved for 15 minutes at 121 ^oC.
M9 medium	¶ Minimal (M9) medium (2x) salts solution ¶ 2 mM $MgSO_4$ ¶ 0.1 mM $CaCl_2$ ¶ 0.2 % Glucose ¶ 0.5 % Casamino acids Preparation of 100 mM of $MgSO_4$ and 100 mM $CaCl_2$ Solutions 100 mM of $MgSO_4$ and $CaCl_2$ was prepared by weighting out 1.204 g of $MgSO_4$ and 1.110 g of $CaCl_2$ then transferring the compounds to each their 100 mL volumetric flask. The volume was adjusted to 100 mL with ddH_2O. Preparation of 4 % of glucose and 10 % Casamino acids solution 4 % of glucose and 10 % Casamino acids solutions was prepared separately by transferring the following 4 g and 10 g of compounds to each their 100 mL volumetric flask. The final volume was adjusted to 100 mL with ddH_2O. Preparation of M9 medium To a non-sterile 1 L GL-45 glass bottle 500 mL M9 medium (2x) salts solution along with 50 mL of 4 % glucose solution and 50 mL of 10 % Casamino acids solution, 20 mL of 100 mM $MgSO_4$

	and 1 mL of 100 mM $CaCl_2$ was added. The finale volume was adjusted to 1 L with ddH_2O. The M9 solution was autoclaved for 15 minutes at 121 ^oC. The solution was stored at 4 ^oC.

3.1.2 Stock solutions

Table3-2. Overviewof stock solutionsprepareddurin the thesis project.

Kanamycin monosulfate (50 mg/mL)	¶ 0.5 g of Kanamycin monosulfate Kanamycin monosulfate was weighted out and transferred to a 10 mL volumetric flask and dissolved in 10 mL ddH_2O using a vortex MS 2 minishaker. Once fully dissolved the solution was filtrated using a 0.20 µm filter and a 10 mL syringe. 1 mL aliquots for kanamycin monosulfate solution in 1.5 mL Eppendorf tubes were prepared. The aliquots were stored at -20 ^oC.
Sodium Chloride (NaCl, 5 M)	¶ 146.1 g of NaCl NaCl was weighted out and then transferred to a 500 mL volumetric flask. Approximately 470 mL ddH_2O was added such that NaCl would fully dissolve. The solution was homogenized using a magnet stirrer. Once fully dissolved the volume was adjusted to 500 mL. The solution was sterilized using a 0.22 µm Steritop® filter concurrent with transferring the solution to a sterile 500 mL GL-45 glass bottle.
Imidazole (2 M)	¶ 33.8 g Imidazole Imidazole was weighted out and transferred to a 250 mL volumetric flask and dissolved in 200 mL ddH_2O using a magnet stirrer. Once dissolved the volume was adjusted to 250 mL with

	ddH_2O. The solution was sterilized using a 0.22 µm Steritop® filter concurrent with transferring the solution to a sterile 250 mL GL-45 glass bottle.
Isopropyl β-D-1-thiogalactopyranoside (IPTG, 1 M)	¶ 2.383 g of IPTG IPTG was weighted out and then transferred to a 10 mL volumetric flask and dissolved in 10 mL ddH_2O using a vortex MS 2 minishaker. Sterilization was achieved by passing the solution through a 0.20 µm filter using a 10 mL syringe. Aliquots were prepared by transferring 1 mL of IPTG to 1.5 mL Eppendorf tubes. The aliquots were stored at -20 ^oC.
Lysozyme (100 mg/mL)	¶ 1.0 g of Lysozome Lysozome was weighted out and transferred to a 10 mL volumetric flask and dissolved in 10 mL ddH_2O using a vortex MS 2 minishaker. Once fully dissolved sterilization was achieved by passing the solution through a 0.20 µm filter using a 10 mL syringe. The solution was divided into 10 aliquots of 1 mL and stored at -20 ^oC.
Potassium phosphate monobasic (KH_2PO_4, 0.17 M)	¶ 11.565 g of KH_2PO_4 KH_2PO_4 was weighted out and then transferred to a 500 mL beaker. The compound was dissolved in 400 mL ddH_2O using a magnet stirrer. Once the salt had fully dissolved, the solution was transferred to a 500 mL volumetric flask and final volume was adjusted to 500 mL. The solution was transferred to a non-sterile 500 mL GL-45 glass bottle and autoclaved for 15 minutes at 121 ^oC.

Potassium phosphate dibasic (K_2HPO_4, 0.72 M)	¶ 62.7 g of K_2HPO_4 K_2HPO_4 was weighted out and then transferred to a 500 mL beaker. The compound was dissolved in 400 mL ddH_2O using a magnet stirrer. Once the salt had fully dissolved, the solution was transferred to a 500 mL volumetric flask and final volume was adjusted to 500 mL. The solution was transferred to a non-sterile 500 mL GL-45 glass bottle and autoclaved for 15 minutes at 121 ^oC.
1% Triton X-100 in PBS solution	¶ 1 mL Triton X-100 ¶ PBS solvent To a 100 mL volumetric flask 1 mL of Triton X-100 was added and dissolved in 80 mL PBS solution using a magnet stirrer. Once solution was homogenized the finale volume was adjusted to 100 mL. The solution was filtrated using Steritop® 0.22 µm Filtration System and stored in a 100 mL GL-45 glass bottle.
Phenylmethylsulphonyl fluoride (PMSF, 50 mM)	¶ 871 mg PMSF PMSF was weighted out and transferred to a 100 mL volumetric flask. The compound was dissolved in 100 mL ddH_2O utilizing a magnet stirrer. Once fully dissolved sterilization was achieved by passing the solution through a 0.20 µm filter and a 60 mL syringe. The solution was divided in aliquots of 10 mL and stored in 15 mL Cellestar® tubes at -20 ^oC.
Magnesium Chloride ($MgCl_2$, 20 mM)	¶ 476.1 mg of $MgCl_2$ $MgCl_2$ was weighted out and transferred to a 250 mL volumetric flask. The compound was dissolved in 200 mL ddH_2O, and the finale volume was adjusted to 250 mL. Solution was sterilized

	using a 0.22 µm Steritop® filter and stored in a 250 mL GL-45 glass bottle at 4 °C.
Calcium Chloride ($CaCl_2$, 1 M)	¶ 1.1098 g $CaCl_2$ $CaCl_2$ was weighted out and transferred to a 10 mL volumetric flask. The compound was dissolved in 8 mL ddH_2O utilizing a magnet stirrer. Once dissolved finale volume was adjusted to 10 mL and sterilized using a 0.20 µm filter and 10 mL syringe. The solution was stored in a 15 mL Cellestar® tube at 4 °C.
Zink Chloride ($ZnCl_2$, 1 M)	¶ 1.363 g $ZnCl_2$ $ZnCl_2$ was weighted out and transferred to a 10 mL volumetric flask. The compound was dissolved in 8 mL ddH_2O using a magnet stirrer. Once dissolved finale volume was adjusted to 10 mL and sterilized using a 0.20 µm filter and 10 mL syringe. The solution was stored in a 15 mL Cellestar® tube at 4 °C.
Sodium hydroxide (NaOH, 0.5 M)	¶ 10 g of NaOH NaOH was weight out and transferred to a 500 mL volumetric flask. The compound was dissolved in 400 mL ddH_2O using a magnet stirrer. Once dissolved the finale volume was adjusted to 500 mL. The solution was sterilized using a 0.22 µm Steritop® filter and stored in a 500 mL GL-45 glass bottle.
3,5-Dinotrosalicylic acid (DNSA, 2x)	¶ 1.0 g of DNSA ¶ 30 g of Sodium potassium tartrate ($KNaC_4H_4O_6 \cdot 4H_2O$) ¶ 80 mL of 0.5 M NaOH

	The compounds were weight out and transferred to a 100 ml volumetric flask. The compounds were then dissolved with 80 mL of 0.5 M NaOH in a water bath at 65 ^{o}C. Once dissolved the DNSA reagent was transferred to a sterile 100 mL GL-45 glass bottle and covered with aluminum foil. The reagent was stored in an area with limited light access at room temperature.
3-methyl-2-benzothiazolinone hydrazone hydrochloride (MBTH, 3 mg/ mL)	¶ 30 mg of MBTH MBTH was weight out and transferred to a 10 mL volumetric flask. The compound was dissolved in 10 mL ddH_2O. Once dissolved the solution was filtrated using a 0.20 µm filter and 10 mL syringe. The solution was stored in a 15 mL Cellestar® tube at 4 ^{o}C.
Dithiothreitol (DTT, 1 mg/mL)	¶ 10 mg of DTT DTT was weight out and transferred to a 10 mL volumetric flask. The compound was dissolved in 10 mL ddH_2O. Once dissolved the solution was filtrated using a 0.20 µm filter and 10 mL syringe. The solution was stored in a 15 mL Cellestar® tube at 4 ^{o}C.
Ammonium iron (III) sulfate ($FeNH_4(SO_4)_2 \cdot 12H_2O$, 2 %)	¶ 200 mg of $FeNH_4(SO_4)_2 \cdot 12H_2O$ $FeNH_4(SO_4)_2) \cdot 12H_2O$ was weight out and transferred to a 10 mL volumetric flask. The compound was dissolved in 10 mL ddH_2O. Once dissolved the solution was filtrated using a 0.20 µm filter and 10 mL syringe. The solution was stored in a 15 mL Cellestar® tube at 4 ^{o}C.
Sulfamic acid (H_3NSO_3, 2 %)	¶ 200 mg of H_3NSO_3

	H_3NSO_3 was weight out and transferred to a 10 mL volumetric flask. The compound was dissolved in 10 mL ddH_2O. Once dissolved the solution was filtrated using a 0.20 µm filter and 10 mL syringe. The solution was stored in a 15 mL Cellestar® tube at 4 ºC.
Hydrochloric acid (HCl, 1 M)	¶ 821,2 µL of 37 % HCl To a 10 mL volumetric flask 5 mL of ddH_2O was added followed by HCl. The solution was mixed, and the finale volume was adjusted to 10 mL. Then filtrated using a 0.20 µm filter and 10 mL syringe. The solution was stored in a 15 mL Cellestar® tube.
Sulfuric acid (H_2SO_4, 5 mM)	¶ 556 µl of H_2SO_4 To a 2 L volumetric flask 1.5 L of ddH_2O was added followed by H_2SO_4. The solution was mixed, and the finale volume was adjusted to 2 L.
Ammonium acetate pH 6.77 (NH_4Ac, 10 mM)	¶ 0.771 g of NH_4Ac NH_4Ac was weight out and transferred to a 1 L volumetric flask. The compound was dissolved in 800 mL ddH_2O using a magnet stirrer. Once dissolved the pH was measured and adjusted to be 6.77. The finale volume was adjusted to 1 L. The solution was sterilized using a 0.22 µm Steritop® filter and transferred to a 1 L GL-45 glass bottle.
8x SYPRO orange dye	¶ 8 µL of 1000x SYPRO orange dye 8 µL of 1000x SYPRO was pipetted to a 1.5 mL Eppendorf tube. The substance was diluted with with ddH_2O to a final volume of 1

	mL. The Eppendorf tube was wrapped in aluminon foil to limit light pollution and stored at -20 ^{o}C.
Disodium EDTA·2H_2O pH 8.0 (EDTA, 0.5 M)	¶ 18.61 g EDTA EDTA was weight out and transferred to a 100 mL volumetric flask. The compound was dissolved in 80 mL ddH_2O using a magnet stirrer. The pH was measured and adjusted to 8.0. Once dissolved the finale volume was adjusted to 100 mL. The solution was sterilized using a 0.22 µm Steritop® filter and transferred to a 100 mL GL-45 glass bottle.
70 % Ethanol	¶ 73 mL of 96 % ethanol Ethanol was transferred to a 100 mL volumetric flask and diluted with ddH_2O. The solution was sterilized using a 0.22 µm Steritop® filter and transferred to a 100 mL GL-45 glass bottle.
10% Crystal violet (CV)	¶ 1 g of CV CV was weighted out and transferred to a 15 mL Cellestar® tube. The compound was dissolved in 8 mL 100 % ethanol. Once dissolved finale volume was adjusted to 10 mL and sterilized using a 0.20 µm filter and 10 mL syringe.
2.5-Dihydroxybenzoic acid (DHB) matrix	¶ 20 mg of DHB 2,5-DHB was dissolved in 30 % ACN and 0.1 % TFA. 1 mM NaCl was added. The final volume was adjusted to 1 mL and stored at 4 ^{o}C.

3.1.3 Buffer solutions

Table3-3. Overviewof buffer solutionspreparedduring the thesis project.

IMAC binding buffer	¶ 2.5 mL of 2M Imidazole ¶ 20 mL of 1M Tris-HCl pH 7.5 ¶ 40 mL of 5M NaCl To a 1 L volumetric flask NaCl was transferred using a 100 mL graduated cylinder while Imidazole and Tris-HCl was transferred using serological pipettes. The mixture was diluted with ddH_2O to a final volume of 1 L. The solution was sterilized using a 0.22 µm Steritop® filter and transferred to a 1 L GL-45 glass bottle.
IMAC washing buffer	¶ 10 mL of 2M Imidazole ¶ 20 mL of 1M Tris-HCl pH 7.5 ¶ 40 mL of 5M NaCl Tris-HCl, NaCl and Imidazole was transferred to a 1 L volumetric flask using separate 100 mL graduated cylinder. The mixture was diluted with ddH_2O to a final volume of 1 L. The solution was sterilized using a 0.22 µm Steritop® filter and transferred to a 1 L GL-45 glass bottle.
IMAC elution buffer	¶ 125 mL of 2 M Imidazole ¶ 10 mL of 1 M Tris-HCl pH 7.5 ¶ 20 mL of 5 M NaCl Tris-HCl and NaCl were transferred to a 500 mL volumetric flask using 25 mL serological pipettes. While Imidazole was transferred using a 250 mL graduated cylinder. The mixture was diluted with ddH_2O to a final volume of 500 mL. The solution was sterilized

	using a 0.22 µm Steritop® filter and transferred to a 500 mL GL-45 glass bottle.
Spheroplast buffer	¶ 171.15 g of Sucrose ¶ 100 mL of 1 M Tris-HCl pH 8.0 ¶ 1 mL of 0.5 M EDTA pH 8.0 Sucrose was weighted out and transferred to a 1 L volumetric flask. 100 mL of 1 M Tris-HCl pH 8.0 and 1 mL of 0.5 M EDTA pH 8.0 was added to the volumetric flask. The substances were dissolved in 600 mL of ddH_2O. The finale volume was adjusted to 1 L and sterilized using a 0.22 µm Steritop® filter and transferred to a 1 L GL-45 glass bottle.
Citrate phosphate buffer pH 5.4	¶ 4.8 g of Citric acid ($C_6H_8O_7$, 0.1 M) ¶ 8.9 g of Sodium phosphate dibasic dihydrate ($Na_2HPO_4 \cdot 2H_2O$, 0.2 M) Compounds were weighed out and transferred to separate 250 mL volumetric flask. The salts were dissolved in 200 mL ddH_2O using a magnet stirrer. Once dissolved the finale volumes were adjusted to 250 mL. The solutions were transferred to 250 mL GL-45 glass bottles. To a 100 mL beaker 22.2 mL of $C_6H_8O_7$ and 27.8 mL $Na_2HPO_4 \cdot 2H_2O$ was added. The pH was measured using pH meter 913. Once pH was checked the solution was transferred to a 100 mL volumetric flask and the final volume was adjusted to 100 mL with ddH_2O. The solution was sterilized with a 0.22 µm Steritop® filter and transferred to a GL-45 glass bottle.
Citrate buffer pH 4.0 (0.1 M)	¶ 3.182 g of Citric acid ($C_6H_8O_7$) ¶ 2.482 g of Sodium citrate dihydrate ($C_6H_9Na_3O_9$)

	Compounds were weighed out and transferred to 250 mL beaker. The salts were dissolved in 200 mL ddH_2O using a magnet stirrer. Once dissolved the pH was measured and adjusted using pH meter 913. The finale volume was adjusted to 250 mL with ddH_2O. The solution was sterilized with a 0.22 µm Steritop® filter and transferred to a 250 mL GL-45 glass bottle.
Bis-tris buffer pH 6.5 (1 M)	¶ 20,924 g of Bis-Tris Bis-Tris was weighted out and transferred to a 100 mL beaker. The compound was dissolved in 50 mL ddH_2O using a magnet stirrer. pH was adjusted to 6.5 using 37% hydrochloric acid (HCl) and by a pH meter 913. Buffer solution was transferred to a 100 mL volumetric flask and finale volume was adjusted to 100 mL with ddH_2O. Solution was sterilized using a 0.22 µm Steritop® filter and transferred to a 100 mL GL-45 glass bottle.
Tris-HCl buffer pH 7.5 and 8.5 (1M)	¶ 30.3 g of Tris base ¶ 37% hydrochloric acid (HCl) Tris base was weighted out and then transferred to a 250 mL beaker. Compound was dissolved in 150 mL ddH_2O using a magnet stirrer. pH was adjusted to 7.5 or 8.5 using 37% hydrochloric acid (HCl) and by a pH meter 913. Final volume was adjusted to 250 mL with ddH_2O. The solution was sterilized using a 0.22 µm Steritop® filter and transferred to a 250 mL GL-45 glass bottle.

3.1.4 Substrates

Table7-4. Overviewof substratespreparedduring the thesis project.

Curdlan (30 mg/mL)	¶ 300 mg of Curdlan ¶ 0.25 M NaOH Curdlan was weight out directly into a 15 mL Cellestar® tube and 8 mL of 0.25 M NaOH was added using a 10 mL serological pipette. The Cellestar® tube was incubated in a water bath for approximately 1.5 hours at 80 ^{o}C with continuous vortexing. Once the substances had dissolved the pH was adjusted to 7.0 using pH meter 913. Finale volume was adjusted to 10 mL.
Lichenin (30 mg/mL)	¶ 300 mg of Lichenin Lichenin was weight out directly into a 15 mL Cellestar® tube and 8 mL ddH_2O was added using a 10 mL serological pipette. The Cellestar® tube was incubated in a water bath for approximately 45 minutes at 80 ^{o}C with continuous vortexing. Once the substances had dissolved the pH was adjusted to 7.0 using pH meter 913. Finale volume was adjusted to 10 mL.
Avicel Cellulose (30 mg/mL)	¶ 300 mg of Avicel Cellulose Avicel cellulose was weight out and transferred to a 15 mL Cellestar® tube and dissolved in 10 mL ddH_2O using a 10 mL serological pipette.

3.2 Gel electrophoresis

Gel electrophoresis is a laboratory method for separation of complex DNA, RNA, or protein mixtures with high resolution according to their charge and molecular size. The process involves applying an electric current to macromolecules facilitating migration through a gel from the negative electrode towards the positive electrode. Different molecules migrate at different rates depending on the physical characteristics and experimental system. Smaller molecules migrate further in a gel in comparison to their large counterparts however several other factors can impact mobility such as molecular shape, temperature, porosity and viscosity of the gel matrix (Reddy & Raju, 2012).

3.2.1 DNA agarose gel electrophoresis

Agarose gel electrophoresis is an effective technique for separation of DNA fragments of varying sizes ranging from 100 bp to 25 kb. Agarose polymers associate non covalently creating a network of agarose pores whose size determine sieving properties of the agarose gel. The phosphate backbone of DNA is negatively charged and as a result when placed in an electric field will migrate towards the positively charged anode. The distance traveled for a DNA fragment is inversely proportional to the log of the fragments molecular weight allowing for separation based on size alone (Lee, Costumbrado, Hsu, & Kim, 2009).

Material

Chemicals

- DNA samples
- SeaKem LE Agarose (Lonza)
- 1xTAE Electrophoresis Buffer buffer (Thermo scientific)
- Peqgreen (Peqlab)
- 4x NuPAGE LDS Sampler buffer
- Ladder
    - Quick-Load® 1 kb (NEB)

Equipment and instruments

- Erlenmeyer flask
- Eppendorf tubes, 1.5 mL (Axygen)
- Microwave oven, MD142 (Whirlpool)
- Mini-sub GT cell (Bio-Rad Laboratories)
- PowerPac™ Basic 300 V Power supply (Bio-Rad Laboratories)
- Gel Doc™ EZ imager (Bio-Rad Laboratories)

Method

To prepare 1 % agarose gel solution 0.5 g SeaKem LE Agarose was weighted out and transferred to a 250 mL Erlenmeyer flask. 50 mL 1x TAE electrophoresis buffer was added to the agarose gel powder. The mixture was heated periodically in the microwave until complete dissolution of the agarose powder. Once dissolution was achieved the solution was cooled down to approximately 50 ^{o}C by running the Erlenmeyer flask under cold tap water. To the agarose solution 2.5 µL PeqGREEN was added and gently mixed. The agarose solution was cast in a transferable mold and let to solidify. The gel was transferred to a Mini-Sub GT cell and completely covered with 1x TAE electrophoresis buffer. The DNA samples were loaded into the wells along with a Quick-Load 1 kbp DNA ladder and run at 90 V for approximately 45 minutes. Once a purple line appeared midway in the gel, the electrophoresis was complete. Agarose gel was removed from the mold and UV imaging was performed using Gel Doc EZ imager.

3.2.2 Sodium Dodecyl Sulphate Polyacrylamide Gel Electrophoresis (SDS-PAGE)

SDS-PAGE gel electrophoresis is a technique for separation of complex mixtures of proteins. Its primarily used for determining the purity of protein samples or protein size (Zhu & Lu, 2012). Proteins have a distinct charge based on the composition of the amino acid side chains and are folded in different configuration based on side chain polarity and (non)covalent interactions (Schmid , Prinz, Stabler, & Sangerlaub, 2016). Initially the proteins are denatured by sodium dodecyl sulphate (SDS), an anionic detergent and SDS buffer then binds the amino acid residues leaving the polypeptide negatively charged. In response to the electric field the

negatively charged polypeptides will travel through a network of pores towards the positively charged anode (Nowakowski, Wobig, & Petering, 2014). The polypeptides are separated by size where smaller proteins migrate faster in the gel matrix due to less resistance than larger proteins (Zhu & Lu, 2012).

Material

Chemicals

- Protein samples
- 1x Tris/Glycine/SDS buffer (Bio-Rad Laboratories)
- 4x NuPAGE LDS Sample buffer
- BenchMark™ Protein Ladder

Equipment

- Mini-PROTEAN® TGX Stain Free Gels 10/15 wells (Bio-Rad Laboratories)
- Mini-PROTEAN® Tetra cell (Bio-Rad Laboratories)
- PowerPac™ Basic 300 V Power supply (Bio-Rad Laboratories)
- Gel Doc™ EZ Imager (Bio-Rad Laboratories)
- ThermoMixer C (Eppendorf)
- Eppendorf tubes, 1.5 mL (Axygen)

Method

SDS-PAGE gel electrophoresis was performed on protein samples of either pure protein or protein extracts. 15 µL of each protein sample were transferred to an Eppendorf tube along with 5 µL of 4x NuPAGE LDS Sample buffer. The mixture was incubated in a Thermomixer C for 10 minutes at 70 ^{o}C. Mini-PROTEAN® TGX Stain Free gels were placed in a Mini-PROTEAN® Tetra cell and filled to the 4x gel mark with 1x Tris/Glycine/SDS buffer. To each well in the Mini-PROTEAN® TGX Stain Free Gels 15 µL of sample or BenchMark™ Protein Ladder were injected with a 0.5 – 10 µL finnpipette. The electrophoresis system was connected to the PowerPac™ Basic 300 V Power supply and run at 200 V for approximately 30 minutes. Upon completion the gel was removed from the Mini-PROTEAN® Tetra cell and it's Mini-

PROTEAN® TGX Stain Free Gel mold. The gel was imaged with Gel Doc™ EZ Imager using the high sensitivity option in the Image Lab software.

3.3 Determination of DNA concentration

Spectrophotometric analysis of DNA concentration and purity is based on the principle that DNA and RNA absorbs specific wavelength of ultraviolet (UV) light and reflect others. Nucleic acids contain conjugated double bonds in their purine and pyrimidine rings which absorbs UV light at 260 nm and reflect the rest. The wavelengths that are reflected are measured in a photo detector. The more UV light that is absorbed by molecules in the sample the higher the nucleic acid concentration is (Li, et al., 2014).

Beer-Lambert's law is utilized for determining the concentration of DNA in a sample. Beer-Lambert's law given in equation 1 states that the absorbance (A) equals the extinction coefficient (ε) of double stranded DNA times path length of the UV light (l) times the concentration (c) (Mamouei, Budidha, Baishya, Qassem, & Kyriacou, 2021).

ö سي - ᶻ ὰᶻ ὦ (1)

Nanodrop™ One generates an absorbance spectrum that represents the absorbance of pure DNA, RNA, and protein. DNA and RNA have absorption peak at 260 nm while proteins have optimal absorbance at 280 nm. To assess the purity the absorbance at 260 nm is divided by absorbance at 280 nm. For pure DNA a ratio of 1.8 is expected (Lucena-Aguilar, et al., 2016).

Material

Chemicals

- Purified plasmid DNA samples
- NE plasmid elution buffer
- ddH_2O

Equipment and instruments

- NanoDrop™ One
- Lens tissue paper

Method

The Nanodrop™ One pedestal was prior to use cleaned with ddH_2O and wiped with lens tissue paper. The instrument system was blanked by pipetting 2 µL of NE plasmid elution buffer onto the pedestal then lowering the sample carrier arm on the pedestal creating an optical pathway for light absorption. The pedestal was once again cleaned with ddH_2O and wiped with lens tissue paper before DNA concentration was measured. DNA concentration for each of the plasmid samples was measured following the same procedure as the blank sample. Absorbance was measured at 260 nm and outputs of DNA concentration given in µg/ mL.

Sample purity was given as a measurement of A260/280 where a high DNA purity fell between 1.80 and 2.00.

3.4 Cloning of *Pa*GH50A and constructing a recombinant pNIC-CH plasmid

DNA cloning is a molecular biology process to produce numerous identical copies of a DNA fragment of interest (Miles & Wolf, 1989). The DNA fragment is inserted into a plasmid using restriction enzymes to produce a recombinant DNA. The recombinant DNA is then introduced into a laboratory strain of *E. coli* and the bacterium with inserted DNA construct gets selected for (Miles & Wolf, 1989).

3.4.1 PCR amplification of *Pa*GH50A

Recombinant DNA is a construct of plasmid and a DNA fragment. To build the recombinant DNA both plasmid and gene must first be amplified through polymerase chain reaction (PCR).

PCR amplification of DNA is a technique for generating millions of copies of a selected DNA sequence in a short period of time. For DNA synthesis the sample must contain the DNA of interest, Deoxyribonucleotide triphosphate (dNTPs), forward and reverse primer and heat resistant DNA polymerase. The technique is a thermocycling process where the temperature is raised and lowered for denaturation and reannealing of reagents to the DNA sample (Roberts, 2019).

The process follows a thermocycle which is repeated 35 times. Each thermocycle consist of three phases with different temperatures called the following, denaturation, annealing and extending. The first phase is the separation of the double stranded DNA by denaturing the hydrogen bonds between the two strands of DNA (Roberts, 2019). For this the temperature is increased to 95 - 98 ^{o}C for a period of 20 - 30 seconds. The time and temperature in the first phase are depended on the guanine-cytosine concentration and therefore may vary. Guanin (G) and cytosine (C) are bound together by three hydrogen bonds while adenine (A) and tyrosine (T) are bound together by two hydrogen bonds. In the second phase called the annealing step, primers of 15 - 30 nucleotides are hybridized to the separated DNA strands. Primers hybridize upstream of specific DNA fragment towards the 3' end due to DNA being synthesized in the 5' - 3' direction. For each of the complementary strand a different primer is needed for the template DNA. A forward primer that recognizes a sequence located upstream the 5'- 3' strand DNA of interest while a reverse primer binds the upstream complementary 3'- 5' strand of the same DNA fragment. The temperature in this phase is reduced to 50 - 65 ^{o}C for a period of 20 - 40 seconds. The temperature in the second phase depends on at which temperature the primer can hybridize upstream the target DNA. If the temperature is to low the primer won't hybridize to the DNA, on the contrary if the temperature is too high the primer will bind DNA nonspecifically. Ideal annealing temperature is often in a range of 4 - 5 ^{o}C lower than the melting temperature of primers. The third phase, elongation the DNA polymerase binds the hydroxyl group on the 3' end of the primer. The complementary DNA strand is synthesized utilizing free nucleotides dATP, dTTP, dGTP, dCTP to expand the developing DNA strand. The temperature in this phase is raised to 75 - 80 ^{o}C for 2 minutes. The newly synthesized DNA is then used as templates in the next thermocycle and process repeats (Lorenz, 2012) (Powlegde, 2004). The total number of DNA copies after the PCR amplification is finished is equal to 2^{n}. n referring to the number of cycles and each cycle lasting approximately 3 minutes (Kralik & Ricchi, 2017).

Material

Chemicals

- Q5® High-Fidelity 2X master mix
- PA14_GH50_conf_seq_Forward [10 µM]
- PA14_GH50_conf_seq_Reverse [10 µM]

- Ultrapure™ distilled water (Invitrogen)
- pCCI plasmid with *PA14_50830* (5 ng/µL)
- Ice

Equipment and instruments

- Thermocycler, SimpliAMP (Thermo Scientific)
- PCR tubes, 0.2 mL (Axygen)
- Eppendorf tubes, 1.5 mL (Axygen)
- Vortex MS 2 minishaker (IKA®)

Method

Purified pCC1 plasmid with *PA14_50830* from *P. aeruginosa* strain PA14 were provided by my co-supervisor Per Kristian Thorén Edvardsen.

Primer stock solutions were prepared by transferring 20 µL of forward and reverse primer to each their own Eppendorf tube. The samples were diluted with 180 µL of Ultrapure™ distilled water and vortexed. Ultrapure™ distilled water - For/Rev primer solution was prepared by pipetting 190 µL Ultrapure™ distilled water along with 2.0 µL of both reverse and forward primer stock solution to an Eppendorf tube. The samples were kept cool in ice. The PCR samples were prepared in 0.2 mL PCR tubes as described in **Table 3-5**. For insert amplification PCR conditions and settings in **Table 3-6** were applied. Two sample parallels were prepared.

Table 3-5. Reaction scheme for PCR reaction in PCR amplification for PA14_50830.

PCR reagents	Sample concentration	Volume
Q5® High-Fidelity 2X master mix	1X	25 µL
Ultrapure™ distilled water - For/Rev primer solution	0.2 µM	23 µL
Pa14$_{Pa\text{GH50A}}$	5 ng/ µL	2.0 µL
Total	-	50 µL

Table 3-6. PCR conditions and settings for PA14_50830 amplification.

PCR conditions		
Temperature	Time	Cycles
98 ºC	5 minutes	1x
98 ºC	10 seconds	35x
63/ 66/ 68 ºC	30 seconds	
72 ºC	90 seconds	
72 ºC	5 minutes	1x

3.4.2 Isolation of high-copy pNIC-CH plasmid from top 10 *E. coli*.

Isolation and purification of plasmids from bacterial cells is an important step in the cloning process. The first step in plasmid purification is cell lysis, freeing DNA, and other intracellular components (Gupta, 2019). A cell sample is centrifuged to form a cell pellet and the pellet is then completely resuspended in a buffer. The alkaline lysis buffer is then added to the sample turning it blue once all the cells have lysed, raising the pH. The high pH will cause the DNA strands to separate and no longer be able to form base pairs, but still associate with each other. In addition, the high pH will cause proteins to denature and unfold. In the next step cellular components other than plasmid DNA are removed from the sample. The solution is neutralized which results in the double strand plasmid DNA reconstructing base pairs while genomic DNA won't as efficiently form base pairs. This results in genomic DNA, proteins, and lipids to aggregate. The aggregates are insoluble and is removed from the sample (Sasagawa, 2018). The sample now mainly contains plasmid DNA with a few cell contaminants and ions from the buffers. These contaminants are removed by transferring the solution to a spin column with a silica membrane. The silica selectively binds to the DNA using a buffer with high ionic strength and thus the solution can be washed multiple times before eluting the plasmid DNA with low ionic strength (Vandeventer, Mejia, Nadim, Johal, & Niemz, 2013).

Material

Chemicals

- Top 10 *E. coli* with pNIC-CH plasmid
- NucleoSpin® Plasmid/ Plasmid (NoLid) kit (Machrey-Nagel)
- Ultrapure™ distilled water (Invitrogen)
- LB medium
- 50 mg/mL Kanamycin monosulfate

Equipment and instruments

- Cellstar™ Tubes, 15 mL (Greiner Bio-One)
- Nucleospin® plasmid column with a 2 mL collection tube (Machrey-Nagel)
- Eppendorf tubes, 1.5 mL (Axygen)
- Nanodrop™ One (Themo scientific)
- Benchtop centrifuge, Allegra X-30R (Beckmann Coulter)
- Benchtop centrifuge, 5418R (Eppendorf)

Method

5 mL LB medium supplemented with 50 µg/ mL kanamycin monosulfate overnight culture inoculated with Top 10 *E. coli* with pNIC-CH plasmid was prepared as described in section 3.7. Two parallel overnight cultures were prepared.

5 mL overnight culture was transferred to a 15 mL Cellstar™ Tube and centrifuged for 10 minutes at 4225 x g at 4 ^{o}C. Following centrifugation, the supernatant was discarded. The cell pellet was resuspended in 250 µL of A1 buffer by pipetting up and down till the solution had reached homogeny. The resuspended pellet solution was transferred to a 2.0 mL Eppendorf tube. 250 µL of A2 buffer was added and gently mixed by inverting the Eppendorf tube until the sample turned blue. The sample was incubated for 5 minutes at room temperature. 300 µL of buffer A3 was added and mixed by inverting the Eppendorf tube until the sample turned colorless. Sample was centrifuged for 5 minutes at 11,000 x g at room temperature.

750 µL of supernatant that contained the plasmid DNA were transferred to Nucleospin® plasmid column with a 2 mL collection tube. Sample was centrifuged for 1 minute at 11,000 x g and the flow-through was discarded. The rest of the sample was transferred to the same

NucleoSpin® column and centrifuged again for 1 minute at 11,000 x g. 500 µL of AW Buffer was added to the column and sample was centrifuged for 1 minute at 11,000 x g and the flow-through was discarded. 600 µL of A4 buffer A4 was added to the column and centrifuged for 1 minute at 11,000 x g and the flow-through was discarded. The NucleoSpin® column was dry centrifuged for 2 minutes at 11,000 x g and the 2 mL collection tube was replaced with a 1.5 mL Eppendorf tube. To the NucleoSpin® column in an Eppendorf tube 25 µL Ultrapure™ distilled water was added and then incubated for 5 minutes at room temperature. Sample was then centrifuged for 1 minute at 11,000 x g. Two sample parallels were prepared.

Plasmid DNA concentration and purity was measured with Nanodrop™ One as described in section 3.3.

3.4.3 Restriction digestion of pNIC-CH plasmid vector

Restriction enzymes are endodeoxyribonucleases that recognize specific palindromic sequences in the DNA and catalyzes the cleavage of phosphodiester bonds in both DNA strands (Castro-Chavez, 2012). After digestion with restriction enzymes the resulting DNA fragment is linearized and separated from undesired DNA fragments by agarose gel electrophoresis. In a double digestion process two different restriction enzymes are used to linearize the plasmid DNA in a single reaction. The restriction enzymes cleavage sites are located on either side of where the gene will be inserted. Digesting DNA with two restrictions enzymes instead of one makes self-ligation of the vector impossible and makes the gene insertion unidirectional (Jamal-Livani, Nikokar, & Safdari, 2020).

Material

Chemicals

- Purified pNIC-CH plasmid
- Cutsmart® buffer 10x (New England biolabs®)
- Calf intestinal alkaline phosphatase, CIP (New England biolabs®)
- Ultrapure™ distilled water (Invitrogen)
- Restriction enzymes

- Aflii restriction enzyme (New England biolabs®)
- PstI-HF (New England biolabs®)

Equipment and instruments

- ThermoMixer™ C (Eppendorf)
- Eppendorf tubes, 1.5 mL (Thermo Scientific)

Method

The forward and reverse primers used in amplification of *PA14_50830* added restriction sites Aflii and Pstl-HF resulting in sticky ends that are an identical match to the complementary restriction sites on the linearized pNIC-CH plasmid. To generate linearized pNIC-CH plasmid the sample was prepared as described in **Table 3-7**.

Table 3-7. Reaction mixtures for double digestion of pNIC-CH plasmid and controls.

Restriction digestion reagents	End concentration	Sample double digest	Control 1	Control 2
pNIC-CH (109.8 ng/ µL)	1.0 µg	9.1 µL	9.1 µL	9.1 µL
Cutsmart® buffer 10x	1x	5.0 µL	5.0 µL	5.0 µL
Aflii	10 units	1.0 µL	1.0 µL	-
PstI-HF	10 units	1.0 µL	-	1.0 µL
Ultrapure™ distilled water	-	33.9 µL	34.9 µL	34.9 µL
Total	-	50 µL	50 µL	50 µL

Samples were incubated in a ThermoMixer™ C for 2 hours at 37 ^{o}C with 600 rpm agitation. 1 hour and 40 minutes into the reaction process 1 µL calf intestinal alkaline phosphates (CIP) was added. The sample was incubation for an additional 25 minutes at 65 ^{o}C to inactivate the restriction enzymes. Two parallels were prepared from different pNIC-CH samples. pNIC-CH concentration in the secondary sample was measured to be 120.9 ng/ µL.

pNIC-CH plasmid fragments were separated by agarose gel electrophoresis following the method described in section 3.2.1. The DNA band at 5279 bp in the agarose gel represented the linearized pNIC-CH plasmid and was excised and purified as described in section 3.4.4.2.

DNA concentration of purified linearized pNIC-CH was measured with Nanodrop™ One as described in section 3.3.

3.4.4 DNA extraction and purification from agarose gel and PCR clean-up

Nucleospin® Gel and PCR gel Clean-up kit allows for purification of DNA from PCR reactions as well as from agarose gels. The process begins my mixing the sample with binding buffer which allows for the binding of DNA to the silica membrane in the column. Sample contaminants are removed through multiple washing steps with ethanolic washing buffer. The final step elution is achieved through utilizing an alkaline buffer under low salt conditions (Obrador-Sanchez, Tzec-Sima, Higuera-Ciapara, & Canto-Canche, 2017) .

Material

Chemicals

- Nucleospin® Gel and PCR gel Clean-up kit (Machery-Nagel)
- PCR mix with *PA14_50830*
- Agarose gel fragments with linearized plasmid DNA

Equipment and instruments

- Nucleospin® column with a 2 mL collection tube (Machrey-Nagel)
- Eppendorf tubes, 1.5 mL (Thermo Scientific)
- Vortex MS 2 minishaker (IKA®)
- Benchtop centrifuge, 5418R (Eppendorf)
- Nanodrop™ One (Themo scientific)
- Scalpel (Swann Moton)
- Benchtop UV transilluminator (UVP)
- Gel Doc™ EZ imager (Bio-Rad Laboratories)
- Scale (Entris Satorious)
- Vortex MS 2 minishaker (IKA®)

3.4.4.1 PCR cleanup of paGH50A after amplification

Method

45 µL of PCR mixture was transferred to a 1.5 mL Eppendorf tube and 90 µL NTI binding buffer was added. The solution was mixed by vortex. The solution was transferred to a Nucleospin® Gel and PCR gel Clean-up column with a 2 mL collection tube and centrifuged for 30 seconds at 11,000 x g, the flow through was discarded. 700 µL of NT3 wash buffer was added to the NucleoSpin® gel PCR clean-up column and centrifuged for 30 seconds at 11,000 x g, flow through was discarded and sample wash was repeated. To completely remove NT3 wash buffer the sample was dry centrifuged for 1 minute at 11,000 x g. The NucleoSpin gel PCR clean-up column was transferred to a 1.5 mL Eppendorf tube and 20 µL NE elution buffer was added and incubated at room temperature for 1 minute. Then the solution centrifuged for 1 minute at 11,000 x g. Two sample parallels were prepared.

Concentration and purity of *PA14_50830* was measured with Nanodrop™ One as described in section 3.3.

3.4.3.2 Gel extraction of linearized pNIC-CH plasmid

Method

The agarose gel with double digestion pNIC-CH plasmids was placed on a benchtop UV transilluminator coupled to a Gel Doc™ EZ imager. The DNA band at 5279 bp was excised from the gel with a clean scalpel and all excess agarose gel was removed. The gel was transferred to a 1.5 mL Eppendorf tube and weighted. For each 100 mg of agarose gel 200 µL NTI buffer was added. The sample was incubated for 10 minutes at 50 ^{o}C in 2-3 min increment with vortexing in between until the agarose gel had completely dissolved.

The plasmid was then purified in accordance with the Nucleospin® Gel and PCR gel Clean-up method given in section 3.4.4.1. Once purified the plasmid DNA concentration and purity was measured with Nanodrop™ One as described in section 3.3.

3.4.5 Ligation of insert: In-Fusion® Cloning

In-Fusion® cloning is a ligation independent cloning method based on annealing of the complementary ends of the DNA insert and linearized plasmid vector. PCR primers are designed to generate flanking homologous overlaps on either side of the DNA insert. During In-Fusion® the In-Fusion enzyme mixture recombine the DNA insert and the linearized plasmid by generating a single stranded 5' end overhang at the terminals of both reagents. The complementary overhang sites are annealed to create a recombinant circular DNA construct that will be incorporated into an expression vector (Throop & LaBaer, 2015).

Material

Chemicals

- Purified and amplified *PA14_50830* (151.4 ng/ µL and 197.6 ng/ µL)
- Linearized pNIC-CH plasmid (16.8 ng/ µL)
- In-Fusion® HD cloning kit (Takara Bio)
- Ultrapure™ distilled water (Invitrogen)

Equipment and instruments

- ThermoMixer™ C (Eppendorf)
- Eppendorf tubes, 1.5 mL (Thermo Scientific)
- Ice

Method

The following In-Fusion reaction mixtures were prepared as described in **Table 3-8**. The samples were vortexed and incubated in a ThermoMixer™ C for 1 hour at 50 ^{o}C. Once In-Fusion was completed the samples were put on ice until transformation of Top 10 *E. coli* expression vector was performed.

Table 3-8. In-Fusion reaction mixture for recombination of PA14_50830 and linearized pNIC-CH plasmid.

	End concentration for cloning reaction	Cloning reaction	Negative control	Positive control
*Pa*GH50A insert (2274 bp)	40 ng/ µL	2.16 µL	-	-
Control insert (2000 bp)	-	-	-	2 µL
Linearized pNIC-CH plasmid (5279 bp)	100 ng/ µL	5.95 µL	1 µL	-
Linearized pUC19 plasmid (5279 bp)	-	-	-	1 µL
5X In-Fusion HD Enzyme premix	-	2 µL	2 µL	2 µL
Ultrapure™ distilled water	-	-	7 µL	5 µL
Total	-	10.11 µl	10 µL	10 µL

3.4.6 Bacterial transformation and selection of transformed *E. coli*

Transformation is the process of which a recombinant plasmid is introduced into a competent cell. The bacterial cells will then replicate and express the recombinant DNA which can be isolated for downstream applications. The transformation process involves producing competent cells capable of exogenous plasmid DNA uptake. Methods for transformation are chemical transformation and electroporation. During a chemical transformation the competent cells are chemically prepared by undergoing calcium chloride ($CaCl_2$) treatment. The purpose of $CaCl_2$ treatment is to bring the recombinant plasmid in close proximity to the lipopolysaccharides in the cell membrane for uptake. Both the cell membrane and the plasmid are negatively charged and to overcome the repulsion a divalent cation such as Ca^{2+} is used. Ca^{2+} bind both cell membrane and recombinant plasmid thus neutralizing the charges. The calcium bound DNA further aids the recombinant plasmid be absorbed into the competent cell during heat shock. The recombinant plasmid-competent cell mixture is in the next step exposed to a heat shock. The heat shock allows for the recombinant plasmid to enter the cytoplasm of the competent cell (Asif, Mohsin, Tanvir, & Rehman, 2017). In the last step transformed bacterial cells are selected for. For selection the bacteria are plated on selective agar plates that

contains antibiotics. The antibiotic prevents growth of non-resistant competent cells without recombinant plasmid (Samuels, Drecktrah, & Hall, 2017).

Material

Chemicals

- In-Fusion® samples: Cloning reaction, negative and positive control (3.4.5)
- Competent cell kit
  - ONE SHOT™ TOP 10 chemically competent *E. coli* (Invitrogen)
  - ONE SHOT™ BL21 (DE3) chemically competent *E. coli* (Invitrogen)
- LB agar plates supplemented with Ampicillin
- LB agar plates supplemented with 50 µg/ mL Kanamycin monosulfate
- Ultrapure™ distilled water (Invitrogen)
- Ice

Equipment and instruments

- Culture tube, 13 mL (Sarstedt)
- Water bath (Thermo Scientific)
- Microcentrifuge, Ministar (VWR)
- Incubator, static (Termaks)
- Incubator, New Brunswick™ Scientific Innova 44 (Eppendorf)

Method

LB agar plates with ampicillin were provided by my co-supervisor Per Kristian Thorén Edvardsen.

In-Fusion® recombinant plasmid prepared as described in section 3.4.5 were micro-centrifuged to spin down the sample and placed on ice. ONE SHOT™ TOP 10 chemically competent *E. coli* or ONE SHOT™ BL21 (DE3) chemically competent *E. coli* were thawed on ice and the LB agar plates along with S.O.C media were warmed up at room temperature and incubated at 37 ºC.

In a LAF bench 50 µL of competent cells were transferred from cryogenic vials to pre-cooled culture tubes. To one culture tube 5 µL of cloning reaction, to another culture tube 5 µL of negative control and to a third culture tube 5 µL of positive control. The samples were gently mixed by flicking the culture tubes. The samples were incubated on ice for 30 minutes. Following ice incubation, the samples were transferred to a 42 ^{o}C water bath for 45 seconds before being placed back on ice for 2 minutes. 200 µL of S.O.C media was added to the culture tubes and gently mixed before incubating the samples at 37 ^{o}C for 60 minutes with 200 rpm agitation.

After incubation the competent cells with cloning rection were plated in aliquots of 10, 50 and 100 µL on LB agar plates supplemented with 50 µg/ mL kanamycin monosulfate. 100 µL of Negative control were transferred to an LB agar plate supplemented with 50 µg/ mL kanamycin monosulfate while 100 µL of positive control were transferred to a LB agar plate supplemented with ampicillin. The LB agar plates were dried in the LAF bench prior to overnight incubation at 37 ^{o}C. The following day, eleven colonies were selected. Colony PCR confirmation and DNA sequencing were performed as described in section 3.5 and 3.6. From the colonies with incorporated recombinant plasmid glycerol stocks were prepared for long term storage as described in section 3.8.

3.5 Colony PCR for confirmation of the cloning process

Colony PCR is a method for rapidly screening bacterial colonies following transformation and growth on selective media. This to verify that the recombinant plasmid is present in the bacterial colonies or to amplify the plasmid (Jamal, et al., 2017). The process begins by randomly selecting visible colonies from a selective agar medium. The colonies are then transferred to PCR tubes along with a master mix. The samples are run in a thermocycler before being visualized in an agarose gel (Liu, Gerken, & Li, 2014).

Material

Chemicals

- Redtaq DNA polymerase master mix 2x (VWR)
- pNIC-CH Plasmid_Forward [10 µM]
- pNIC-CH Plasmid_Reverse [10 µM]
- Ultrapure™ distilled water (Invitrogen)
- LB agar plates supplemented with 50 µg/ mL kanamycin monosulfate
- Transformed competent cells:
    - ONE SHOT™ TOP 10 chemically competent *E. coli* (Invitrogen)
    - ONE SHOT™ BL21 (DE3) chemically competent *E. coli* (Invitrogen)

Equipment and instruments

- Disposable inoculating loops (Thermo Scientific)
- Eppendorf tubes, 1.5 mL (Axygen)
- Thermocycler, SimpliAMP (Thermo Scientific)
- PCR tubes, 0.2 mL (Axygen)

Method

In a LAF bench 11 colonies of transformed ONE SHOT™ TOP 10 chemically competent *E. coli* or 6 ONE SHOT™ BL21 (DE3) chemically competent *E. coli* were selected for colony PCR.

A bacteria colony were picked using an inoculating loop and transferred to a 1.5 mL Eppendorf tube before being dissolved in 20 µL of sterile Ultrapure™ distilled water. Utilizing the same inoculation loop the remaining bacteria were transferred to a split LB agar plate supplemented with 50 µg/ mL kanamycin monosulfate and numbered.

PCR reaction mixture was prepared as described in **Table 3-9**. Ultrapure™ distilled water was added first, secondly Redtaq master mix and primers and lastly transformed competent cells. The PCR reaction mixtures were run in a Thermocycler following the PCR settings given in **Table 3-10** or **Table 3-11**. Once PCR reaction was complete the reaction mixture was analyzed by agarose gel electrophoresis as described in section 3.2.1.

Table 3-9. PCR reaction mixturees for colony PCR.

Reagents	End concentration	Volume
Redtaq DNA polymerase master mix 2x	1x	12.5 µL
pNIC-CH Plasmid_Forward [10 µM]	0.43 µM	1.0 µL
pNIC-CH Plasmid_Reverse [10 µM]	0.43 µM	1.0 µL
Ultrapure™ distilled water	-	8.5 µL
Transformed competent cells	-	2.0 µL
Total	-	23 µL

Table 3-10. PCR conditions for colony PCR of transformed ONE SHOT É

PCR conditions		
Temperature	Time	Cycles
94 ºC	10 minutes	1x
94 ºC	30 seconds	35x
58 ºC	30 seconds	
72 ºC	150 seconds	
72 ºC	5 minutes	1x

Table 3-11. PCR conditions for colony PCR of transformed ONE SHOT É

PCR conditions		
Temperature	Time	Cycles
98 ºC	10 minutes	1x
98 ºC	10 seconds	35x
63 ºC	30 seconds	
72 ºC	150 seconds	
72 ºC	5 minutes	1x

3.6 DNA sequencing for confirmation of the cloning process

DNA sequencing providers a complete characterization of recombinant DNA and allows for confirmation of DNA insert size, insert orientation, and possible mutation in the catalytic sites. To identify any DNA deviations a reference of the DNA insert is used.

Sanger sequencing technique is a commonly used method for determining the DNA sequence of recombinant plasmids. A primer is bound to the template DNA next to the insert DNA. A DNA polymerase in the presence of free nucleotides (dATP, dTTP, dGTP and dCTP) extends the primer by adding on the complementary nucleotides based on nucleotides in the template strand. To determine composition of a particular DNA sequence a fluorescent dideoxynucleotide (ddNTPs: ddATP, ddTTP, ddGTP and ddCTP) is used. A ddNTP functions as a chain terminator due to it lacking a hydroxyl group on carbon 3 and each time a ddNTP binds to the expanding DNA strand, DNA synthesis ends. This creates DNA fragments of various lengths which can be separated by gel electrophoresis. The various ddNTP have fluorescents markers which can be detected and allow for the nucleotide sequence to be determined (Sanger, Nicklen, & Coulson, 1977).

Material

Chemicals

- pNIC-CH Plasmid_Forward [10 µM]
- pNIC-CH Plasmid_Reverse [10 µM]
- Transformed and selected competent cells:
  - ONE SHOT™ TOP 10 chemically competent *E. coli* (Invitrogen)
  - ONE SHOT™ BL21 (DE3) chemically competent *E. coli* (Invitrogen)
- Ultrapure™ distilled water (Invitrogen)

Equipment and instruments

- Eppendorf tubes, 1.5 mL (Axygen)
- Eurofins Genomics barcodes (Eurofins Genomics)

Method

The DNA samples were prepared as described in **Table 3-12**. The Eppendorf tubes were marked with Eurofins Genomics barcodes. The samples were delivered to a GATC pick up point and sequencing was performed by The LightRun service of Eurofins Genomics.

Sequencing data was analyzed in Jalview version 2 (Waterhouse, Procter, Martin, Clamp, & Barton, 2009) using Muscle algorithm for multiple sequence alignment. Moreover, the sequence chromatogram was used to examine sequence conservation.

Table 3-12. Recombinant DNA samples prepared for sequencing by The LightRun service of Eurofins Genomics. Two samples per colony were prepared, one containing forward primer and the other containing reverse primer.

Reagents	Concentration	For. Primer sample	Rev. Primer sample
pNIC-CH Plasmid_Forward [10 µM]	4.5 µM	5.0 µL	-
pNIC-CH Plasmid_Reverse [10 µM]	4.5 µM	-	5.0 µL
Recombinant plasmid (Stock: 25 ng/ µL)	150 ng	6.0 µL	6.0 µL
Total	-	11 µL	11 µL

3.7 Bacterial overnight cultures

Material

Chemicals

- Glycerol stocks with *E. coli* BL21 cell suspension
- LB agar plates supplemented with 50 µg/ mL kanamycin monosulfate
- 50 mg/ mL Kanamycin monosulfate
- LB medium

Equipment and instruments

- Incubator, New Brunswick™ Scientific Innova 44 (Eppendorf)
- Static incubator (Termaks)
- Sterile Erlenmeyer flask, 100-250 mL
- Culture tubes, 13 mL (Starstedt)
- Inoculation loops (Thermo Scientific)

Method

An inoculation loop was used to pick an inoculum from the glycerol stock with *E. coli* BL21 and with the same inoculation loop the inoculum was streaked out on a LB agar plate supplemented with 50 µg/ mL kanamycin monosulfate. The LB agar plate was incubated for 18 hours at 37 ºC. The following day an overnight culture was prepared.

The size of the Erlenmeyer flask selected for cell cultivation was based on the general rule stating that the growth medium should represent 25 % of the total Erlenmeyer flask volume. For smaller volumes of overnight culture 13 mL culture tubes were utilized. This allowed for adequate aeration. Appropriate volume of sterile LB medium and of 50 mg/ mL Kanamycin monosulfate was added to an Erlenmeyer flask/ culture tube. From the LB agar plate one colony was picked using an inoculation loop and transferred to the LB growth medium supplemented with 50 µg/ mL kanamycin monosulfate. The LB medium was incubated for 18 hours at 37 ºC and 220 rpm agitation.

3.8 Long-term storage of bacteria cultures

Glycerol stocks are cell suspensions meant for long-term storage at -80 ºC. At low temperature ice crystal are formed that can dehydrate and puncture the bacteria. To prevent and reduce such harmful effects bacterial suspensions are stored in a glycerol solution. Glycerol is a cryoprotectant agent that disrupts the formation of ice at low temperature by raising the total concentration of solutes present in a sample. In addition, glycerol forms strong hydrogen bonds with water molecules which out competes water forming hydrogen bonds with other water molecules (Whaley, et al., 2021).

Material

Chemicals

- Bacterial suspensions
- LB medium
- 50 mg/ mL kanamycin monosulfate
- Sterile 85 % glycerol

Equipment and instruments

- Incubator, New Brunswick™ Scientific Innova 44 (Eppendorf)
- Culture tube, 13 mL (Sarstedt)
- Cryogenic tubes, 2 mL (Sarstedt)

Method

Overnight culture with selected transformants were cultivated in 5 mL LB media supplemented with 50 µg/ mL kanamycin and incubated for 18 hours at 37 ^{o}C with 220 rpm agitation. The following day glycerol stocks were prepared by adding 130 µL of sterile 85 % glycerol and 830 µL of cell suspension to a 2 mL cryogenic tube. The glycerol stocks were transferred to an 80 ^{o}C freezer.

3.9 Protein expression in an *E. coli* BL21

Proteins participate in almost all cellular activity and therefore knowledge of proteins is essentials for understanding biological systems. To characterize the function and biochemical properties of proteins they must first be expressed. Ideally the native host organism would be better for expressing the protein, but they are often unsuitable for protein expression for a variety of reasons. To solve this problem, production systems for expressing heterologous proteins have been development. Bacterial protein expression systems are a commonly used due to bacteria being easy to cultivate, reproduce rapidly and scalable. The host organism must fulfill a variety of requirement such as being a genetically tractable, possessing characteristics

of producing recombinant proteins and processing them. The model organism *E. coli* is one of the most used host organisms for heterologous protein expression (Rosano & Ceccarelli, 2014).

3.9.1 Small scale recombinant protein expression in *E. coli* BL21

Before large scale expression of recombinant protein, the expression parameters of *E. coli* BL21 must first be optimized. The recombinant plasmid has an Isopropyl β-D-1-thiogalactopyranoside (IPTG) inducible T7 promoter. IPTG induction is method for regulating protein synthesis. In *E. coli* BL21 without IPTG induction the Lacl repressor binds to the lacO site containing the lac operator sequence. When lacl repressor binds the LacO site it inhibits T7 RNA polymerase from binding to the T7 promoter adjacent to the LacO site and initiating transcription. IPTG is a reagent that mimics inducer allolactose and in the presence of IPTG the T7 RNA polymerase can bind to the T7 promoter by inhibiting Lacl repressor from binding to the LacO site. This leads to synthesis of recombinant proteins (Briand, et al., 2016). Other parameters for heterologous protein expression in *E. coli* BL21 are temperature, growth medium, pH and oxygen levels.

Material

Chemicals

- Growth medium: LB, TB, BHI and M9
- 50 mg/mL kanamycin monosulfate
- 1M IPTG

Equipment and instruments

- Glass tubes, Sterile
- Erlenmeyer flask, 250 mL
- Culture tube, 13 mL (Sarstedt)
- LB agar plates
- Disposable inoculating loops (Thermo Scientific)
- Eppendorf tubes, 1.5 mL (Thermo Scientific)
- Cell density meter, Ultrospec 10 (Biochrom)

- Semi-Micro Cuvette (Brand)
- Benchtop centrifuge, 5418R (Eppendorf)
- Incubator, static (Termaks)
- Incubator, New Brunswick™ Scientific Innova 44 (Eppendorf)

Method

5 mL LB medium supplemented with 50 µg/ mL kanamycin monosulfate overnight culture inoculated with *E. coli* Bl21 transformant was prepared as described in section 3.7. The following day 30 mL of selected growth medium was added to a 250 mL Erlenmeyer flask along with 31 µL of 50 mg/mL kanamycin monosulfate. To the same Erlenmeyer flask 1 mL of overnight culture was added and the culture was incubated for approximately 1 hour and 45 minutes at 37 ^{o}C with 220 rpm agitation. After 1 hour and 45 minutes had passed cell density was measured and OD_{600} determined to be between 0.6 – 0.8. 1 mL of sample was transferred to a 1.5 mL Eppendorf tube and put on ice. The rest of the culture was split into aliquots of 6 mL and transferred to glass tubes. IPTG was added to the samples. Two samples had a final IPTG concentration of 0.2 mM and two samples with a final IPTG concentration of 1 mM. the samples were mixed and 1 mL sample of culture with IPTG concentration 0.2 mM and 1.0 mM were transferred to each their 1.5 mL Eppendorf tube and put on ice. The prepared samples were harvested as described in section 3.10. Two of the cultures were incubated overnight at 20 ^{o}C and two samples were incubated at 37 ^{o}C for 3 hours before taking another 1 mL sample and overnight. The following day 1 mL samples were taken from all the cultures and harvested as described in section 3.10. The samples were analyzed with SDS-PAGE gel electrophoresis as described in section 3.2.2.

3.9.2 Large scale Protein expression in *E. coli* BL21

Once the parameter for recombinant protein expression had been determined. Large scale protein expression was initiated to produce and isolate a greater amount of recombinant protein for characterization studies.

Material

Chemicals

- Growth medium: TB and M9
- 50 mg/mL Kanamycin monosulfate
- 1M IPTG
- Antifoam 204 (Invitrogen)

Equipment and instruments

- Erlenmeyer flask, 250 mL
- 1 L GL-45 threaded glass bottle and sparger lids
- Culture tube, 13 mL (Sarstedt)
- Disposable serological pipettes, 25 mL (VWR)
- Eppendorf tubes, 1.5 mL (Thermo Scientific)
- LB agar plates
- Disposable inoculating loops (Thermo Scientific)
- Eppendorf tubes, 1.5 mL (Thermo Scientific)
- Cell density meter, Ultrospec 10 (Biochrom)
- Semi-Micro Cuvette (Brand)
- Benchtop centrifuge, 5418R (Eppendorf)
- Incubator, static (Termaks)
- Incubator, shaker (Infors HT)
- Lex-48 bioreactor (Epiphyte3)

3.9.2.1 Large scale cultivation in Erlenmeyer flasks

Method

20 mL LB medium supplemented with 50 µg/ mL kanamycin monosulfate overnight culture inoculated with *E. coli* Bl21 transformant was prepared as described in section 3.7. The following day 15 mL of overnight culture was pipette over to a 2 L Erlenmeyer flask containing 500 mL of a selected growth medium, 515 µL of 50 mg/mL kanamycin monosulfate and 150 µL of Antifoam 204. The culture media was incubated at 37 ^{o}C with 220 rpm agitation until an

OD_{600} of 0.6 – 0.8 had been reached. 1 mL of culture was transferred to a 1.5 mL Eppendorf tube before adding 514 µL of 1 M of IPTG such that the final concentration was 1 mM IPTG in the culture medium. The culture medium was mixed, and another 1 mL of culture was taken and put on ice. The 1 mL samples were harvested as described in section 3.10. The culture medium was incubated for a total of 18 hours at 37 ^{o}C with 220 rpm agitation. The following day the cell culture was harvested as described in section 3.10 and purified using immobilized metal affinity chromatography (IMAC) as described in section 3.11.

3.9.2.2 Large cultivation in Lex-48 bioreactor

Lex-48 bioreactor system is an alternative method for cultivating bacteria. The system allows for agitation and aeration throughout the medium by directing filtrated and compressed air through a sparger into the culture. The culture bottles are immersed into a temperature-controlled water bath to maintain optimal cell growth conditions (Isopencu, Tanase, Joseceanu, & Lavric, 2014).

Method

20 mL LB medium supplemented with 50 µg/ mL kanamycin monosulfate overnight culture inoculated with Bl21 transformant was prepared as described in section 3.7. The following day, to a 1 L sterile GL-45 bottle 500 mL of selected growth medium, 515 µL of 50 mg/mL kanamycin monosulfate, 150 µL of Antifoam 204 and 15 mL of overnight culture. Sparger lids were placed on the glass bottles and transferred from the LAF bench to a laminar flow water bath in the Lex-48 bioreactor system. The temperature was set to 37 ^{o}C and the sparger lid was loosened before turning on a moderate air flow. The culture medium was incubated in the bioreactor until an OD_{600} of 0.6 – 0.8 had been reached. 1 mL sample was taken from the culture before adding 514 µL of 1 M IPTG such that the final concentration was 1 mM IPTG in the culture medium. Culture medium was mixed, and another 1 mL sample was taken and transferred to a 1.5 mL Eppendorf tube and put on ice. The 1 mL samples were harvested as described in section 3.10. The culture medium was placed back in the Lex-48 bioreactor water bath and incubated for a total of 18 hours at 37 ^{o}C and moderate aeration. The following day,

the cell culture was harvested as described in section 3.10 and purified using IMAC as described in section 3.11.

3.10 Protein extraction from the cytoplasm and periplasm

Proteins are large complex biomolecules that are essential for physiological processes (Watford & Wu, 2018). Initially, protein extraction involves mechanical disruption of the cells by applying force such as sonication. In addition, for extraction of intracellular proteins chemical detergents are often used to disrupt the outer cell membrane. Protease inhibitors are added to the protein extract to prevent loss of protein due to proteolysis (Structural Genomics Consortium, et al., 2008).

Protein extraction happens in several steps due to the heterogeneity of cell cultures. The first step involves separating the selected growth medium from the cells. This is done by applying a centrifugal force field and separating the sample according to particle density. The process continues with adding chemical buffers that allows for degradation of undesirable DNA, proteins, etc. (Trabbic-Carlson, Liu, Kim, & Chilkoti, 2004). At this step depending on whether the recombinant protein is isolated from the cytoplasm or periplasm, cell suspension can undergo the following processes. Either be mechanically homogenized with sonication (cytoplasmic extraction) or extracted with specific buffers (periplasmic extraction). In the end, the crude protein extract contains the recombinant protein along with other proteins isolate from the same location (Latifi, Khajeh, Farnoosh, Hassanpour, & Khodi, 2015) .

3.10.1 Extraction of cytosolic proteins

For extraction of cytosolic proteins an important step is cell lysis by sonification. Sonication is process of disrupting the cell membrane to either introduce compounds into the cytoplasm or extract certain compounds. For this process ultra-sonic soundwaves are utilized. The cell membrane is composed of a bilayer of phospholipids and associated proteins (Casares, Escriba, & Rossello, 2019). A large sonic pressure at a specific point in the cell membrane is applied creating a cavitation bubble. Through this pore compounds can be introduced into the cells without causing cell apoptosis. As the sonic pressure is increased over time the size of the pore

expands to a point of cell implosion. This causes the cell to lyse, and all its contents to spill into the buffer solution (Karthikesh & Yang, 2021).

Material

Chemicals

- Cell suspension
- IMAC binding buffer
- Complete™ Mini EDTA free protease inhibitor cocktail tablets (Roche)
- 1% Triton X-100 PBS solution
- Lysozyme, 100 mg/ mL
- Dnase 1 (NEB)
- ddH_2O
- ice

Equipment and instruments

- Syringe, 60 mL
- CellStar® tubes, 50 mL (Greiner Bio-One)
- Stericup®, 0.22 µm (Merck)
- Eppendorf tubes, 1.5 mL (Thermo Scientific)
- Centrifugal bottle, 50 mL, 1 L (Thermo Scientific)
- Benchtop centrifuge 5418R (Eppendorf)
- Centrifuge Avanti J25-S (Beckmann Coulter)
- Centrifuge, Sorvall lynx 4000 (Thermo Scientific)
- Beaker, 100 and 250 mL
- Vibra Cell (Sonics)

3.10.1.1 Small scale cytoplasmic harvesting

Method

1 mL samples taken from cell suspensions described in section 3.9 were centrifuged for 10 minutes at 16.900 g at 4 ^{o}C and supernatant was discarded. The harvested cell pellets were resuspended in 196 µL of PBS + 1% Triton X-100 and 4 µL of Complete™ Mini EDTA free protease inhibitor solution (Complete™ Mini EDTA free protease inhibitor dissolved in 2 mL ddH_2O). The samples were kept on ice. Prior to sonication of each sample the sonication probe was cleaned with 70 % ethanol. Each sample for sonication were transferred to a 100 mL beaker with ice and the sonication probe was submerged approximately 1 cm into the 1.5 mL Eppendorf tube. Each sample were sonicated in five rounds with 5 seconds on and 5 seconds off sonication and an amplitude of 27 %. The samples were centrifuged for 10 minutes at 16.900 g at 4 ^{o}C. Samples were analyzed by SDS-PAGE gel electrophoresis as described in section 3.2.2.

3.10.1.2 Large scale cytoplasmic harvesting

500 mL cell suspension was harvested by transferring the solution to a 1 L centrifugal flask and filling the flask to the 1 L mark with ddH_2O. The cells were harvested using a JA-10 rotor for 15 minutes at 7500 rpm at 4 ^{o}C. The supernatant was discarded, and the cell pellet was resuspended in 30 mL ice cold IMAC binding buffer supplemented with three Complete™ Mini EDTA free protease inhibitor cocktail tablets (final concentration of 1 cocktail tablet per 10 mL solution). The cell pellet was resuspended using a 60 mL syringe and the resuspended solution was transferred to a 50 mL CellStar® tube. To the solution 3 µL DNase 1 and 30 µL of 100 mg/ mL lysozyme was added. The mixture was incubated on ice for 30 minutes with shaking every 10 minutes. After 30 minutes, sonication was performed for 10 minutes with 5 seconds on and 5 seconds off at an amplitude of 30 %. Prior to sonication the sonication probe was cleaned with 70 % ethanol and submerged into the 50 mL CellStar® tube in a 250 mL beaker with ice. The cell lysate was transferred to a 50 mL centrifugal bottle and centrifuged using a JA-25.50 rotor for 30 minutes at 30 000 rpm at 4 ^{o}C. The crude cytoplasmic extract was filtered through a 0.22 µm Stericup® to remove cell debris and DNA contaminates. The protein extract was stored at 4 ^{o}C until purification, performed as described in section 3.11.

3.10.2 Extraction of periplasmic proteins

Extraction of recombinant protein from the periplasm utilizes osmotic shock to disrupt the outer cell membrane in Gram negative *E. coli*. The outer membrane is made of a thin layer of peptidoglycan which is vulnerable to osmotic pressure. The disintegration of the outer membrane happens by either physical force e.g., heat or osmotic pressure or by using chemical reagents. Osmotic shock relies on the principle of osmosis in which water moves across a semi permeable outer membrane to an area with low concentration of water. The cell pellet resuspended in cold water before incubating it for 45 seconds with dilute $MgCl_2$ causes the membrane permeability to change as the outer membrane perforation occurs (Schimek, et al., 2020).

Material

Chemicals

- Cell suspension
- Spheroplast buffer
- PMSF, 50 mM
- $MgCl_2$, 20 mM
- Complete™ Mini EDTA free protease inhibitor cocktail tablets (Roche)
- Ice cold ddH_2O
- ice

Equipment and instruments

- Syringe 5 mL and 60 mL (BD plastpak)
- Disposable injection needle
- CellStar® tubes, 15 and 50 mL (Greiner Bio-One)
- Stericup®, 0.22 µm (Merck)
- Eppendorf tubes, 1.5 mL (Thermo Scientific)
- Centrifugal bottle, 50 mL, 1 L (Thermo Scientific)
- Vortex MS 2 minishaker (IKA®)
- Benchtop centrifuge 5418R (Eppendorf)

- ¶ Centrifuge Avanti J25-S (Beckmann Coulter)
- ¶ Centrifuge, Sorvall lynx 4000 (Thermo Scientific)

3.10.2.1 Smale scale periplasmic harvesting

Metode

1 mL samples taken from cell suspensions described in section 3.9 were centrifuged for 10 minutes at 16.900 g at 4 ^{o}C and the supernatant was discarded. The harvested cell pellets were resuspended in 100 µL spheroplast-PMSF solution (prepared by mixing 3 mL Spheroplast buffer and 6 µL of 50 mM PMSF). The samples were vortexed and centrifuged for 20 minutes at 7500 rpm at 4 ^{o}C. The supernatant was discarded, and the samples were incubated at room temperature for 30 minutes. Post incubation cell pellets were resuspended in 96 µL cold ddH_2O supplemented with 4 µL of Complete™ Mini EDTA free protease inhibitor solution (Complete™ Mini EDTA free protease inhibitor dissolved in 2 mL ddH_2O). The samples were incubated on ice for 45 seconds before 5 µL of 20 mM $MgCl_2$ was added to a final concentration of 1 mM $MgCl_2$. The resuspended samples were vortexed and centrifuged for 15 minutes at 16.900 g at 4 ^{o}C. Samples were analyzed by SDS-PAGE gel electrophoresis as described in section 3.2.2.

3.10.2.2 Large scale periplasmic harvesting

Method

500 mL cell suspension was harvested by transferring the solution to a 1 L centrifugal flask and filling the flask to the 1 L mark with ddH_2O. The cells were harvested using a JA-10 rotor for 15 minutes at 7500 rpm at 4 ^{o}C. The supernatant was discarded, and the cell pellet was resuspended in 30 mL Spheroplast-PMSF solution (prepared by mixing 30 mL Spheroplast buffer and 60 µL of 50 mM PMSF). The cell pellet was resuspended using a 60 mL syringe and then transferred to a 50 mL centrifugal flask. The cell suspension was centrifuged using a JA-25.50 rotor for 20 minutes at 7500 rpm at 4 ^{o}C. The supernatant was discarded, and the cell pellet was incubated at room temperature for 30 minutes. After incubation the cell pellet was

resuspended in 30 mL ice cold ddH_2O supplemented with three Complete™ Mini EDTA free protease inhibitor cocktail tablets (final concentration of 1 cocktail tablet per 10 mL solution) using a 5 mL syringe with injection needle. Once cells were resuspended the sample was incubated on ice for 45 seconds and 1.5 mL of 20 mM $MgCl_2$ was added to a final concentration of 1 mM $MgCl_2$. The cell suspension was centrifuged using a JA-25.50 rotor for 15 minutes at 20 000 rpm at 4 ^oC. The crude periplasmic extract was filtered through a 0.22 µm Stericup® to remove cell debris and DNA contaminates. To the 30 mL sterile extract 600 µL of 50 mM PMSF was added such that final concentration was 1 mM. The protein extract was stored at 4 ^oC until purification, performed as described in section 3.11.

3.11 Purification method

3.11.1 Immobilized metal affinity chromatography (IMAC)

Immobilized metal affinity chromatography (IMAC) is a method for purification of recombinant protein. The protein target is designed with an oligo histidine fusion tag at the C-terminal that creates an affinity with the ligand (Kaur & Reinhardt, 2012). The principle of IMAC is based on interactions between the lone electron pairs of nitrogen or oxygen in the amino acids side chains and the immobilized metal ions in the stationary phase. Certain amino acids such as histidine and cysteine form complexes with chelated metals at a neutral pH. HisTrap™ HP column is packed with Ni Sepharose high performance (HP) affinity resin. While the His-tag allows for strong interaction with the stationary phase other proteins in the extract will either not bind to the resin or binding weakly. Imidazole in the IMAC buffers competes with the his-tag for binding to the stationary phase. The IMAC binding buffer and IMAC washing buffer have a very low concentration of imidazole and disrupts binding of weakling bonded proteins to the HisTrap™ HP Column. The recombinant protein with His-tag gets eluted by an IMAC elution buffer with a high imidazole concentration (Riguero , et al., 2020).

Material

Chemicals

- Cytosolic or periplasmic protein extract.
- IMAC binding buffer
- IMAC washing buffer
- IMAC elution buffer
- 20 % ethanol
- ddH_2O

Equipment and instruments

- CellStar® tubes, 50 mL (Greiner Bio-One)
- HisTrap™ HP 5 mL column (GE Healthcare)
- Äkta Pure (GE Healthcare)

Method

Protein purification was performed manually with a flow rate of 2 mL/ min and pressure below or at 0.4 MPa. Äkta Pure along with the HisTrap™ HP 5 mL column was stored in 20 % ethanol solution. Therefore prior to purification the system tubes S2 and A1 was washed with sterile ddH_2O. The system was then flushed with 5 column volumes of ddH_2O to prevent interactions between IMAC buffers and ethanol. The flow rate was reduced to 0.4 mL/ min before inserting the HisTrap™ HP 5 mL column into the column space in Äkta Pure. The flowrate was increased to 2 mL/ min and the column was flushed with 5 column volumes of IMAC binding buffer. Before applying the protein extract the UV detector was autozeroed. The extract was loaded into the column using the S2 inlet and applicator pump. After sample application, sample tube was flushed with IMAC binding buffer until the UV signal had decreased slightly. The flow through fraction was collected in a 50 mL CellStar® tube. IMAC washing buffer was introduced into the column through the A1 pump. The wash fraction was collected in a 50 mL CellStar® tube. Once UV signal had stabilized IMAC elution buffer was introduced into the column. From the moment the UV signal started to increase the elution fraction was collected in a 50 mL CellStar® tube until the UV signal had stabilized. After purification was completed the system tubing and column was first flushed with 5 column volumes of ddH_2O and secondly 5 column volumes of 20 % ethanol. The flow rate was decreased to 0.5 mL/ min to remove the HisTrap™ HP 5 mL column and the Äkta Pure instrument was shot down.

During purification flowthrough, wash and elution was collected. These samples were analyzed by SDS-PAGE gel electrophoresis as described in section 3.2.2 Followed by buffer exchange as described in section 3.12.

3.12 Buffer exchange

3.12.1 Diafiltration

Diafiltration is technique in which a solution is forced through is semi permeable membrane that separates macromolecules from compounds with low molecular weight. Macromolecules with a higher mass then the molecular weight cut off (MWCO) will remain in the reservoir compartment of the centrifugal concentrator. During diafiltration both the solvent and the low molecular weight solutes are eluted through the membrane filter and the solutes with higher mass than the MWCO become concentrated (Loewe, Dieken, Grein, Salzig, & Czermak, 2018).

Material

Chemicals

- Purified protein sample
- Tris-HCl pH 7.5, 20 mM

Equipment and instruments

- Vivaspin 20 centrifugal concentrator 10K MWCO (Sartorius)
- Syringe, 1 mL (BD Plastipak)
- Filter, 0.22 µm (BD Plastipak)
- Disposable injection needle (BD Plastipak)
- Benchtop centrifuge, Allegra X-30R (Beckmann Coulter)

Method

The protein sample was loaded into the reservoir compartment of the Vivaspin centrifugal concentrator, and the volume was adjusted to 20 mL with exchange buffer 20 mM Tris-HCl pH 7.5. The sample was centrifuged for 22 minutes at 4255 g at 4 ^{o}C or until the sample volume equaled 500 µL. This process was repeated four times, once to concentrate the protein solution and three for the buffer exchange process. Once the buffer exchange was completed the 500 µL sample was diluted to 1 mL with exchange buffer. The protein sample was sterilized using a 1 mL syringe with 0.22 µm filter and the protein concentration was determined as described in section 3.13.1.

3.12.2 Dialysis

Dialysis is a passive separation technique that facilitates the removal of micro-molecules from a solution by diffusion through a semi-permeable membrane. The dialysate is transferred to dialysis cassette with pore sizes in the membrane determined by the MWCO value. The cassette with dialysate is placed in a buffer solution with a volume 500-1000 times greater than the dialysate volume. Low molecular weight compounds diffuse though the cassette membrane and into the buffer solution while macromolecules with greater mass than the MWCO will remain in the cassette. Dialysis is a slow process that usually last 24 hours and the buffer solution is exchanged twice to avoid contaminates diffusing back into the dialysate (Phillips, 1995).

Material

Chemicals

- Purified protein sample
- Tris-HCl pH 7.5, 20 mM

Equipment and instruments

- Beaker, 1 L
- Vivaspin 20 centrifugal concentrator 10K MWCO (Sartorius)
- Syringe, 2 and 1 mL (BD Plastipak)
- Filter, 0.22 µm

- Disposable injection needle
- Slide-A-Lyzer® Dialysis Cassette 10K MWCO (Thermo Scientific)
- Benchtop centrifuge, Allegra X-30R (Beckmann Coulter)
- Magnet stirrer RCT basic (IKA)

Method

The protein sample was concentrated as described in section 3.12.1. The 1 mL dialysate was transferred to a Slide-A-Lyzer® dialysis cassette by injecting the dialysate through the gasket via one of the injection ports. Prior to removing the injection needle from the gasket, excess air was withdrawn. A float buoy was attached to the cassette before submerging it into 1 L of 20 mM Tris-HCl buffer. The buffer solution was mixed using a magnet stirrer and covered with aluminum foil to avoid contamination. Dialysis was performed in a cool room. Three hours into the dialysis process the buffer was exchanged with new batch of 20 mM Tris-HCl pH 7.5, and this was repeated after six hours. 24 hours later the sample was withdrawn from the cassette using a 2 mL syringe. The protein sample was sterilized using a 1 mL syringe with 0.22 µm filter. The protein concentration was determined as described in section 3.13.1.

3.13 Protein concentration determination

3.13.1 Spectrophotometric quantification of protein

Spectrophotometric quantification of protein is depended on the aromatic residue content.. The aromatic amino acids are tryptophan, tyrosine and phenylalanine and these residues exhibit strong UV light absorption at 280 nm. Tryptophan residues have the highest UV absorption at 280 nm followed by tyrosine. While phenylalanine UV absorption at 280 nm is negligible along with disulfide bonded cysteines. Protein is quantified by measuring the absorbance of tryptophan and tyrosine at 280 nm and thus determine the total amount of protein in a sample by using the Beer-Lambert law. Beer-Lamberts law defines the dependence of the UV

absorption on its extinction coefficient, concentration, and the lights pathlength (Anthis & Clore, 2013).

ö سي آ ώ ّ ü ά (2)

- A: Absorbance at 280 nm
- ε: Extinction coefficient (M^{-1} cm^{-1})
- c: Protein concentration (mg/ mL)
- L: Optical pathlength (cm)
- Mm: Molecular weight of protein (Da)

Proteins and peptides have distinct extinction coefficient. The theoretical extinction coefficient can be determined by inputting the amino acid sequence without signal peptide into Protparam bioinformatics tool supplied by Expasy (Gasteiger, et al., 2005).

Material

Chemicals

- Protein sample
- Tris-HCl pH 7.5, 20 mM
- ddH_2O

Equipment and instruments

- BioPhotometer D30 (Eppendorf)
- µCuvette® (Eppendorf)
- Lens tissue paper
- Vortex MS 2 minishaker (IKA®)

Method

µCuvette® was cleaned with ddH_2O and wiped with lens tissue paper. 20 mM of Tris-HCl pH 7.5 buffer was vortexed and 2 µL was pipetted onto the sample holder before closing the

µCuvette® creating an optical pathlength of 1 mm. After blanking the BioPhotometer the µCuvette® was cleaned using ddH_2O and wiped with lens tissue paper. 2 µL of 5x diluted protein sample was placed within the sample holder before closing the µCuvette® and sample absorbance was measured at 280 nm. Three sample parallels were measured to get an accurate representation of protein concentration. Concentration was calculated using equation 2.

3.13.2 Bradford protein assay

Bradford assay is technique for protein quantification. It utilizes the colorimetric properties of a specific dye to determine the total protein content in a buffer solution. The dye used in this assay is Coomassie brilliant blue G-250 and at low pH this reagent becomes protonated and forms a blue color complex. In an acidic environment Coomassie brilliant blue G-250 disrupts the native protein structure exposing the amino acid side chains by donating its free electrons to ionizable amino acids such as arginine and lysine. This exposes the hydrophobic amino acids residues which binds non covalently to the non-polar region of Coomassie brilliant blue G-250 forming a protein-dye complex with a blue color. The formation of the protein-dye complex shifts the UV absorption to 595 nm. Protein is quantified by measuring absorbance at 595 nm (Brady & Macnaughtan, 2015). The protein concentration was calculated using equation 3 and 4.

(3)

(4)

- DF: Protein dilution factor
- $V_{measured\ ample}$: Volume of protein in measured sample
- V_{ddH2O}: Volume of ddH_2O in measured sample
- $C_{measured\ sample}$: Concentration of protein in measured sample
- $C_{protein\ sample}$: Concentration of protein

Material

Chemicals

- Protein sample
- Bio Rad protein assay (Bio-Rad Laboratories)
- Ultrapure™ distilled water (Invitrogen)
- ddH_2O

Equipment and instruments

- BioPhotometer D30 (Eppendorf)
- Vortex MS 2 minishaker (IKA®)
- Micro cuvettes (Eppendorf)
- Eppendorf tubes, 1.5 mL (Thermo Scientific)
- Lens tissue paper

Method

Bradford protein assay sample was prepared following the reaction scheme in **Table 3-13**. To the 1.5 mL Eppendorf tube, Ultrapure™ distilled water and protein was added prior to the Bio Rad protein assay solution. A triplicate of the measured sample was prepared. The Bradford samples was vortexed to ensure colorimetrical homogeny followed by 5 minute incubation at room temperature. The sample was diluted 10x such that the concentration could be measured at 595 nm. Sample concentration was quantified using a Bradford protein assay software program on the BioPhotometer D30. The BioPhotometer was blanked prior to measuring the triplicates at 595 nm. The triplicates were averaged, corrected for the 10x dilution factor before concentration was calculated using equation 3 and 4.

Table 3-13. Reaction scheme for quantification of protein using the Bradford protein assay.

Reagents	Blank	Measured sample
Ultrapure™ distilled water	800 µL	795 µL
Protein sample	-	5 µL
Bio Rad protein assay	200 µL	200 µL

3.14 Enzyme activity assay

3.14.1 3,5-dinitrosalicylic acid (DNSA) activity assay

3,5-dinitrosalicylic acid (DNSA) method is a method for rapid estimation of reducing sugars in a solution. Reducing sugars are characterized by having a free aldehyde or a free ketone group bound. DNSA detects reducing sugars liberated by enzymes with hydrolase activity. During this reaction DNSA is reduced to 3-amino-5-nitrosalicyclic acid (ANSA) at 100 ^{o}C. In an alkaline environment ANSA has an orange-brown color. With the increase in concentration of reducing sugars in a sample the orange pigment intensifies. The OD for samples treated with DNSA is 540 nm (Gusakov, Kondratyeva, & Sinitsyn, 2011).

Material

Chemicals

- *Pa*GH50A
- Substrates
  - Lichenin, 30 mg/ mL (Megazyme)
  - Curdlan, 30 mg/ mL (Megazyme)
- Buffers with various pH
  - Tris-HCl buffer pH 7.5 and 8.5, 20 mM
  - Bis-tris buffer pH 6.5, 20 mM
  - Citrate buffer pH 4.0, 20 mM
- Positive control
  - Celluclast® (Novozyme)
  - Citrate phosphate buffer pH 5.4, 20 mM

- Avicel cellulose, 30 mg/ mL

¶ 3,5-Dinotrosalicylic acid (DNSA) reagent, 2x

¶ Ice

Equipment and instruments

¶ Eppendorf tubes, 1.5 and 2 mL (Thermo Scientific)

¶ 96-Well Polystyrene Microwell plate (Sarstedt)

¶ Plate reader, VarioSkan Lux (Therno Scientific)

¶ Vortex MS 2 minishaker (IKA®)

¶ ThermoMixer™ C (Eppendorf)

¶ Benchtop centrifuge 5418R (Eppendorf)

¶ Boiling water bath, SBB Aqua 5 plus (Grant)

¶ Membrane dry vacuum pump/ compressor, VCP 80 (VWR)

¶ Multiscreen®HTS 96-Well Plates, 0.45 µm Durapore® (Merck Millipore)

Method

DNSA reaction mixtures were prepared by mixing different reagents as shown in in **Table 3-14**. To an Eppendorf tube selected buffer was added first before adding *Pa*GH50A and substrate due to the viscosity of the substrates. The reaction mixtures were vortexed and incubated in ThermoMixer™ C for a 24 hour period at 37 ^{o}C with 700 rpm agitation. After 15 min, 30 min, 45 min, 60 min, 6 h and 24 h, 50 µL aliquots were withdrawn from the reaction. The reaction was stopped by incubating the samples in a water bath at 100 ^{o}C for 5 minutes followed by adding 100 µL of DNSA reagent. Samples were returned to the water bath at 100 ^{o}C for 15 minutes. The samples were kept on ice until their cooled to room temperature. 150 µL of the samples were transferred to Multiscreen®HTS 96-Well Plates, 0.45 µm Durapore® and filtered in a Membrane dry vacuum pump/ compressor, VCP 80. 100 µL of samples was transferred to a 96-Well Polystyrene Microwell plate. OD was measured at 540 nm.

Table 3-14. Reaction scheme for analysis of PaGH50A activity using DNSA method.

Reagents	End concentration	Volume
Substrate	5. 4 mg/ mL	72 µL
*Pa*GH50A	5.9 µM	160 µL
Buffer	8.4 mM	168 µL
Total volume	-	400 µL

Table 3-15. Reaction scheme for analysis of positive control using DNSA method.

Reagents	End concentration	Volume
Avicel cellulose	3.0 mg/ mL	40 µL
Celluclast® Cellulase	16,89 µg/ mL	0.8 µL
Citrate phosphate buffer pH 5.4	8.4 mM	199 µL
Total volume	-	400 µL

3.14.2 3-methyl-2-benzothiazolinone hydrazone (MBTH) activity assay

3-methyl-2-benzothiazolinone hydrazone (MBTH) method is an alternative method to DNSA for quantification of total reducing sugar (Horn & Eijsink, 2003). The reaction between the reducing sugars and MBTH is a two-step process. In the first step the aldehyde group of glucose condenses with a single MBTH molecule to form an abduct and the secondary step occurs at a low pH and in this step the abduct reacts with a second MBTH molecule to create a colored product with an OD of 620 nm (Anthon & Barrett, 2002).

Material

Chemicals

- *Pa*GH50A
- Substrate
  - Purified Psl, pH 7.5
- Buffers with various pH

- Tris-HCl buffer pH 7.5 and 8.5, 20 mM
- Bis-tris buffer pH 6.5, 20 mM
- Citrate buffer pH 4.0, 20 mM

¶ Positive control
- Celluclast® (Novozyme)
- Citrate phosphate buffer pH 5.4, 20 mM
- Avicel cellulose, 30 mg/ mL

¶ Ultrapure™ distilled water (Invitrogen)

¶ MBTH, 3 mg/mL

¶ DTT, 1 mg/mL

¶ $(FeNH_4(SO_4)_2) \cdot 12H_2O$, 2 %

¶ Sulfamic acid, 2 %

¶ HCl, 1 M

¶ NaOH, 0.5 M

¶ Ice

Equipment and instruments

¶ Eppendorf tubes, 1.5 and 2 mL (Thermo Scientific)

¶ CellStar® tubes, 50 mL (Greiner Bio-One)

¶ Disposable serological pipettes, 5 mL (VWR)

¶ 96-Well Polystyrene Microwell plate (Sarstedt)

¶ Plate reader, VarioSkan Lux (Therno Scientific)

¶ Vortex MS 2 minishaker (IKA®)

¶ Membrane dry vacuum pump/ compressor, VCP 80 (VWR)

¶ Multiscreen®HTS 96-Well Plates, 0.45 µm Durapore® (Merck Millipore)

¶ ThermoMixer™ C (Eppendorf)

Method

MBTH reagent was prepared before use by transferring equal volumes of 3 mg/mL MBTH and 1 mg/mL DTT. The acidic solution was prepared by pipetting 2.5 mL of 2 % $F(FeNH_4(SO_4)_2) \cdot 12H_2O$, 2.5 mL of 2 % sulfamic acid, 2.5 mL of HCl and 2.5 mL of Ultrapure™ distilled water to a 15 mL CellStar® tubes.

Reaction mixtures were prepared by mixing different reagents as shown in in **Table 3-16** and **Table 3-15** (section 3.14.1). To a 1.5 mL Eppendorf tube, selected buffer was added prior to adding purified Psl pH 7.5 and *Pa*GH50A. The reaction mixtures were vortexed and incubated in ThermoMixer™ C for a 24 hour period at 37 ^{o}C with 700 rpm agitation. After 15 min, 30 min, 45 min, 60 min, 6 h and 24 h, 50 µL aliquots were withdrawn from the reaction. The reaction was stopped by adding 50 µL of 0.5 M NaOH and 50 µL of 1:1 (v/v) 1 mg/ mL DTT: 3 mg/ mL MBTH. Samples were then incubated in a ThermoMixer™ C for 15 minutes at 80 ^{o}C with 700 rpm agitation. Immediately after removal from the ThermoMixer™ C 100 µL of a solution containing 0.5 % $F(FeNH_4(SO_4)_2) \cdot 12H_2O$, 0.5 % sulfamic acid and 0.25 M HCl was added to the samples. The samples were inverted a few times for homogenization and kept on ice until the samples cooled to room temperature. 250 µL of the samples were transferred to Multiscreen®HTS 96-Well Plates, 0.45 µm Durapore® and filtered in a Membrane dry vacuum pump/ compressor, VCP 80. 150 µL of samples was transferred to a 96-Well Polystyrene Microwell plate and OD was measured at 620 nm.

Table 3-16. Reaction scheme for analysis of PaGH50A activity using MBTH method

Reagents	End concentration	Volume
Purified Psl pH 7.5	-	160 µL
*Pa*GH50A	5.9 µM	160 µL
Buffer	8.4 mM	80 µL
Total volume	-	400 µL

3.14.3 MALDI-TOF MS

Matrix-assisted laser desorption-ionization time of flight mass spectrometry (MALDI-TOF MS) is an analytical technique where molecules are separated according to their mass-to-charge ratio (m/z). The MALDI-TOF MS data are exhibited as a mass spectrum with m/z represented on the x-axis and signal intensity along the y-axis (Singhal, Kumar, Kanaujia, & Virdi, 2015).

The MALDI-TOF MS process is divided into two phases. In the first phase ionization of macromolecules-matrix sample fixed in a crystalline matrix occurs. During ionization the sample is bombarded by a laser that releases the sample molecules from the plate. The sample

molecules are vaporized while simultaneously being ionized. High voltage is applied to the vacuum chamber accelerating the charged molecules through an electric field. In the second phase referred to as the time-of-flight mass spectrometry (TOF MS) phase. The molecules travel linearly towards a detector after ionization. Higher mass molecules arrive later than molecules with lesser mass. Flight time allows for determination of mass and each peak along the x-axis in a mass spectrum corresponds to a specific molecule (Lai & Wang, 2017).

Material

Chemicals

- β-glucan samples
- 2.5-Dihydroxybenzoic acid (DHB, Bruker)
- Standard with chitin oligomer 1-6

Equipment and instruments

- Eppendorf tubes, 1.5 mL (Thermo Scientific)
- Vortex MS 2 minishaker (IKA®)
- Microcentrifuge, Ministar (VWR)
- ThermoMixer™ C (Eppendorf)
- Ultraflextreme MALDI-TOF MS (Bruker)
- MTP 384 ground steel BC MALDI-TOF MS target plate (Bruker)
- MTP Target Frame III (Bruker)
- Hair dryer (Solis)

Method

Reaction mixtures were prepared following the procedure described in section 3.14.1 **Table 3-14** and **Table 3-15** and section 3.14.2 **Table 3-16**. 1 μL of β-glucan sample was transferred to a PCR tube cap and mixed with 1 μL of DHB matrix by pipetting up and down. 1 μL β-glucan sample-DHB mixture was transferred to an MTP 384 ground steel BC MALDI-TOF MS target plate. The spot was dried with a hair dryer till a crystalline structure was formed. The MTP 384 ground steel BC MALDI-TOF MS target plate with sample was fitted on an MTP Target Frame III and placed into the Ultraflextreme MALDI-TOF MS instrument.

The laser intensity utilized was at 85 % with a 2000 frequency. The instrument was calibrated with standard of chitin oligomers. The mass spectrum for each sample was created by taking the sum of ten mass spectra. The mass spectra were saved prior to opening them in an analysis software where the mass peaks were automatedly annotated.

3.15 Quantification of oligosaccharide products with HPLC

High performance liquid chromatography (HPLC) is a high-resolution analytical technique for separation, identification, and quantification of components in a sample. The mobile phase is comprised of aqueous buffers which are forced through the HPLC system by a pump. The column is in an oven where the temperature is regulated for analyte mixture separation (Yan, 2014).

The HPLC process begins with the vacuum pump forcing the mobile phase through the column and detector under high pressure. The vacuum pump connected to a degasser removes dissolved gasses in the mobile phase and drives the solvents into a mixing chamber where they can be mixed before entering the column. In HPLC analysis either isocratic or gradient elution mode is used. Isocratic elution refers to when the mobile phase composition remains constant throughout the analysis while gradient elution is when the mobile phase composition is changed during the analysis. The sample is introduced into the system through automatic injection using an auto sampler. Once the sample is loaded into the system it travels via a loop. Excess sample exits the loop via a vent port while a part of the sample forced into the column by the mobile phase (Hashim, 2018). Separation in the column is based on the degree of interaction between the sample components and the absorbent particles. The components with higher affinity to the mobile phase travels faster through the column and eluded out first. While the components with higher affinity for the stationary phase interact with the stationary phase and are eluted later. Separation is carried out according to either reverse phase HPLC or normal phase HPLC. In reverse phase HPLC the stationary phase is non-polar while the mobile phase is relatively polar. During reverse phase separation the hydrophobic analytes have higher affinity towards the stationary phase and polar molecules will be eluded first. While in normal phase HPLC the stationary phase is polar and the mobile phase nonpolar. During separation the more polar analytes are retained for longer in the column. After separation the compounds are directed towards the detector. Multiple detectors can be used such as UV-Vis, refractive index (RI), etc.

The detector data is displayed in a chromatogram. The chromatogram is comprised of peaks on the x-axis that represents retention time for each analyte and the y-axis (peak area) represents the quantity of each analyte there is present in a sample (Yan, 2014)

3.15.1 High performance liquid chromatography (HPLC) with RI detector

In this experiment a Rezex™ ion exclusion column is used. The principle for ion exclusion chromatography (IEC) is that the charged stationary phase repels ionic compounds thus leading to early elution while non-ionic analytes have a high affinity for stationary phase and are retained longer (Fasciano, Mansour, & Danielson, 2016).

In addition, a refractive index (RI) detector is utilized for analyte detection after separation. RI detector is used when the analytes has limited or no UV absorption capabilities. The principle for RI detection is measuring the refractive index when light is passed through the mobile phase with analyte compared to a reference. When light leaves one material and enters another it refracts, and thus the refractive index of a material is a measure of how much light bends when it enters a different material. Light created by a light source in the detector is passed through a flow cell comprised of solvent and analyte and a different flow cell comprised solely of solvent. The light is then passed through both flow cells a second time using a mirror before being sent to the detector where the intensity is measured. When RI of an analyte sample and a reference sample is the same little to no bending of light occurs at the interface between the flow cells causing a large amount of light to reach the RI detector. As the analytes in the Rezex column are eluded the RI of solution in the sample flow cell will vary from the reference flow cell causing the light to bent as it passes between the flow cells. The amount of light reaching the detector will change producing a signal response. This response is displayed as peaks in the chromatogram (Wade & Bailey, 2013).

Material

Chemicals

- β-glucan samples
- H_2SO_4, 5 mM

Equipment and instruments

- Eppendorf tubes, 1.5 mL (Thermo Scientific)
- Snap Ring Micro-Vials with Snap Ring Caps, 0.3 mL (VWR)
- Vortex MS 2 minishaker (IKA®)
- ThermoMixer™ C (Eppendorf)
- Finnpipette™ 10 - 100 µL (Themo scientific)
- Membrane dry vacuum pump/ compressor, VCP 80 (VWR)
- Multiscreen®HTS 96-Well Plates, 0.45 µm Durapore® (Merck Millipore)
- HPLC, Dionex Ultimate 3000 system (Thermo Scientific)
- Rezex™ ion exclusion LC column, 300 x 7.8 mm (Phenomenex)

Method

Reaction mixtures were prepared following the procedure described in section 3.14.1 **Table 3-14** and **Table 3-15** and section 3.14.2 **Table 3-16**. 20 µL of β-glucan samples were pipette over to 0.3 mL Snap Ring Micro-Vials and vials were capped with Snap Ring Caps.

HPLC analysis was performed using a 300 x 7.8 mm Rezex™ LC column in the Dionex Ultimate 3000 system. Prior to innating sample run the column oven temperature was raised to 65 ^{o}C and the mobile phase flow rate increased stepwise to 0.6 mL/ min. RI detector was selected for analysis of β-glucan samples and the system was then purged for 15 minutes. While the purge was in progress a sample queue was prepared. The three first samples in the queue were blanks with 5 mM of H_2SO_4 buffer used to ensure that there were no system errors. 8 µL of each sample was injected into the Rezex™ column after the blanks were run. The duration for each sample in the column was 22 minutes. After the sequence of samples were completed, the chromatograms were analysed using the Chromeleon 7 software.

3.15.2 High performance liquid chromatography (HPLC) with CAD MS

Porous graphitic carbon (PGC) column contains a stationary phase that retains polar analytes (Bapiro, Frances, & Jodrell, 2016). When the analytes are eluted from the PGC column, they are nebulized into aerosols by a counter stream of nitrogen gas. The aerosols travel through a

spray chamber and into an evaporation tube where the solvent is removed. This leaves behind dried analyte particles. The dried particles then exit the evaporation tube and travel to a mixing chamber where they react with positively charged nitrogen gas ions. An ion trap removes unreacted nitrogen gas ions from the mixture. The ionized analyte particles travel further to a CAD electrometer. In the electrometer the analyte charge is converted to a signal. This signal is amplified and displayed as peaks in the chromatogram. CAD detection is independent of analytes chemical structure and is therefore a good alternative for analysis of volatile analytes without chromophores (Almeling, IIko, & Holzgrabe, 2012).

The HPLC system was combined with a Thermo LTQ Velos Pro MS/MS system to provide spectral data for identification and quantification of each analyte. An MS system is comprised of an ion source, a mass analyzer, and an ion detector. Mobile phase with analytes is eluted out the column and a percentage of the sample enters the CAD detection system while another part enters the MS system through an inlet capillary. The sample is vaporized and ionized by electrospray ionization (ESI). ESI is an atmospheric pressure ionization technique in which high voltage is applied across the atmospheric interface creating an electric field. This electric field turns the sample meniscus into a Taylor cone which is pulled into a jet of liquid and is further disrupted into a series of aerosols. Once the sample has been dispersed the solvent vaporize creating ionized ions which can enter the MS system. The ions accelerate through a magnetic field that sorts the ions based on their mass and charge. Ions are deflected by the mass analyzer at different rates with lighter ions being deflected first due less mass and greater charger. Deflected ions accelerate towards an ion detector that detects ions and organize them by their m/z values and relative abundance in a sample. The m/z signal are displayed as peaks in a mass spectrum (Ho, Lam, Chan, & et, al., 2003).

Material

Chemicals

- β-glucan samples
- Buffer A: Ammonium acetate, NH_4Ac 10 mM
- Buffer B: Acetonitrile (ACN), 100 %
- ddH_2O

Equipment and instruments

- Eppendorf tubes, 1.5 mL (Thermo Scientific)
- Snap Ring Micro-Vials with Snap Ring Caps, 0.3 mL (VWR)
- Vortex MS 2 minishaker (IKA®)
- ThermoMixer™ C (Eppendorf)
- Membrane dry vacuum pump/ compressor, VCP 80 (VWR)
- Multiscreen®HTS 96-Well Plates, 0.45 µm Durapore® (Merck Millipore)
- HPLC, Dionex Ultimate 3000 RS system (Thermo Scientific)
- PGC Column, 150 x 2.1 mm (Thermo scientific)
- CAD detector (Corona Ultra)
- Thermo LTQ Velos Pro MS/MS (Thermo Scientific)

Method

Reaction mixtures were prepared following the procedure described in section 3.14.1 **Table 3-14** and **Table 3-15** and section 3.14.2 **Table 3-16**. 20 µL of β-glucan samples were pipette over to 0.3 mL Snap Ring Micro-Vials and vials were capped with Snap Ring Caps. In addition, a blank with 70 µL of ddH_2O was prepared.

HPLC analysis was performed using a 150 x 2.1 mm PGC column in the Dionex Ultimate 3000 RS system coupled to a Thermo LTQ Velos Pro MS/MS and a CAD detector. MS system was switched on and column temperature was set to 70 ^oC. The flow rate was increased to 0.2 mL/ min with 100 % ACN for 10 minutes. After 10 minutes flow rate was slowly raised to 0.4 mL/ min and the mobile phase composition was adjusted to 50 % of ACN and 50 % of 10 mM NH_4Ac for 15 minutes. The acetonitrile content in the mobile phase was adjusted to 0 % for 15 minutes. Following the PGC column equilibration a sample queue was prepared in the Xcalibur software. Once the HPLC system was ready for analysis, 2.5 µL of a blank with ddH_2O was injected into the column to ensure that there were no system errors. Once the blank run was complete 2.5 µL of β-glucan samples were injected into the PGC column. Analytes were detected with a CAD detector and a MS system. The duration for separation in the column and analysis in the CAD and MS was 40 minutes. After the sequence of samples were completed, the chromatograms were analysed using the Xcalibur software.

3.16 Thermal shift assay

Thermal shift assay is a biochemical method for assessing protein stability under a set of experimental conditions to determine the thermal profile of a protein. Proteins contain hydrophobic residues that under normal circumstances are unexposed. A fluorescent dye with affinity for hydrophobic residues is mixed with the protein and at low temperatures the fluorescent dye remains in the solution unbound to the protein, but as the temperature is gradually increased the protein unfolds exposing the hydrophobic core permitting the fluorescent dye to interact with the hydrophobic residues and fluoresce. During the analysis the change in fluorescent signal is measured. The temperature induced denaturation of a protein is displayed in a melting curve. The melting temperature (Tm) represents the denaturation midpoint (Benedetti, et al., 2022).

Material

Chemicals

- ¶ *Pa*GH50A, 15 µM
- ¶ Tris-HCl pH 7.5, 20 mM
- ¶ SYPRO orange dye (Thermo Fisher)
- ¶ ddH_2O
- ¶ Ice

Equipment and instruments

- ¶ qPCR StepOnePlus™ (Applied Biosystems)
- ¶ Plate centrifuge, Plate spin II (Kubota)
- ¶ MicroAmp™ optical 96-well reaction plate (Applied Biosystems)
- ¶ MicroAmp™ Adhesive optical cover (Applied Biosystems)
- ¶ Eppendorf tubes, 1.5 mL (Thermo Scientific)
- ¶ Vortex MS 2 minishaker (IKA®)
- ¶ Aluminum foil

Method

8X SYPRO orange dye solution was placed on ice and covered with aluminum foil to limit light pollution and degradation. The reaction mixtures were prepared as described in **Table 3-17** and vortexed. To a MicroAmp™ optical 96-well reaction plate placed on ice 20 µL of either blank or protein sample were pipetted over to a plate well. Four replicates for each sample were prepared. The MicroAmp™ optical 96-well reaction plate with samples was sealed with MicroAmp™ Adhesive optical cover. The plate was centrifuged for 1 minute at 1000 g and subsequently transferred to the qPCR StepOnePlus™ system where the thermal shift analysis was performed. Following the qPCR settings that samples were incubated at 25 ^{o}C for 2 minutes before increasing the temperature from 25 to 97 ^{o}C over 50 minutes. Once the temperature reached 97 ^{o}C the samples were incubated for an additional 2 minutes. The melting curve was displayed in the StepOne software.

Table 3-17. Reaction mixtures for analysis of thermal shift assay of PaGH50A.

Reagent	End Concentration	Blank	Protein sample
*Pa*GH50A	1.5 µM	-	10 µL
Tris-HCl pH 7.5	5 mM	25 µL	25 µL
8X SYPRO orange dye	1x	12.5 µL	12.5 µL
ddH_2O	-	62.5 µL	52.5 µL

3.17 Purifying Psl from *P. aeruginosa* mutant strain PAO1 ΔWspF ΔPel

Material

Chemicals

- Overnight culture of *P. aeruginosa* PAO1 ΔWspF ΔPel.
- EDTA pH 8.0, 0.5 M
- Proteinase K, 20 mg/ mL (NEB)
- 37 % HCl (VWR)
- Ice

Equipment and instruments

- Eppendorf tubes, 1.5 mL (Thermo Scientific)
- Finnpipette™ 0.5 - 10 µL, 10 - 100 µL and 100 - 1000 µL (Themo scientific)
- Vortex MS 2 minishaker (IKA®)
- ThermoMixer™ C (Eppendorf)
- Benchtop centrifuge 5418R (Eppendorf)
- Boiling water bath, SBB Aqua 5 plus (Grant)
- pH paper

Method

The day prior to Psl purification 15 mL overnight culture of *P. aeruginosa* PAO1 ΔWspF ΔPel was prepared as described in section 3.7. The following day 10 mL of the overnight culture was split into 1 mL aliquots. The cell pellets were harvested by centrifugation for 10 minutes at 16.900 g at 4 ^{o}C and resuspended in 100 µL of 0.5 M EDTA pH 8.0. Once the cells pellets were resuspended, they were boiled in a water bath for 20 minutes at 100 ^{o}C. The samples were vortexed every 5 minutes. After 20 minutes samples were centrifuged for 10 minutes at 16.900 g at 4 ^{o}C and 90 µL of the supernatant fraction was transferred to a new 1.5 mL Eppendorf tube. 45 µL of 1 mg/mL proteinase K was added to the supernatant fraction to remove protein contaminants and the samples were incubated in a ThermoMixer™ C for 1 hour at 60 ^{o}C with 600 rpm agitation. The 1 hour incubation period was followed by an additional 30 minute incubation at 80 ^{o}C with 600 rpm agitation to inactive proteinase K. The purified Psl samples were incubated in ice until samples reached room temperature. The pH of the samples was adjusted to approximately 7.5 with 37 % HCl using pH paper.

3.18 *Pa*GH50A activity in *P. aeruginosa* biofilms

Many species of bacteria associate on surfaces to form biofilms compromised of complex aggregates of microorganisms encapsulated by an ECM. Biofilms play a critical role in a microbial pathogenesis. Most biofilms formed in nature is a consortium of various microorganism, but in certain setting single specie biofilms are formed. *P. aeruginosa* have this intrinsic ability to form robust single species biofilms in for example the lungs of a CF patient or in a clinical setting (Thi, Wibowo, & Rehm, 2020).

Analysis of static biofilm systems were preferred in a laboratory setting rather than a chemostat or continuous flow system for biofilm formation. Static assay allowed for better examination of different aspects and detection of changes in the biofilm under various conditions (Merritt, Kadouri, & O'Toole, 2005).

3.18.1 Agar plate-based *Pa*GH50A activity assay

Agar plate-based activity assay is a method for screening enzyme activity. An agar plate is inoculated with single strain of *P. aeruginosa* together with an enzyme over a period. If the enzyme has biofilm degrading properties a clear halo is formed around the enzyme application zone. The size of the halo indicates the efficiency of the specific enzyme in degrading biofilm (Molitor, et al., 2019)

Material

Chemicals

- Sterile *Pa*GH50A, 1 µM and 5.9 µM
- Tris-HCl pH 7.5, 20 mM
- *P. aeruginosa* strains
  - PAO1
  - PAO1 ΔWspF
  - PAO1 ΔWspF ΔPsl
  - PAO1 ΔWspF ΔPel.
- LB agar plates without antibiotics
- LB medium

Equipment and instruments

- Cell density meter, Ultrospec 10 (BioChrom)
- Static incubator (Termaks)
- Eppendorf tubes, 2 mL (Thermo Scientific)
- Vortex MS 2 minishaker (IKA®)
- Circular membrane filter

Method

15 mL overnight culture without antibiotics inoculated with *P. aeruginosa* strain PAO1, PAO1 ΔWspF, PAO1 ΔWspF ΔPsl or PAO1 ΔWspF ΔPel were prepared as described in section 3.7. The following day a chosen volume of overnight culture depending on the OD_{600} was transferred to a 2 mL Eppendorf tube, diluted to an OD_{600} of 0.1 and a volume of 1.8 mL. The cell suspension was vortexed and OD_{600} was remeasured to ensure the samples had correct OD_{600}.

An LB agar plate was divided into three parts. 1 mL of each *P. aeruginosa* solution was pipette over to separate LB agar plates. The cell suspension was spread in the LB agar plate using an L shaped inoculation loop and excess culture was removed. A sterile circular membrane filter was placed in each of the three parts. To one of the membrane filters 20 µL of 20 mM Tris-HCl pH 7.5 was added and to the two other membrane filters *Pa*GH50A was added with the following concentrations 1 µM and 6 µM. The process was repeated for all the *P. aeruginosa* strains. The plates were dried in the LAF bench before incubating the plates for 18 hours at 37 ^{o}C. The next day the agar plates were examined for halo formation.

3.18.2 *Pa*GH50A activity assessment in microtiter plate biofilm

Microtiter plate biofilm assay for assessing biofilm formation by measuring the OD of adherent biomass stained with crystal violet. Bacteria strains are cultivated in a 96 well plate over a period, followed by exposing and incubating the biofilm with enzyme. Then after incubation removing the planktonic cells and staining the adherent biofilm. The surface associated dye allows for a semi quantitative assessment of formed biofilm (Merritt, Kadouri, & O'Toole, 2005).

Material

Chemicals

- Sterile *Pa*GH50A
- Sterile Ultrapure™ distilled water (Invitrogen)
- *P. aeruginosa* strains

- PAO1
- PAO1 ΔWspF
- PAO1 ΔWspF ΔPsl
- PAO1 ΔWspF ΔPel.

¶ LB agar plates without antibiotics

¶ LB medium

¶ Bleach (Lilleborg)

¶ NaCl solution, 0.9 %

¶ Crystal violet, 0.1 %

¶ Ethanol, 70 %

Equipment and instruments

¶ Cell density meter, Ultrospec 10 (BioChrom)

¶ Static incubator (Termaks)

¶ Plate reader, VarioSkan Lux (Thermo Scientific)

¶ 96-Well Polystyrene Microwell plate (Sarstedt)

¶ Adhesive sealing film

¶ Sterile Eppendorf tubes, 2 mL (Thermo Scientific)

¶ Vortex MS 2 minishaker (IKA®)

¶ Orbital shaker (VWR)

Method

Microtiter plate biofilm assay was executed under sterile conditions. All materials were autoclaved, and solutions filtrated prior to use.

15 mL overnight culture without antibiotics inoculated with *P. aeruginosa* strain PAO1, PAO1 ΔWspF, PAO1 ΔWspF ΔPsl or PAO1 ΔWspF ΔPel were prepared as described in section 3.7. The following day a chosen volume of overnight culture depending on the OD_{600} was transferred to a 2 mL Eppendorf tube, diluted to OD_{595} of 0.01 and a volume of 1.9 mL. The cell suspensions were vortexed and OD_{595} was remeasured to ensure the samples had correct OD_{595}. 100 µL of a cell suspension was transferred to a well in the 96-Well Polystyrene Microwell plate. A total of 16 parallels of each strain was prepared. In addition, LB controls were prepared by transferring 100 µL of LB medium to the microtiter plate. 8 parallels were

prepared. The 96-Well Polystyrene Microwell plate with samples were incubated under static conditions for 18 hours at 37 ºC.

The following day OD_{595} was measured in a plate reader prior to adding *Pa*GH50A to wells. To 8 out of 16 wells for each strain *Pa*GH50A with a final concentration of 6 µM was added. To the other 8 wells an equal volume of sterile Ultrapure™ distilled water was added. This was repeated for all the *P. aeruginosa* strains. To 4 out of 8 LB controls *Pa*GH50A was added with a final concentration of 6 µM and an equal volume of sterile Ultrapure™ distilled water was added to the other 4 wells. The 96-Well Polystyrene Microwell plate was sealed with adhesive sealing film and incubated statically for 24 hours at 37 ºC. In a different experiment *Pa*GH50A was inoculated along with *P. aeruginosa* suspensions instead of the following day using the same method.

The next day OD_{595} was measured in a plate reader before washing and staining adherent biofilm. The 96-Well Polystyrene Microwell plate was inverted over a container with bleach and shaked to remove the liquid from the wells. This was followed by washing each well three times with 150 µL of 0.9 % NaCl solution to remove the rest of the medium with planktonic cells. Once the liquid was removed from the wells, the plate was let to incubate upside down on dry paper for 5 minutes at room temperature. To each well 120 µL of 0.1 % of crystal violet solution was added. The 96-Well Polystyrene Microwell plate was placed on an orbital shaker shaking at low speed for 30 minutes at room temperature to stain the adherent biofilm. After 30 minutes excess crystal violet solution was disposed of, and the wells were once more washed three times with 150 µL of 0.9 % NaCl solution. The plate was inverted on paper towels and dried for 5 minutes at room temperature. To the wells 120 µL of 70 % ethanol was added and the plate was placed on the orbital shaker for 30 minutes at room temperature to solubilize the stained biofilm. After the incubation period the well contents were mixed by pipetting and 100 µL of each solution was transferred to a clean 96-Well Polystyrene Microwell plate. The OD_{595} was measured.

4. Results

4.1 Bioinformatics

4.1.1 Enzyme properties of *Pa*GH50A

The bioinformatics tool ExpasY Protparam (Gasteiger, et al., 2005) was used to identify the physiochemical properties of mature *Pa*GH50A. Properties such as molecular weight, pI value, extinction coefficients, amino acid composition and instability index were calculated and given in **Table 4-1**.

Table 4-1. Expasy Protparam analysis of mature PaGH50A. The key properties calculated for PaGH50A without signal peptide (SP) were number of amino acids (Aa), molecular weight (MW), extinction coefficient (Ů,) isoelectric point (pI) and instability index (Ii).

Name	Value
Aa	726
MW (Da)	79 300.50
pI	5.76
ε (M^{-1} cm^{-1})	139 925
Ii	48.41

Full-length enzyme contained 757 amino acids which included an SP consisting of 31 amino acids predicted by SignalP-5.0 sever (Armenteros, et al., 2019). The SP was predicted between amino acid residue 1 and the cleavage point at amino acid residue 31 as shown in (**Figure 4-1**). The probability for the cleavage point was given to be 0.4927 and the secretory pathway was predicted to be Sec/SPI with a likelihood of 0.9389.

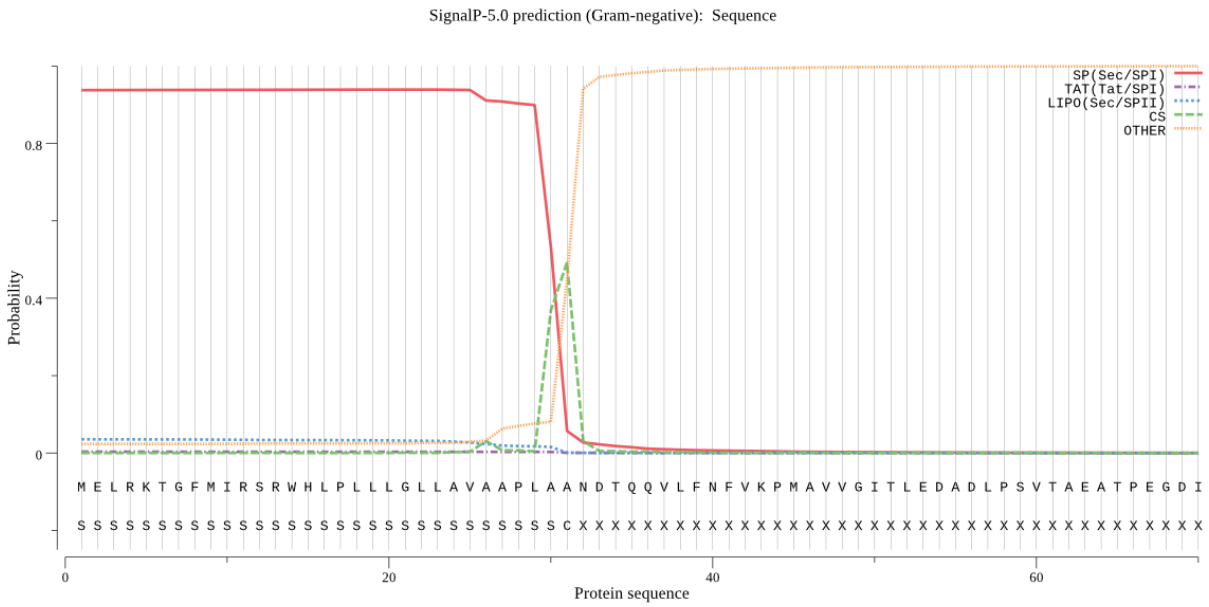

Figure 4-1. Signal peptide (SP) location in PaGH50A. SignalP-5.0 distinguishes between three types of secretion pathways Sec/SPI, Tat/SPI and Sec/SPII depending on whether signal peptidase I or II (SPI/SPII) cleaves the SP during translocation. The cleavage point is between amino acids A and N (i.e., LAA-ND), amino acid residue 31-32. The cleavage point is marked with a green line. Signal P-5.0 predicted that the amino acid sequence had the highest probability of containing SP (Sec/SPI) marked with red. The rest of the amino acid sequence is marked with yellow and referred to as other.

4.1.2 Structure and domain architecture of *Pa*GH50A

The domain architecture of *Pa*GH50A was analysed using Interpro and Phyre2. Interpro (Blum & et. al, 2021) utilizes predictive models called protein signatures, provided by various databases and an Interpro search showed that the protein family and domains of *Pa*GH50A were unknown, however a homologous superfamily of glycoside hydrolase was predicted between amino acid residue 387-714 (**Figure 4-2**).

Figure 4-2. PaGH50A predicted structure. Full length enzmyme consist of a signal peptide of 31 amino acids followed by a glycoside hydrolase familiy 50 catalytic domain of 327 amino acids. The two regions are connceted by a linker region (shown

as a black line) of 356. The full length enzyme also contains a hexa His-tag region (not shown). The structure is predicted based on results from Interpro, Phyre2 and CAZy. .

Phyre2 (Kelley, Mezulis, Yates, Wass, & Sternberg, 2015) generates protein models based on homologous sequences with a sequence identity greater than 25 %. The top template indicated that *Pa*GH50A was functionally and structurally associated with Aga50D found in *Saccharophagus degradans*, with a 33 % sequence identity and an alignment occurring between amino acid residue 34 and 734. The next-best alignment was with AgWH50C found in *Agarivorans gilvus*, with a sequence identity equaling 33 % and an alignment occurring between amino acid residue 53 and 734. The protein model generated for mature *Pa*GH50A is shown in **Figure 4-3**. Furthermore, the CAZy database (Drula, et al., 2022), which classifies carbohydrate active enzymes based on sequences similarity, classified *Pa*GH50A as a member of the GH50 family, a family that until now contained enzymes active towards agarose.

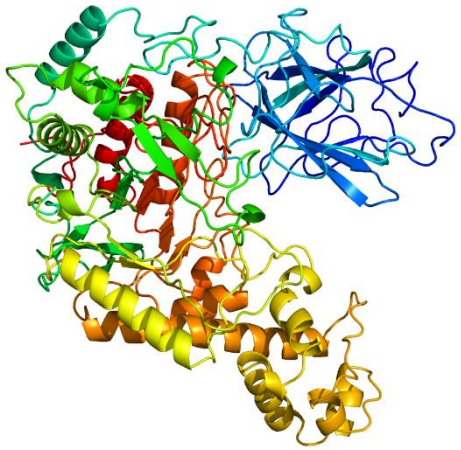

Figure 4-3. The predicted 3D protein structure of mature PaGH50A. The structure was modelled with Phyre2 based homologous sequence.

4.1.3 Functional protein association network

For analysis of protein networks STRING was utilized (Jensen & et. al, 2009) . In graphical representations provided by such analysis, the red node represents the query protein which in this case is PA1046 from *P. aeruginosa* PAO1 due to *Pa*GH50A found in *P. aeruginosa* PA14

not being listed in the STRING database (**Figure 4-4**). It should be noted that PA1046 and *Pa*GH50A are 98.2 % (based on alignment) identical and are believed to perform the same activity in both strains.

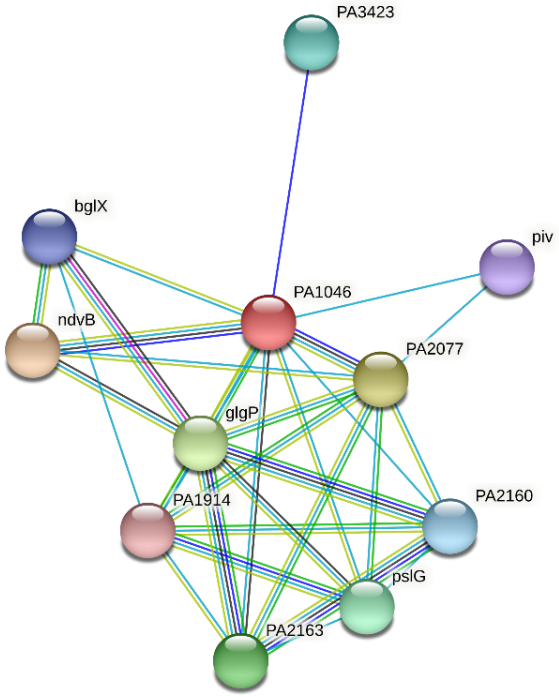

Figure 1-4. STRING analysis of known and predicted protein network of PA1046. The nodes represent the associated proteins while the edges between the nodes represents various types of interactions where light blue and pink represents known interactions, green, orange, and deep blue represents predicted interactions, black represents co-expression and purple for protein homology.

The first shell contained proteins that interacted with PA1046 with the highest order of confidence and are shown in **Table 4-2**. The majority of the predicted functional partners are glycoside hydrolases which further suggests that *Pa*GH50A has hydrolase activity.

Table 4-2. Description of predicted functional partners of PA1046 found in P. aeruginosa PAO1. The gene name, confidence score and protein family are given for the associated proteins.

Gene name	Confidence score	Protein family
NdvB	0.831	Glycosyltransferase 2. Glycoside hydrolase family 17.
PA2077	0.749	Not classified
glgP	0.695	Glycosyltransferase 35
PA2163	0.680	Glycoside hydrolase family 77.
PslG	0.680	Glycoside hydrolase family 39.
PA3423	0.671	Not classified
PA2160	0.668	Glycoside hydrolase family 13.
bglX	0.667	Glycoside hydrolase family 3.
Piv	0.664	S01.281 family (Proteases)
PA1914	0.653	Not classified

4.2 Cloning, expression, and purification

4.2.1 Cloning of *Pa*GH50A

PA14_50830 was amplified using PCR amplification. Agarose gel analysis showed that the PCR products obtained at annealing temperature 66 and 68 ºC were approximately 2.3 kbp which corresponded with the expected size of *PA14_50830* of 2.274 kbp, indicating successful amplification (**Figure 4-5**).

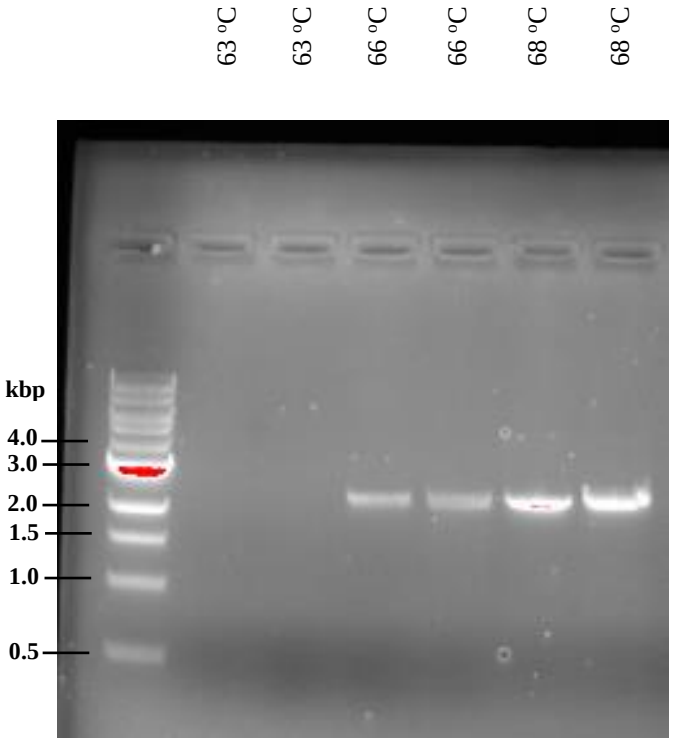

Figure 4-2. Agarose gel analysis of amplified PA14_50830. During PCR amplification primer annealing temperatures 63, 66 and 68 °C were analyzed. Lane 1 contains QuickLoad® 1 kb ladder while lane 2-6 contains PCR products. The annealing temperatures used are indicated above each well. The molecular weight of PA14_50830 is 2.274 kilobases (kbp).

pNIC-CH plasmid was successfully linearized using restriction enzymes AfIii and PstI-HF in a double digestion process. The DNA band at 5.279 kbp in lane 2-5 represents the linearized pNIC-CH plasmid (**Figure 4-6**). In the same lanes smaller bands of approximately 2.0 kbp were observed, these bands represent the DNA fragments which were replaced by *PA14_50830* during In-Fusion® cloning. The DNA bands at approximately 8.0 kbp in lane 6 and 7 represented undigested pNIC-CH plasmid.

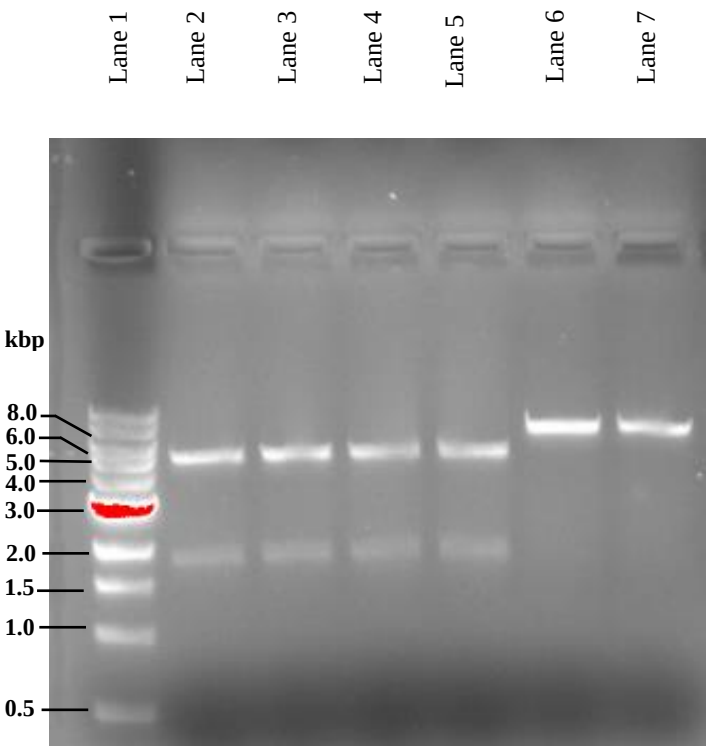

Figure 4-3. Agarose gel analysis of pNIC-CH plasmid after double digestion with restriction enzymes AflIi and PstI-HF. Lane 1 contains QuickLoad® 1 kb ladder while lane 2-7 contain pNIC-CH plasmid after double digestion. In lane 2-5 the DNA band at 5.279 kbp represents the linearized pNIC-CH plasmid while the DNA band at aproximatly 2.0 kbp represents the DNA fragment that is expected to be replaced by PA14_50830. Lane 6-7 contains undigested pNIC-CH.

In-Fusion® Cloning was used to ligate *PA14_50830* into the linearized pNIC-CH vector. This was successful according to the colony PCR performed on the selected transformants, where 7 out of 11 colonies showed the expected PCR product (**Figure 4-7**). Following DNA sequencing of transformants, colony 5 was selected and transformed into ONE SHOT™ BL21 (DE3) chemically competent *E. coli* for protein expression. Six *E. coli* Bl21 colonies were randomly selected for colony PCR. Transformation was successful for all selected colonies and the purified plasmids were sent for DNA sequencing (**Figure 4-8**). After sequence confirmation *E. coli* Bl21 colony 4 was selected for further use in the project.

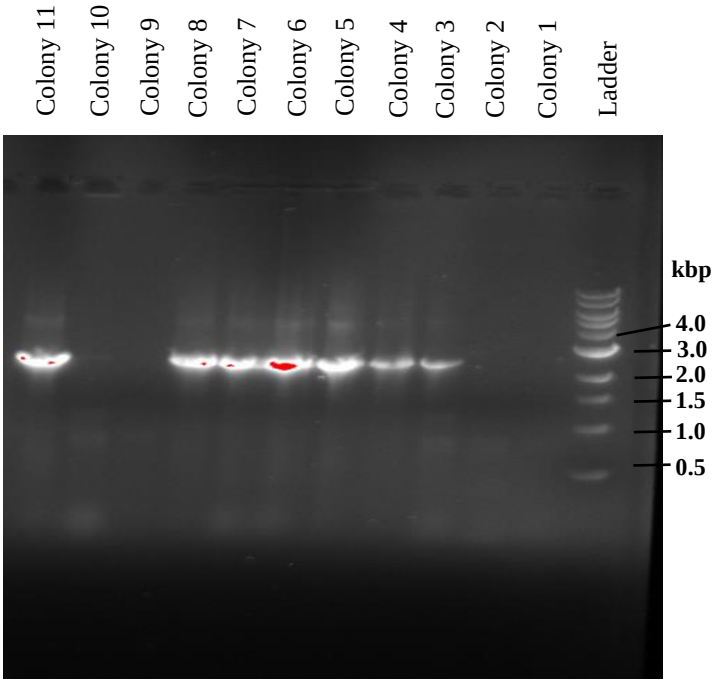

Figure 4-4. Colony PCR of transformed ONE SHOT® BL21 (DE3) chemically competent E. coli cells. The DNA band at 2.274 kbp represents PA14_50830. The transformed colonies are indicated above each well while QuickLoad® ladder is present by the outer right lane and sizes are given in kbp.

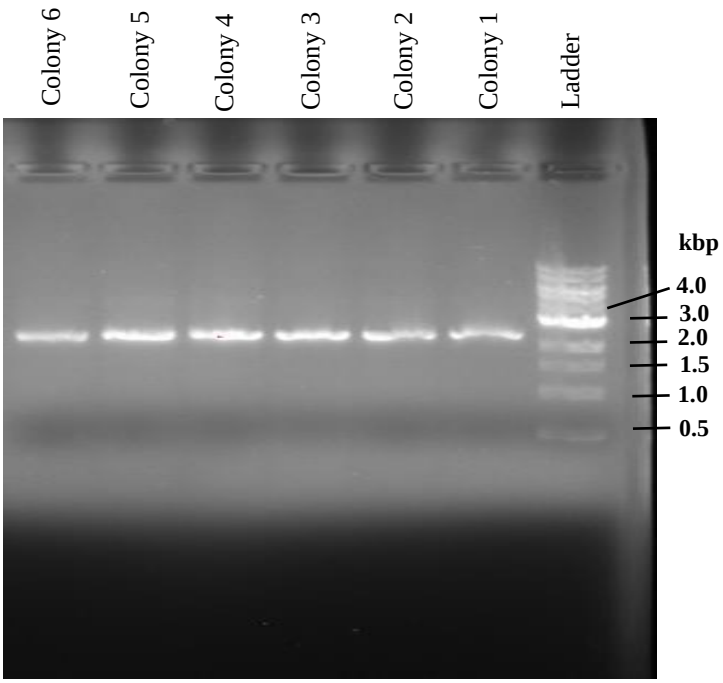

Figure 4-5. Colony PCR of transformed ONE SHOT® BL21 (DE3) chemically competent E. coli cells. The DNA band at 2.274 kbp represents PA14_50830. The colonies are indicated above each well while QuickLoad® ladder is present by the outer right lane and sizes are given in kbp.

4.2.2 Expression and purification

Various expression parameters such as IPTG concentration, temperature, growth medium, incubation time and extraction methods were investigated for optimizing protein expression in *E. coli* Bl21.

Transformants were initially cultivated in LB, TB, BHI medium, however it was unclear whether *Pa*GH50A was expressed after 3 hours and 18 hours due low protein yield or other factors (**Figure 4-9A,B,C**). The experiment was repeated using M9 medium while all other parameters remained the same. Protein expression was induced at both IPTG end concentration after 18 hours at 37 ^{o}C (**Figure 4-9D**). Observations showed that *Pa*GH50A was expressed, however the protein yield remained low. Protein expression was further investigated by extracting *Pa*GH50A from the periplasm instead of the cytoplasm while all other parameters remained the same. Extraction from periplasm reduced contaminates, however cultivation in TB medium did not increase protein yield in comparison to M9 medium (**Figure 4-9E**).

A) LB medium – cytoplasmic extraction

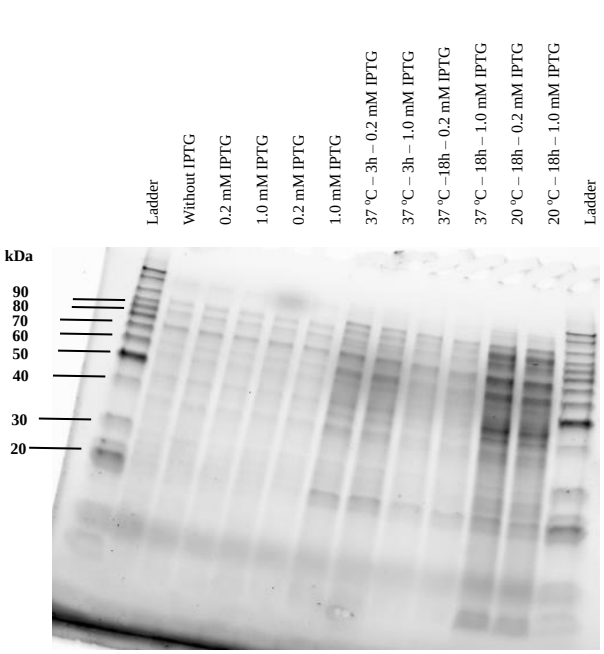

B) TB medium – cytoplasmic extraction

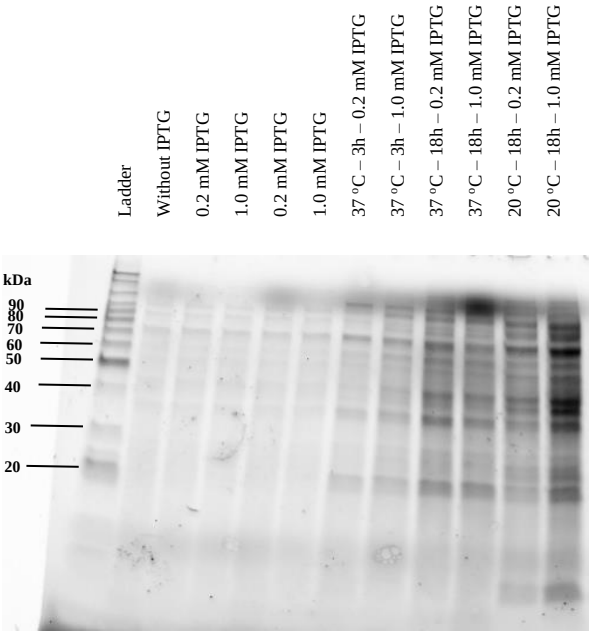

C) BHI media – cytoplasmic extraction

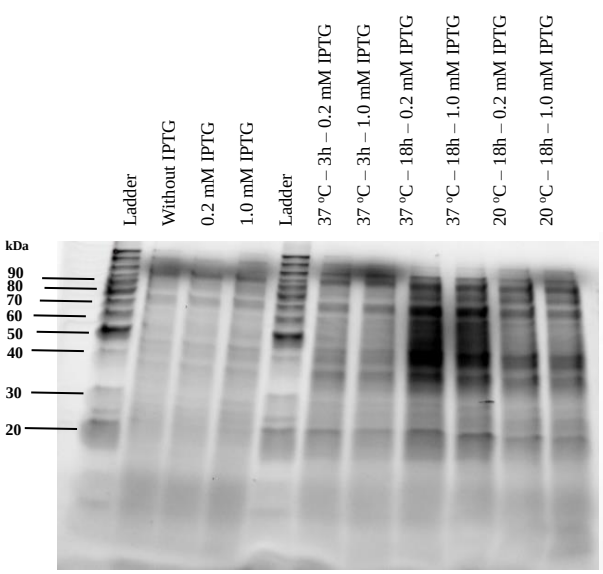

D) M9 media – cytoplasmic extraction

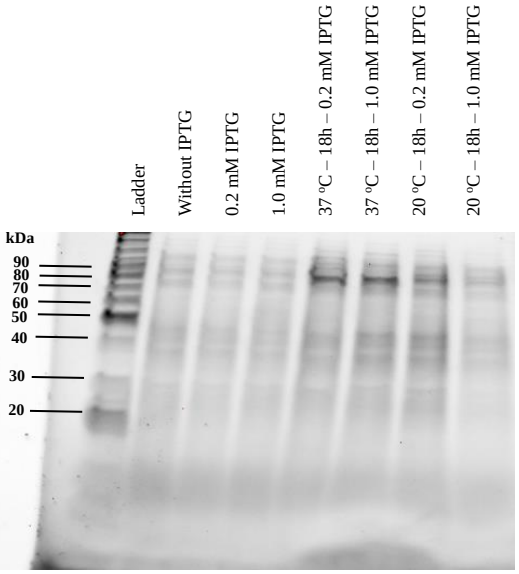

E) TB medium – periplasmic extraction

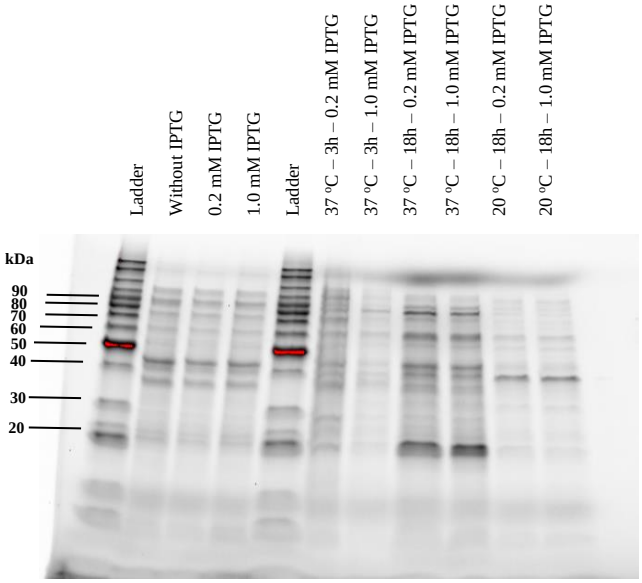

Figure 4-6 SDS-PAGE analysis of PaGH50A expression. Various parameters for protein expression were investigated and optimized. The expression parameters were growth medium, IPTG end concentration of 0.2 and 1 mM, temperature of 20 and 37 ºC, incubation time and extraction methods. A), B), C) and D) shows protein expression in the following mediums LB, TB, BHI and M9 and PaGH50A extracted from the cytoplasm while E) shows protein expression in TB medium with PaGH50A extracted from periplasm. The sources for samples are indicated above each well while B e n c h M a r k Ê p r present i n l a d d e by the outer left lane and sizes are given in kDa. Molecular weight of mature PaGH50A is 79.3 kDa.

Following optimization of parameters, *Pa*GH50A was purified from *E. coli* BL21 using IMAC purification method. IMAC fractions along with samples extracted from the cytoplasm were analyzed and showed that the elution fraction contained *Pa*GH50A, however the fraction was highly contaminated by other proteins co-eluting with *Pa*GH50A (**Figure 4-10A**). Therefore, alternatively *Pa*GH50A was extracted from the periplasm followed by purification. The elution fraction had negligible contaminates, however protein yield remained low (**Figure 4-10B**).

To further increase expression of *Pa*GH50A in *E. coli* BL21, cultivation was performed in Lex-48 bioreactor. *E. coli* BL21 cultivated in Lex-48 bioreactor for 18 hours at 37 ^{o}C with moderate aeration allowed for more cell proliferation and thus more *Pa*GH50A than cultivation in a shaker incubator for 18 hours at 37 ^{o}C with 220 rpm agitation (**Figure 4-10C**). The elution fraction yielded 0.663 mg/L after incubation in a shaker incubator while 0.945 mg/L after incubation in Lex-48 bioreactor.

A) Shaker – cytoplasmic extraction

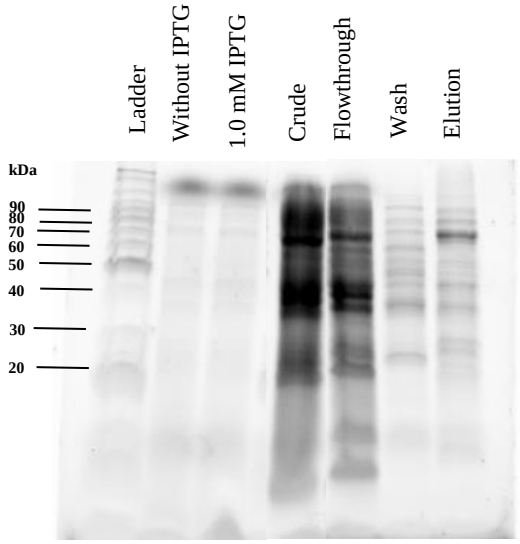

B) Shaker – periplasmic extraction C) Lex-48 bioreactor – periplasmic extraction

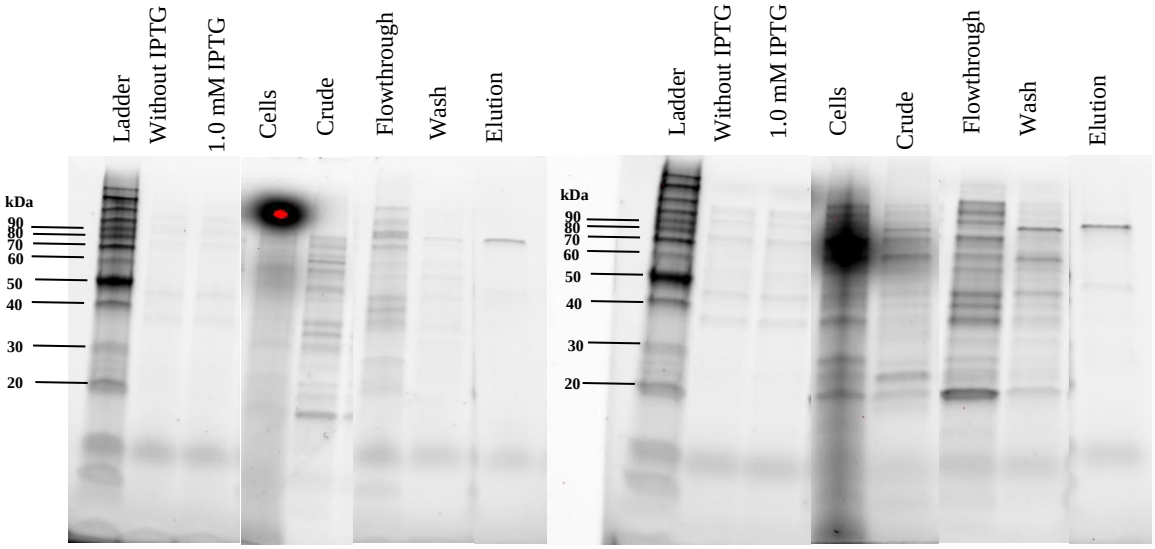

Figure 4-7. SDS-PAGE gel analysis of PaGH50A expression and IMAC purification. A), B), C) shows PaGH50A expression under different conditions. The variable conditions are written in the title and the sources for the samples are indicated above each well while BenchMark™ protein ladder is given in kDa. The flowthrough and the outer fraction was 35 mL, the wash and elution fractions were 20 mL.

4.3 Characterization of *Pa*GH50A

4.3.1 Thermal shift analysis

Thermal shift assay was performed to determine the melting temperature (Tm) of *Pa*GH50A. The melting profile was visualized with the derivative fluorescence data. The steepest incline in fluorescence represents the temperatures at which *Pa*GH50A denatures the fastest and the lowest points represents Tm. Tm was determined to be 28 and 51 ºC, suggesting that *Pa*GH50A consists of two domains which denatures at different temperatures (**Figure 4-11**). Additionally, the melting curve appears uneven with subtle downwards turns indicating that *Pa*GH50A denatures unevenly.

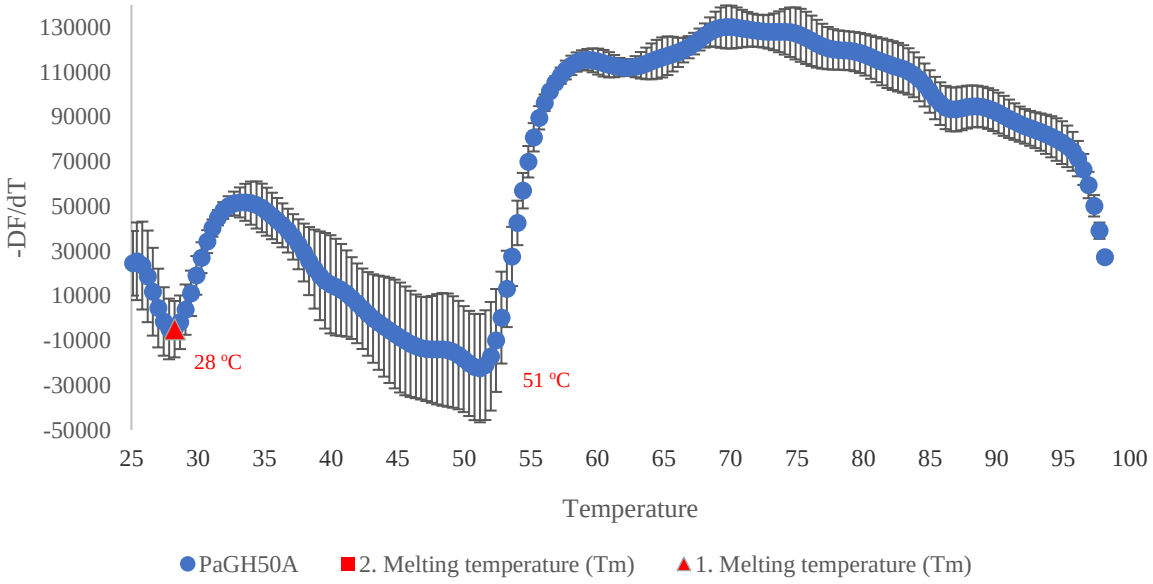

Figure 4-8. Thermal shift analysis of PaGH50A. The lowest points in the melting curve represents the melting temperature (Tm, orange figure). The y-axis represents the derivative of the fluorescence from SYPRO binding to PaGH50A hydrophobic residues. While the x-axis shows the increasing temperature (ºC) over 50 minutes. The melt curve was based on the average of four replicates and the error bars represent standard deviation between the fluorescence measurements.

4.3.2 Enzyme assays

4.3.2.1 Variation of enzyme concentration

Initial characterization of *Pa*GH50A was conducted by examining the activity levels towards the β-1,3 substrates that already have been shown as substrates for *Pa*GH50A (Yi, yan, Jiang, & Wang, 2018) namely curdlan and lichenan using DNSA method. The enzyme did indeed show hydrolytic activity towards both substrates that increased with increasing enzyme concentration (**Figures 4-12 and 4-13**). Interestingly, activity towards both substrates were low within the first 60 minutes but showed an increasing trend after this time point.

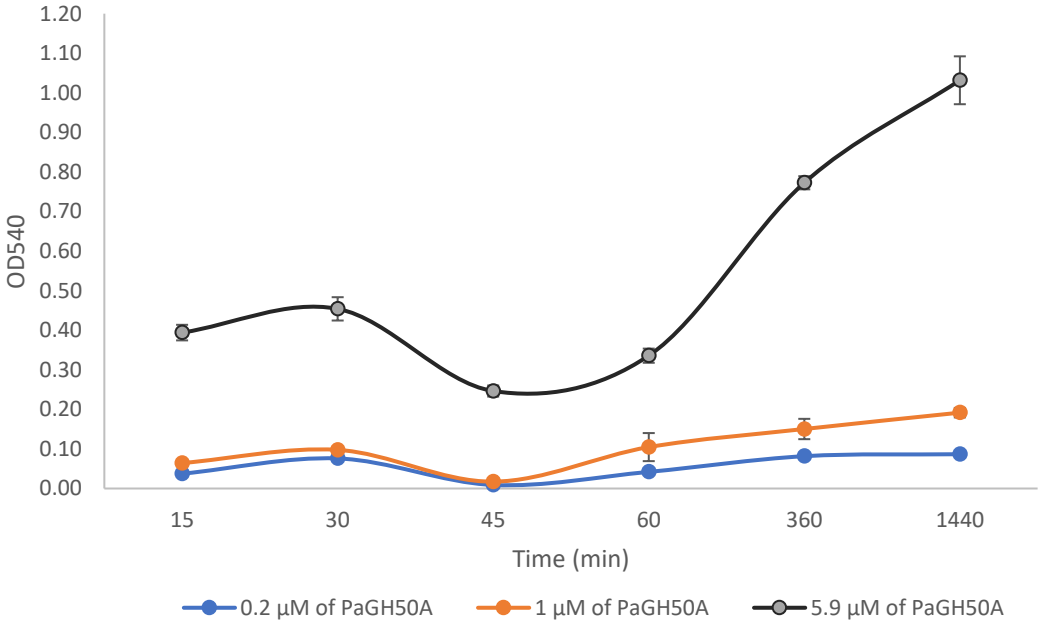

Figure 4-9 PaGH50A activity towards lichenan. Enzyme activity was investigated with 0.2, 1 and 5.9 µM PaGH50A and analysed using DNSA assay. The y-axis represents OD_{540} (since a glucose standard was not prepared, thus the relative activity % was unable to be calculated) while the x-axis represents the time. The progress curve was based on the average of a triplicate and the error bars represent standard deviation between the measurements.

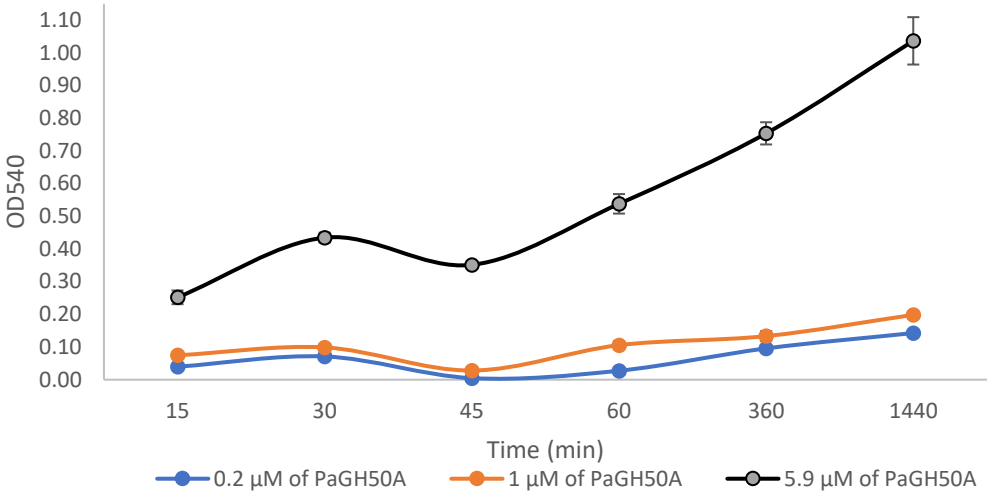

Figure 4-10 PaGH50A activity towards curdlan. Enzyme activity was investigated with 0.2, 1 and 5.9 µM PaGH50A and analysed using DNSA assay. The y-axis represents OD_{540} (since a glucose standard was not prepared, thus the relative activity % was unable to be calculated) while the x-axis represents the time. The progress curve was based on the average of a triplicate and the error bars represent standard deviation between the measurements.

4.3.2.2 Variation of substrate concentration

Activity of *Pa*GH50A were investigated at curdlan concentrations of 18.5, 33.3 and 61.7 mM. *Pa*GH50A showed hydrolytic activity at all examined curdlan concentrations, however showed increasing activity at lower concentrations, optimally at 33.3 mM (**Figures 4-14**).

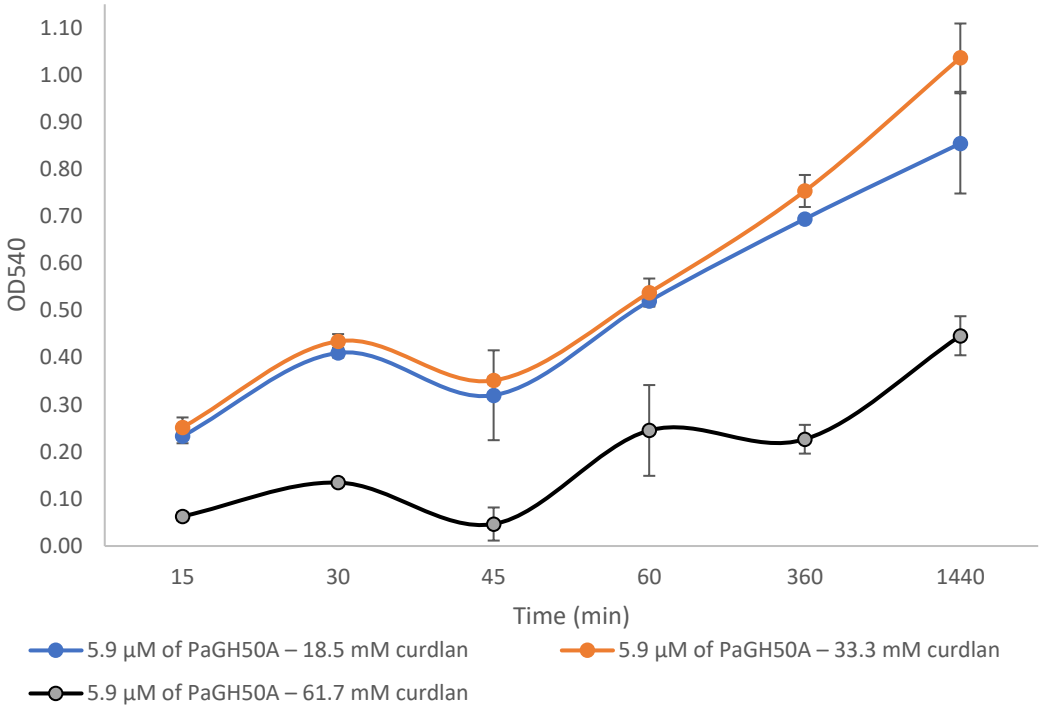

Figure 4-11. Enzyme activity assay with curdlan at various concentrations. PaGH50A activity was investigated with 18.5, 33.3 and 61.7 mM curdlan and analysed using DNSA assay. The y-axis represents OD_{540} (since a glucose standard was not prepared, thus the relative activity % was unable to be calculated) while the x-axis represents the time. The progress curve was based on the average of a triplicate and the error bars represent standard deviation between the measurements.

4.3.2.3 Variation of pH

Activity of *Pa*GH50A was determined by conducting DNSA assay using various buffers with different pH from 8.5 - 4.0. The data showed that *Pa*GH50A is active at all examined pHs, however the progress curve indicates that the enzyme has an optimum pH within the range of pH 6.5 – 8.5, optimally at pH 8.5 (**Figures 4-15**). In comparison to Yi, et al. whom previously characterized PaBglu50A, an orthologous enzyme to *Pa*GH50A found that the optimal pH for enzyme activity was pH 5.5 but retained more than 80 % maximal activity within pH 4.0-8.0 for 30 minutes (Yi, yan, Jiang, & Wang, 2018).

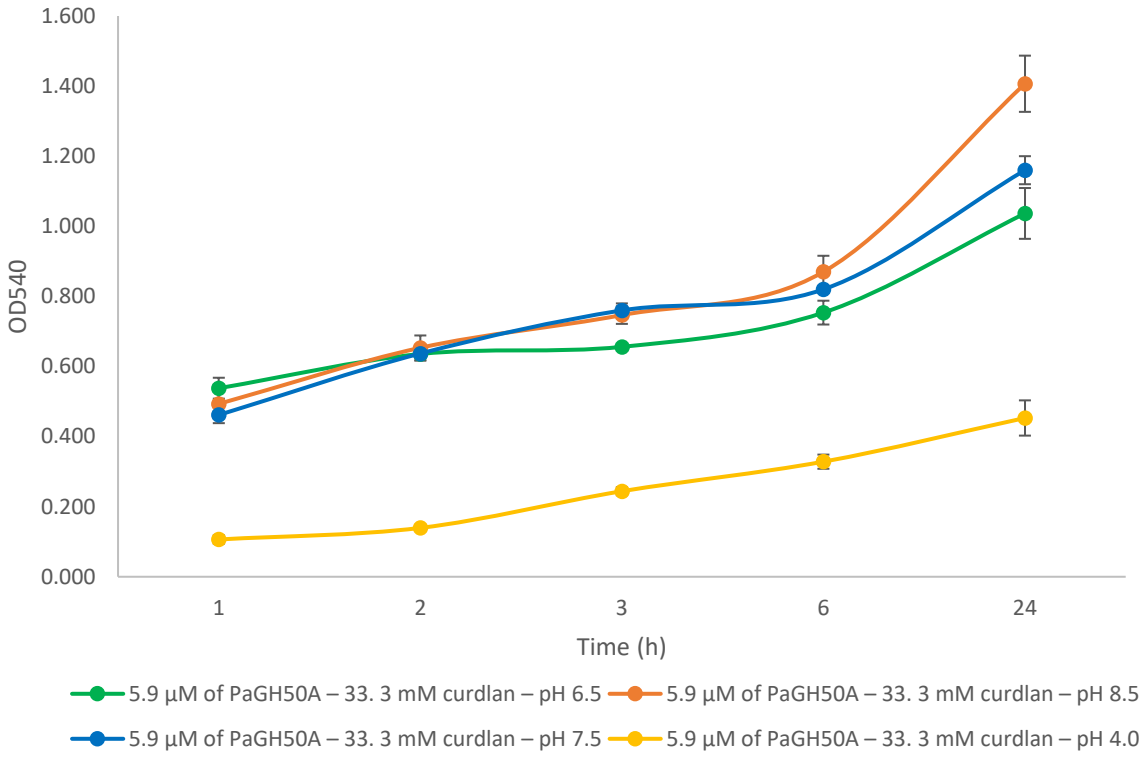

Figure 4-12. Optimum pH for PaGH50A activity. Enzyme activity was investigated at pH 8.5, 7.5, 6.5 and 4.0 and analysed using DNSA assay. The y-axis represents OD_{540} (since a glucose standard was not prepared, thus the relative activity % was unable to be calculated) while the x-axis represents the time. The progress curve was based on the average of a triplicate and the error bars represent standard deviation between the measurements.

4.3.2.4 Adding inert salts

Further investigation involved determining how $CaCl_2$ and $ZnCl_2$ affected *Pa*GH50A activity. The data showed that the inert interfered with the reaction rate indicating that *Pa*GH50A did not need divalent cations as cofactors (**Figures 4-16**).

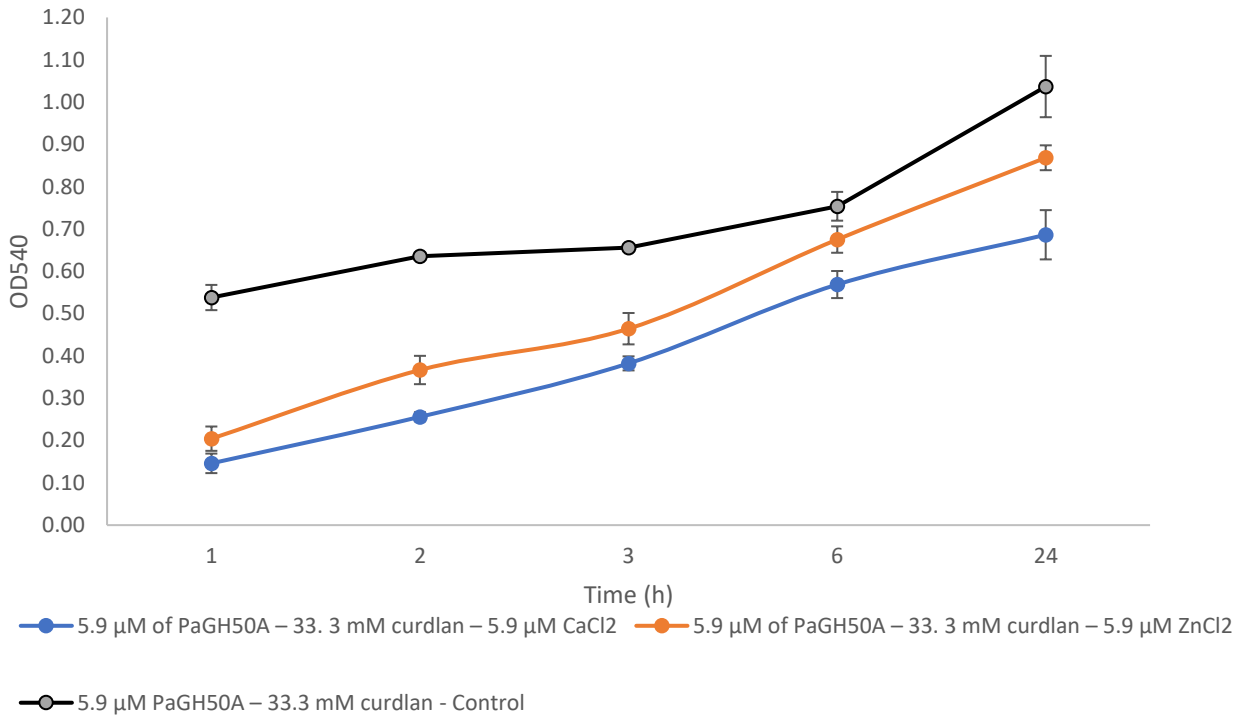

Figure 4-13. Enzyme activity with added inert salts i.e., $CaCl_2$ and $ZnCl_2$. Reducing ends are measured using DNSA assay. The y-axis represents OD_{540} (since a glucose standard was not prepared, thus the relative activity % was unable to be calculated) while the x-axis represents the time. The progress curve was based on the average of a triplicate and the error bars represent standard deviation between the measurements.

4.4 MALDI-TOF analysis

For characterization of β-1,3-oligosaccharide product profiles, the activity of PaGH50A towards curdlan wase investigated by MALDI-TOF analysis. In the initial experiments, reaction suspensions contained 5.9 µM *Pa*GH50A, 33.3 mM curdlan and 9.6 mM Tris-HCl buffer pH 7.5. Product analysis under various conditions showed the presence of hydrolysis products ranged from di- to nonasaccharide given in **Table 4-3**. The major products in the series of the β-1,3-oligosaccarides ranged from di- to pentasaccaride (**Figures 4-17B**). The data suggest that *Pa*GH50A hydrolysis curdlan by an endo-mechanism into β-1,3-oligosaccharides with different degrees of polymerization. These results partially coincided with the data presented by Yi, et al. in which they found that major hydrolysis products ranged from glucose to tetrasaccharide (Yi, yan, Jiang, & Wang, 2018).

To prove that a probable substrate of *Pa*GH50A was in fact β-glucans such as curdlan, mass variations were examined. It was observed that tetrasaccharides did indeed have 1 or 2 m/z variations due to carbon isotope variation in polysaccharides (**Figures 4-17C**).

Table 4-3. b-1,3-oligosaccaride products of curdlan, produced under various conditions. The saccharide type, name given in the MALDI-TOF spectra and m/z value for each -saccharide.

-saccharide	Name	Mass-to-charge ratio (m/z)
Di	$[(Glu)_2\,Na]^+$	365.28
Tri	$[(Glu)_3\,Na]^+$	527.42
Tetra	$[(Glu)_4\,Na]^+$	689.56
Penta	$[(Glu)_5\,Na]^+$	851.70
Heksa	$[(Glu)_6\,Na]^+$	1013.84
Hepta	$[(Glu)_7\,Na]^+$	1175.98
Octa	$[(Glu)_8\,Na]^+$	1338.12
Nona	$[(Glu)_9\,Na]^+$	1500.26

MALDI-TOF analysis is not a quantitative method therefore the varying peak intensities in the mass spectrum were independent of the amount of β-1,3-oligosaccharide. Signal variations could occur with sample composition, instrumental conditions, etc. The method was meant for determining product profile and is applied in combination with other enzymatic assays for quantification.

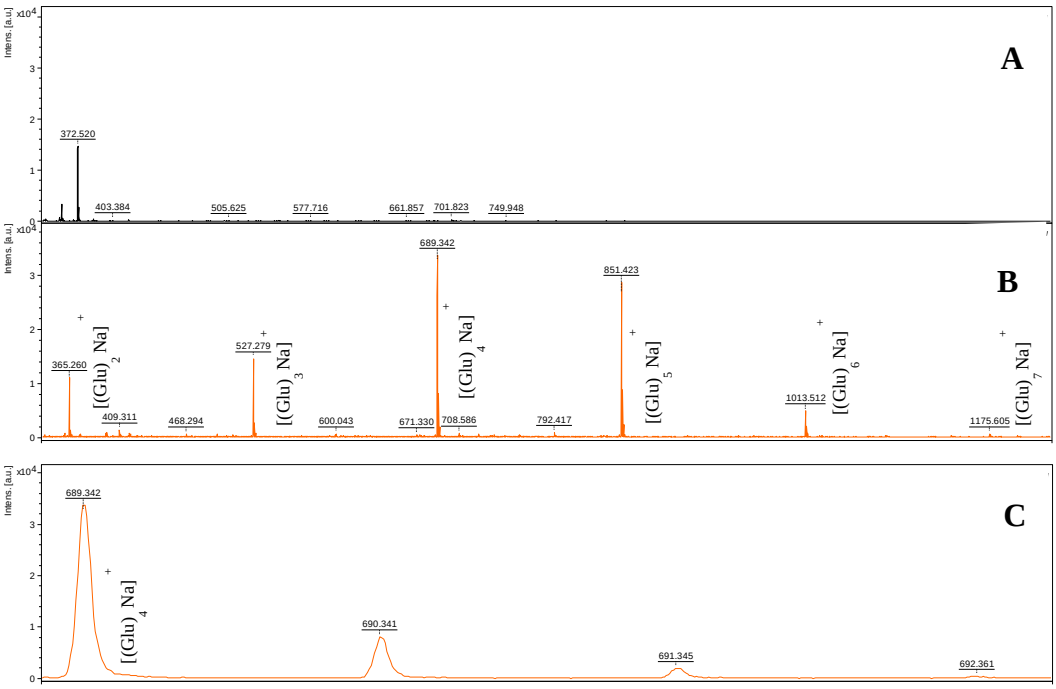

Figure 4-14. Mass spectra of b-1,3-oligosaccaride product profiles. A) shows negative control containing denatured PaGH50A, B) shows hydrolysis products after 24 hour incubation of 33.3 mM curdlan with 5.9 µM PaGH50A at 37 °C and C) shows the carbon isotope pattern of $[(Glu)_4\ Na]^+$. The x-axis represents the mass-to-charge ratio (m/z) while the y-axis represents the signal intensity. The degree of polymerization was annotated in the mass spectra beside their respective masses.

4.4.1.1 Substrate concentration

The substrate concentration can influence the product profile, this was thus investigated for *Pa*GH50A. Curdlan concentration 18.5, 33.3 and 61.7 mM were examined. The data showed that enzyme activity was lower at higher curdlan concentration, however the substrate concentration did not affect the degree of polymerization (**Figure 4-18**).

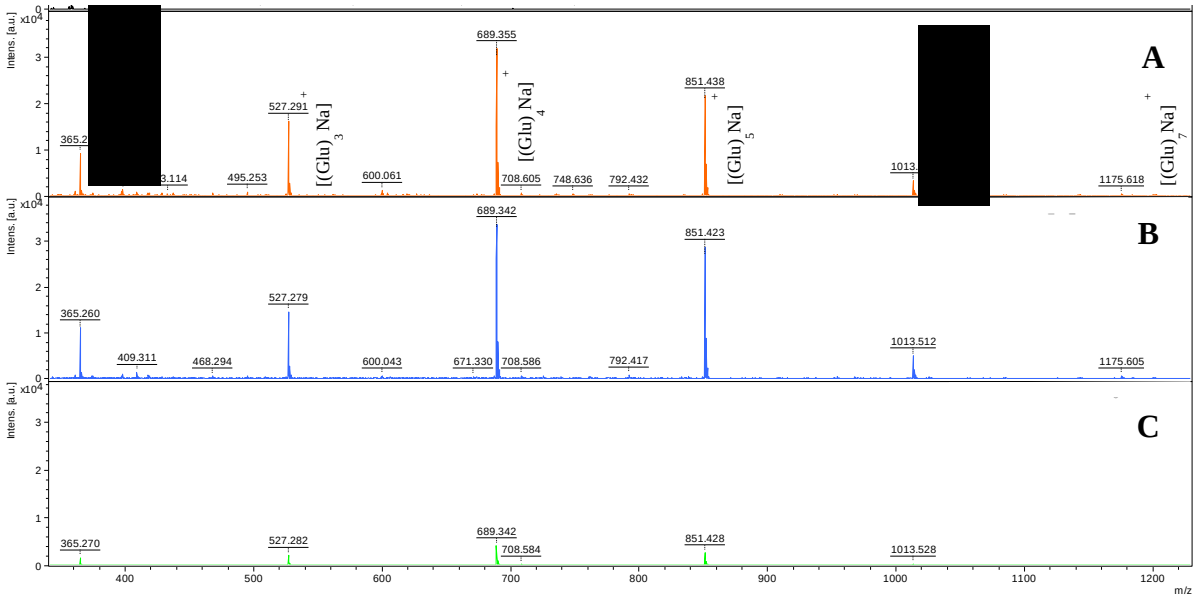

Figure 4-15. Mass spectra of ƃ-1,3-oligosaccaride product profiles. A, B, C) shows PaGH50A hydrolysis at the following curdlan concentration 18.5, 33.3 and 61.7 mM. The x-axis represents the mass-to-charge ratio (m/z) while the y-axis represents the signal intensity. The degree of polymerization was annotated in the mass spectra beside their respective masses.

4.4.1.2 Variation in temperature

The effect of temperature on *Pa*GH50A activity was examined by incubating the enzyme-substrate solution at 23, 37 and 50 ^{o}C while all other parameters remained the same. The results showed that activity was low at 23 and 50 ^{o}C. Additionally, it was observed that at 50 ^{o}C, a larger assortment of β-1,3-oligosaccharides ranging from di- to nonasaccharides, indicating low enzyme activity (**Figure 4-19**). The optimal temperature for *Pa*GH50A activity could conceivably be 37 ^{o}C based on MALDI-TOF analysis, which is different from PaBglu50A analysed by Yi, et al. which had an optimal temperature of 45 ^{o}C (Yi, yan, Jiang, & Wang, 2018).

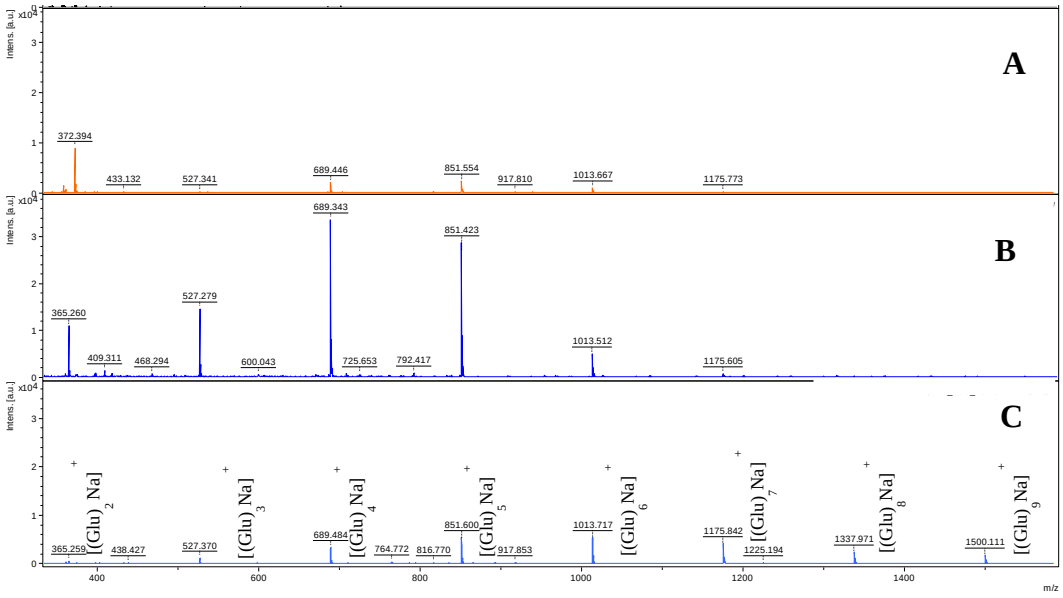

Figure 4-16. Mass spectra of ƃ-1,3-oligosaccaride product profiles. A, B, C) shows PaGH50A hydrolysis of curdlan at the following temperatures 23, 37 and 50 ºC. The x-axis represents the mass-to-charge ratio (m/z) while the y-axis represents the signal intensity. The degree of polymerization was annotated in the mass spectra beside their respective masses.

4.4.1.3 Incubation time

To determine the lengths of β-1,3-oligosaccharides generated by *Pa*GH50A hydrolysis of curdlan over time, the enzyme reaction was sampled at 4, 5, 6 and 24 hours. The data showed that at hour 4 the β-1,3-oligosaccharides ranged from di- to nonasaccharide with pentasaccharide as the major product. Between hour 4 and 6 the signal intensity increased indicating that the enzyme was still active, however the product profile remained to some extent similar. By hour 24 the product profile shifted towards shorter β-1,3-oligosaccharides which ranged from di- to heptasaccharide with tetrasaccharide as the major product (**Figure 4-20**)

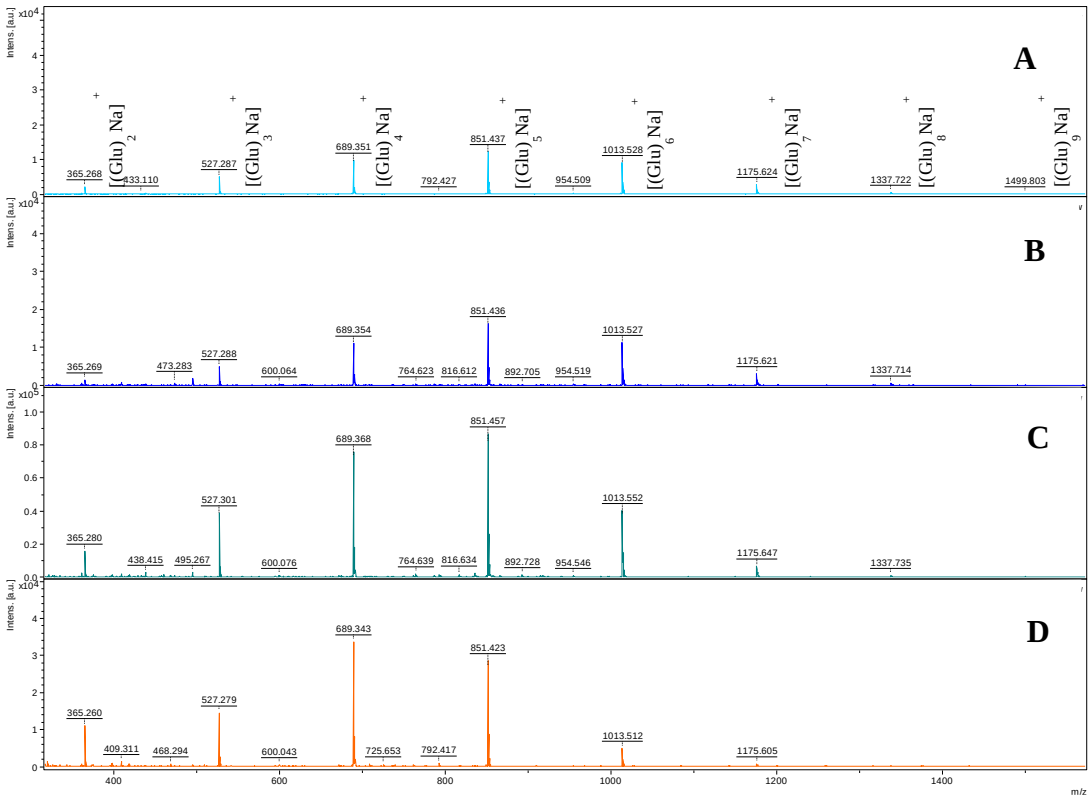

Figure 4-17 Mass spectra of ƃ-1,3-oligosaccaride product profiles. A, B, C) shows hydrolysis products of curdlan by PaGH50A sampled at the following incubation hours 4, 5, 6 and 24. The x-axis represents the mass-to-charge ratio (m/z) while the y-axis represents the signal intensity. The degree of polymerization was annotated in the mass spectra beside their respective masses.

4.4.1.4 pH

pH effects *Pa*GH50A activity by influencing the charge of the active site residues and the enzyme in general (Malthouse, 2020). The results showed that *Pa*GH50A had activity at pH 8.5, 7.5, 6.5 and 4.0, however the product profile varied at the different pHs. At pH 8.5 and 7.5 the major products were tetra- and pentasaccaride, at pH 6.5 the dominating β-1,3-oligosaccharide was tetrasaccharide and at pH 4.0 *Pa*GH50A hydrolysis yielded longer β-1,3-oligosaccharide likely indicating lower enzymatic activity (**Figure 4-21**).

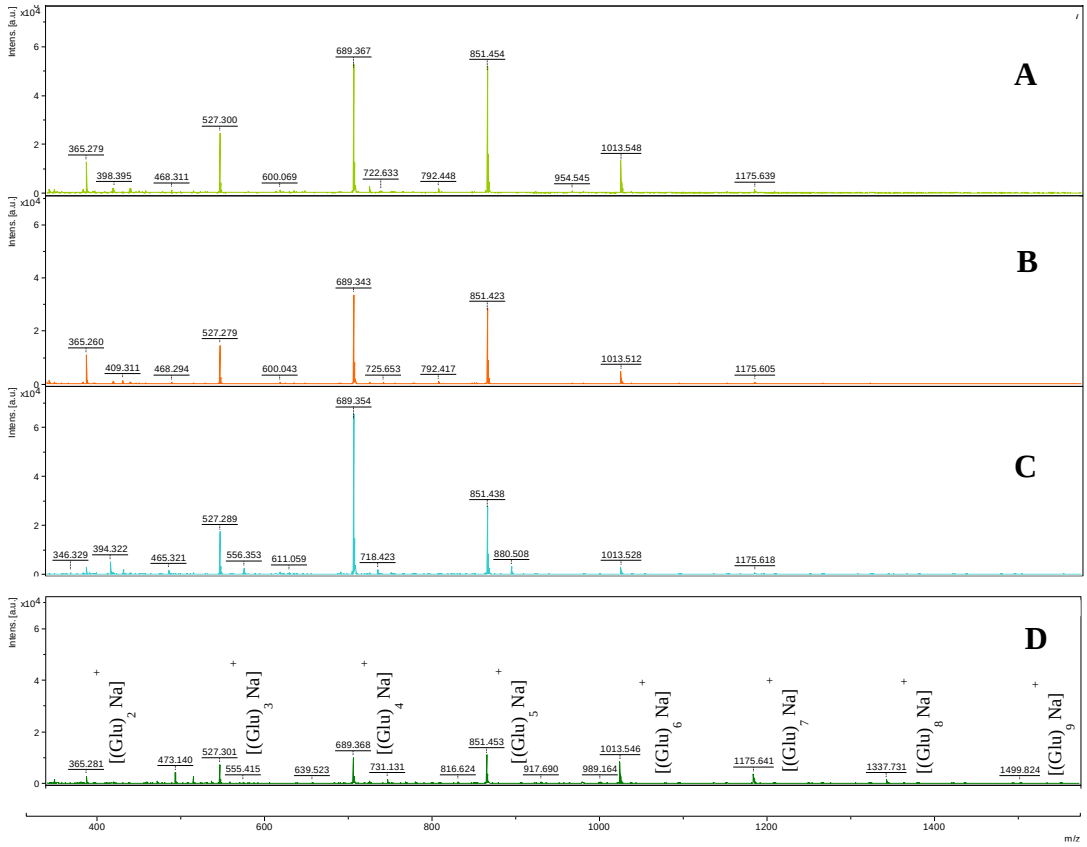

Figure 4-18. Mass spectra of β-1,3-oligosaccaride product profiles. A, B, C, D) shows hydrolysis products of curdlan by PaGH50A at the following pHs 8.5, 7.5, 6.5 and 4.0. The x-axis represents the mass-to-charge ratio (m/z) while the y-axis represents the signal intensity. The degree of polymerization was annotated in the mass spectra beside their respective masses.

4.4.1.5 $CaCl_2$

Previously it was observed that *Pa*GH50A activity declined with added inert salts (**Figure 4-16**), therefore the product profile was examined to see how it was affected. The results for added $CaCl_2$ to solutions with pH 8.5, 7.5, 6.5 and 4.0 showed that the product profile had not been influenced by Ca^{2+}, although enzyme activity fell at all pHs (**Figure 4-22**). This suggest that *Pa*GH50A does not need Ca^{2+} as a cofactor.

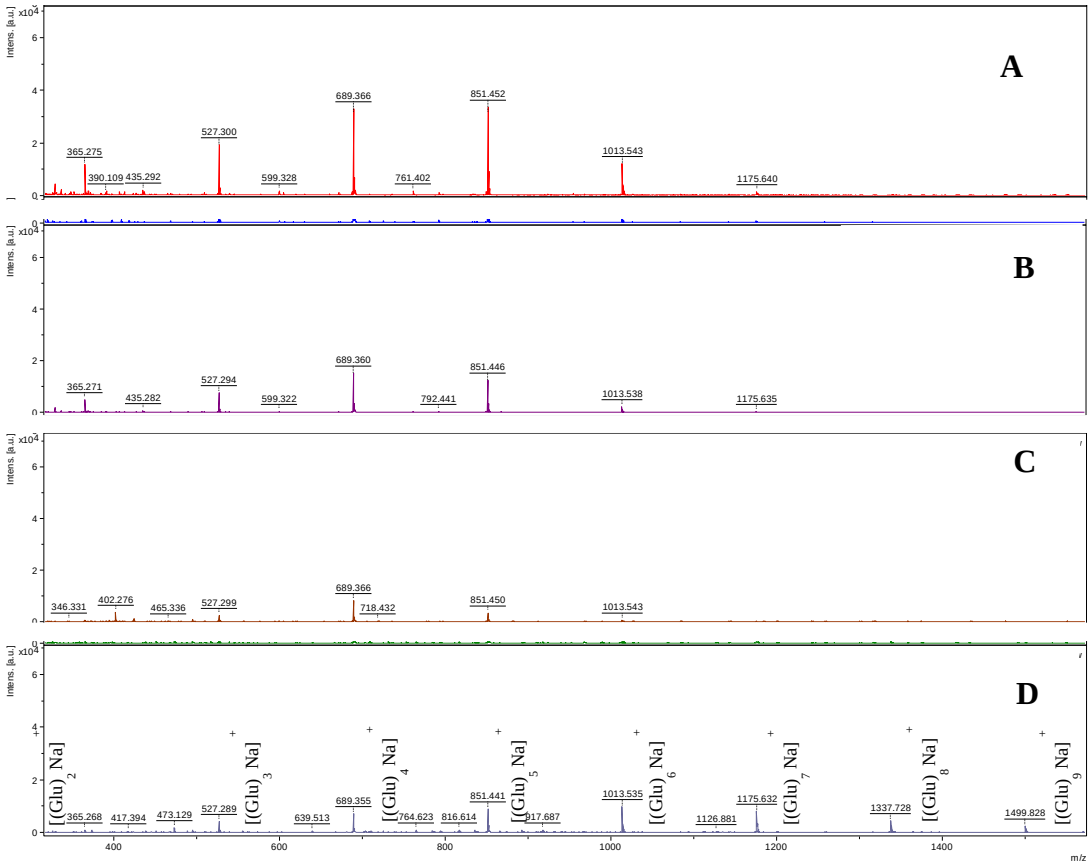

Figure 4-19. Mass spectra of ß-1,3-oligosaccaride product profiles. A, B, C, D) shows hydrolysis products of curdlan by PaGH50A with added $CaCl_2$ at the following pHs 8.5, 7.5, 6.5 and 4.0. The x-axis represents the mass-to-charge ratio (m/z) while the y-axis represents the signal intensity. The degree of polymerization was annotated in the mass spectra beside their respective masses.

4.5 HPLC analysis

*Pa*GH50A were showed to generate β-1,3-oligosaccharides of curdlan and lichenan, and thus quantification were attempted using HPLC-Rezex-RI. Unfortunately, no products were detected when using the setup (**Figure 4-23**). Since the HPLC-Rezex-RI method failed, a different approach was attempted, using a different column and a more sensitive detector, namely the HPLC-PGC-CAD method. Products arising from *Pa*GH50A mediated hydrolysis of curdlan, lichenan and Psl were investigated, however this method did neither result in detection of reaction products (**Figure 4-24**).

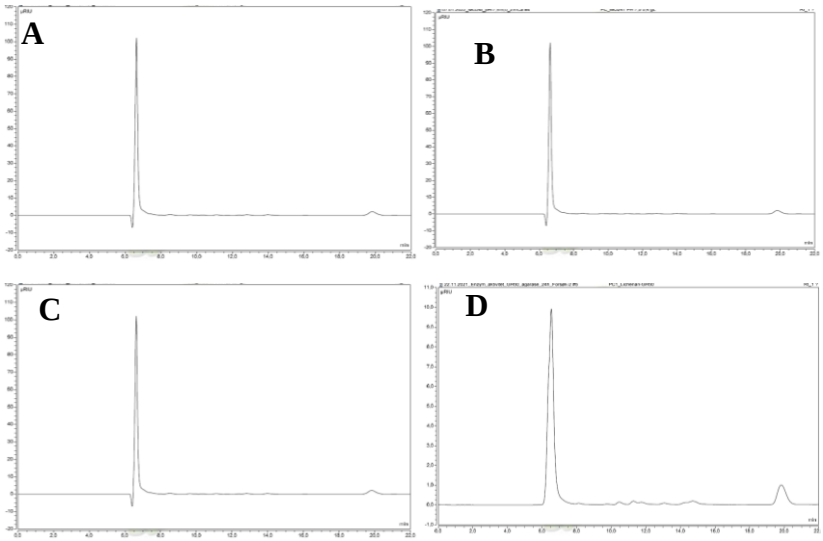

Figure 4-20 HPLC-Rezex-RI chromatogram for quantification of reaction products from PaGH50A hydrolysis of curdlan and lichenan. A, C) shows negative controls for curdlan and lichenan while B, D) shows analysis of sample supernatant. The separation time was 22 minutes. The x-axis represents the retention time for each analyte while the y-axis represents the mili absorbance unit (mAu).

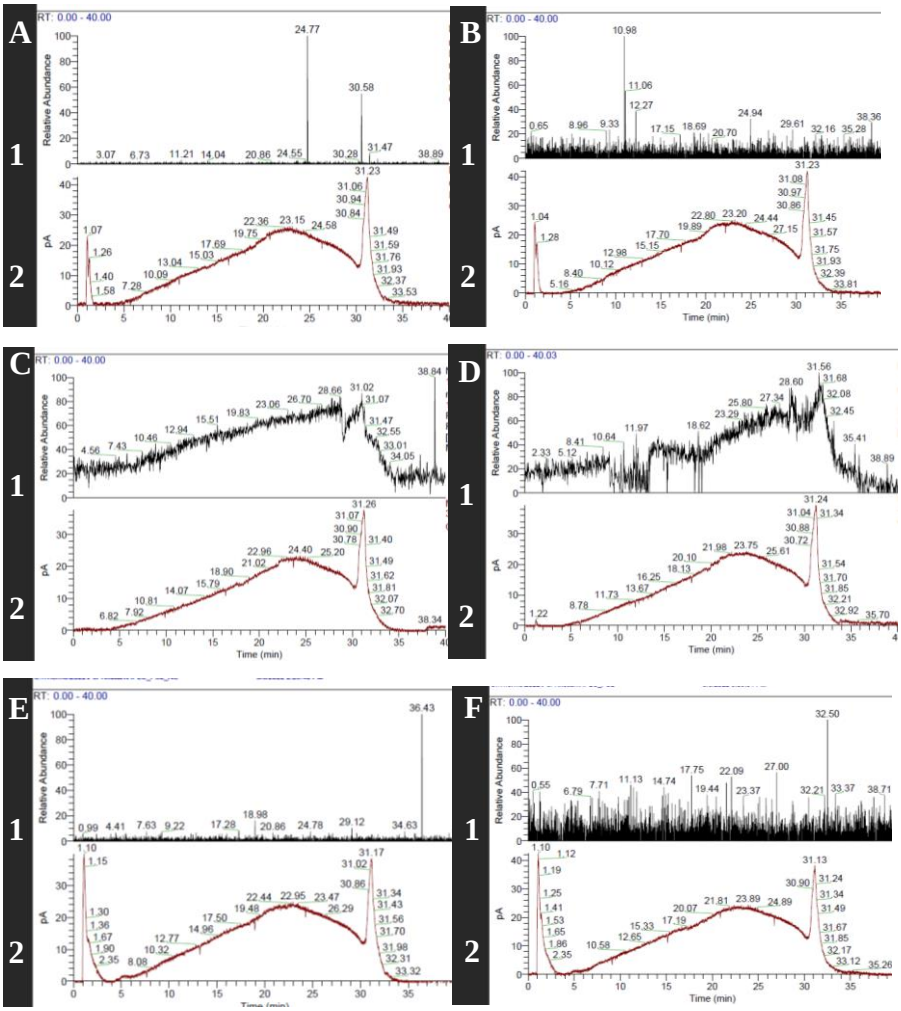

Figure 4-21 HPLC-PGC-CAD chromatogram for quantification of reaction products from PaGH50A hydrolysis of curdlan, lichenan and Psl. A, C, E) shows the negative control for curdlan, lichenan and Psl while B, D, F) shows analysis of supernatant after enzyme activity assay. A1, C1, E1) and B1, D1, F1) shows mass spectra while A2, C2, E2) and B2, D2, F2) show chromatogram. The separation time was 40 minutes. The x-axis represents the retention time for each analyte while the y-axis represents the mili absorbance unit (mAu).

4.6 *P. aeruginosa* biofilm analysis

A key virulence factor for pathogenesis of *P. aeruginosa* is the formation of biofilm. The pathogen produces biofilm specific exopolysaccharides such as alginate, Pel and Psl which are important for attachment and maintenance of the biofilm architecture. As previously noted, Psl is an exopolysaccharide composed of a repeating pentamer with a main chain consisting of D-mannose, L-rhamnose and D-glucose moieties coupled by α/β-1,3-glycosidic linkages and a D-mannose sidechain linked by a α-1,2 glycosidic bond (**Figure 1-4**). Since *Pa*GH50A has been

shown to hydrolyze β-1,3-glycosidic linkages, it was of great interest to investigate if the enzyme could depolymerize Psl and possibly influence the biofilm of *P. aeruginosa*.

4.6.1 *PaGH50A* hydrolysis of Psl

Enzyme activity assay was performed to determine if *Pa*GH50A had an effect on purified Psl isolated from *P. aeruginosa* strain PAO1 ΔWspF ΔPel. For this assay a different reducing end assay was used than what was used for curdlan and lichenan (the MBTH assay) since the DNS assay had proven challenging to use. The result show that *Pa*GH50A indeed was able to depolymerize Psl (**Figure 4-25**), showing activity at pH 7.5 comparable to the that of *Pa*GH50A hydrolysis of curdlan.

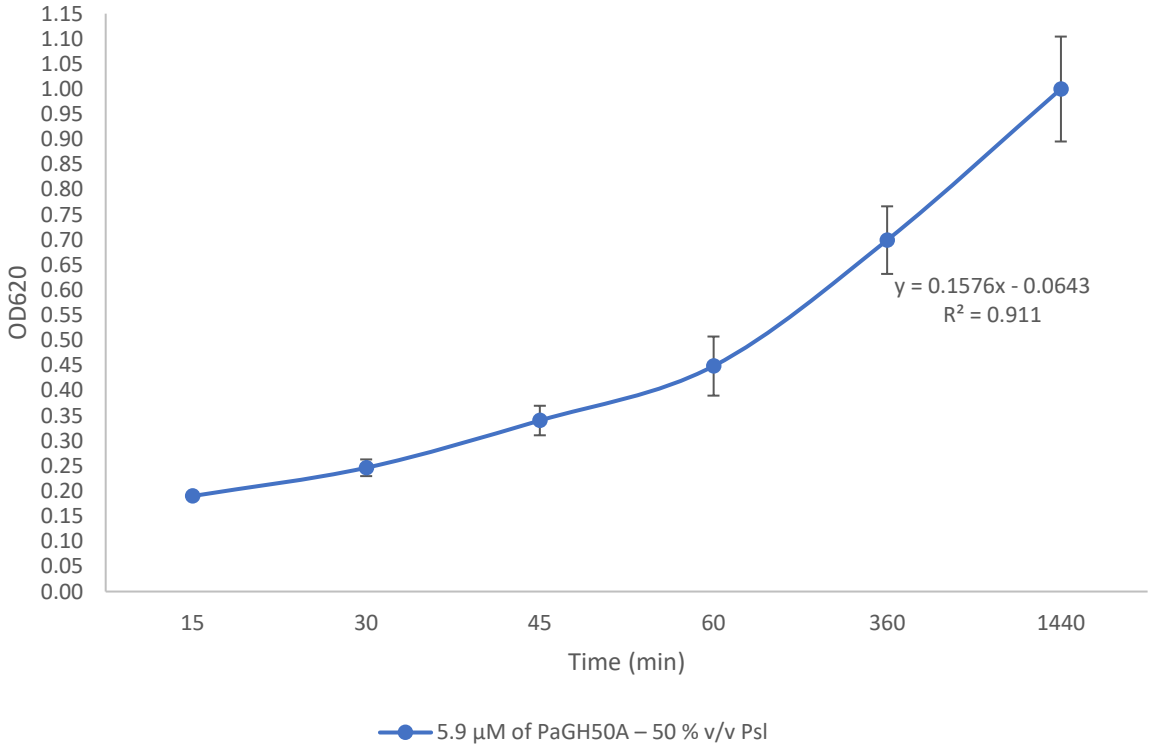

Figure 4-22 PaGH50A activity assay with towards Psl. Enzyme activity was investigated with 50 % v/v Psl and analysed using MBTH assay. The y-axis represents OD_{620} (since a glucose standard was not prepared, thus the relative activity % was unable to be calculated) while the x-axis represents the time. The progress curve was based on the average of a triplicate and the error bars represent standard deviation between the measurements.

4.6.2 Agar plate based *Pa*GH50A activity assay

The effect of *Pa*GH50A on *P. aeruginosa* biofilm cultivated in agar plates were investigated. When *Pa*GH50A was applied concurrently with *P. aeruginosa* suspensions no halo formation was observed (**Figure 4-26**). Further investigation of halo formation on agar plates were explored using the same method, however *Pa*GH50A solution was applied 18 hours after *P. aeruginosa* inoculations. This did neither produce halos around the enzyme application zones (**Figure 4-27**). The results indicate that *Pa*GH50A did not have degradative properties on *P. aeruginosa* biofilm cultivated on agar plates.

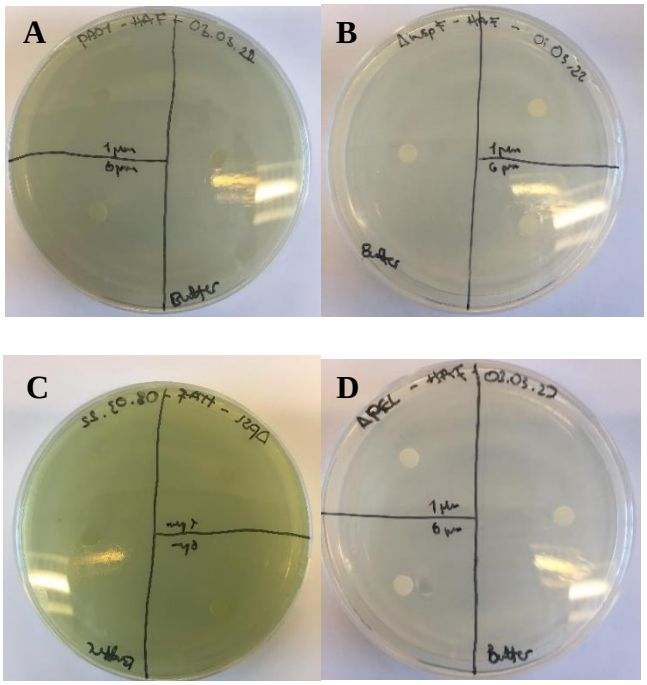

Figure 4-23 Analysis of halo formation on agar plates inoculated with P. aeruginosa PAO1 (A) and mutant strains PAO1 æ W s µ(B), P A O 1 ææPW(C)µ F d P A O 1 æ (D). A, B, C, and D shows a divided agar plate inoculated with P. aeruginosa of various strains incubated concurrently with PaGH50A. To one partition 20 µL Tris-HCl buffer pH 7.5 and to the two other partitions 20 µL of PaGH50A with the following concentrations 1 and 6 µM.

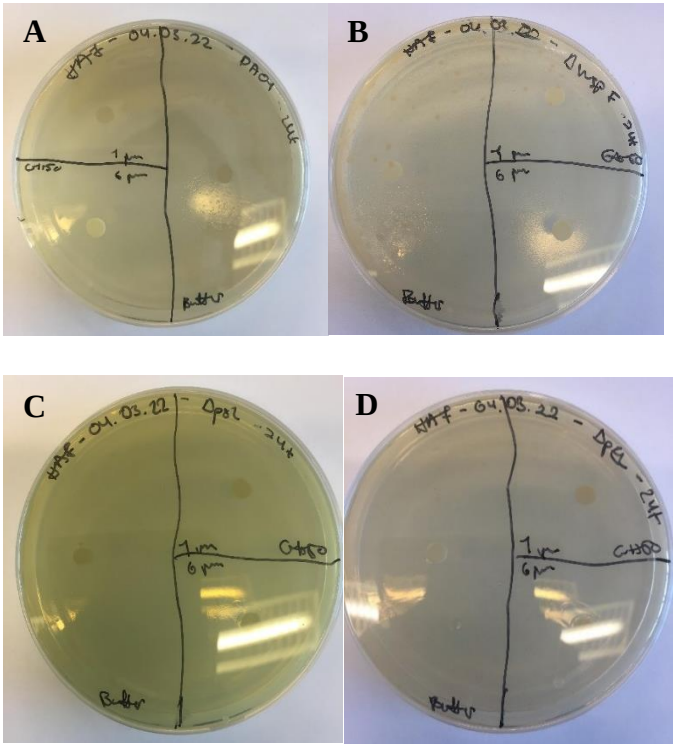

Figure 4-24. Analysis of halo formation on agar plates inoculated with P. aeruginosa PAO1 (A) and mutant strains PAO1 œ W s µ(B), P A O 1 œ W(C)µ Fn d œ HPsAlO 1 œ (D). A, B, C, aD Pshows a divided agar plate inoculated with P. aeruginosa of various strains and PaGH50A applied 18 hours after inoculation. To one partition 20 µL Tris-HCl buffer pH 7.5 and to the two other partitions 20 µL of PaGH50A with the following concentrations 1 and 6 µM.

4.6.3 The effect of *Pa*GH50A on *P. aeruginosa* biofilm formation process

4.6.3.1 Analysis of *P. aeruginosa* biofilms inoculated 18 hours prior to *Pa*GH50A application

To determine the effect of *Pa*GH50A on mature single species biofilm, microbial attachment to abiotic surfaces were investigated. *P. aeruginosa* strains were inoculated in LB liquid media 18 hours prior to applying *Pa*GH50A. Prior to quantitively assessing the effect of *Pa*GH50A, pictures were taken showing colour changes of *P. aeruginosa* cultures in the microtiter wells. *P. aeruginosa* produces pigment compounds pyocyanin, pyorubin, pyomelanin and pyoverdine which gives the cultures the following distinct colors blue, red, brown, yellow-green (Debritto, et al., 2020). The results showed that *Pa*GH50A can trigger pigment production in *P. aeruginosa* biofilms (**Figure 4-28**).

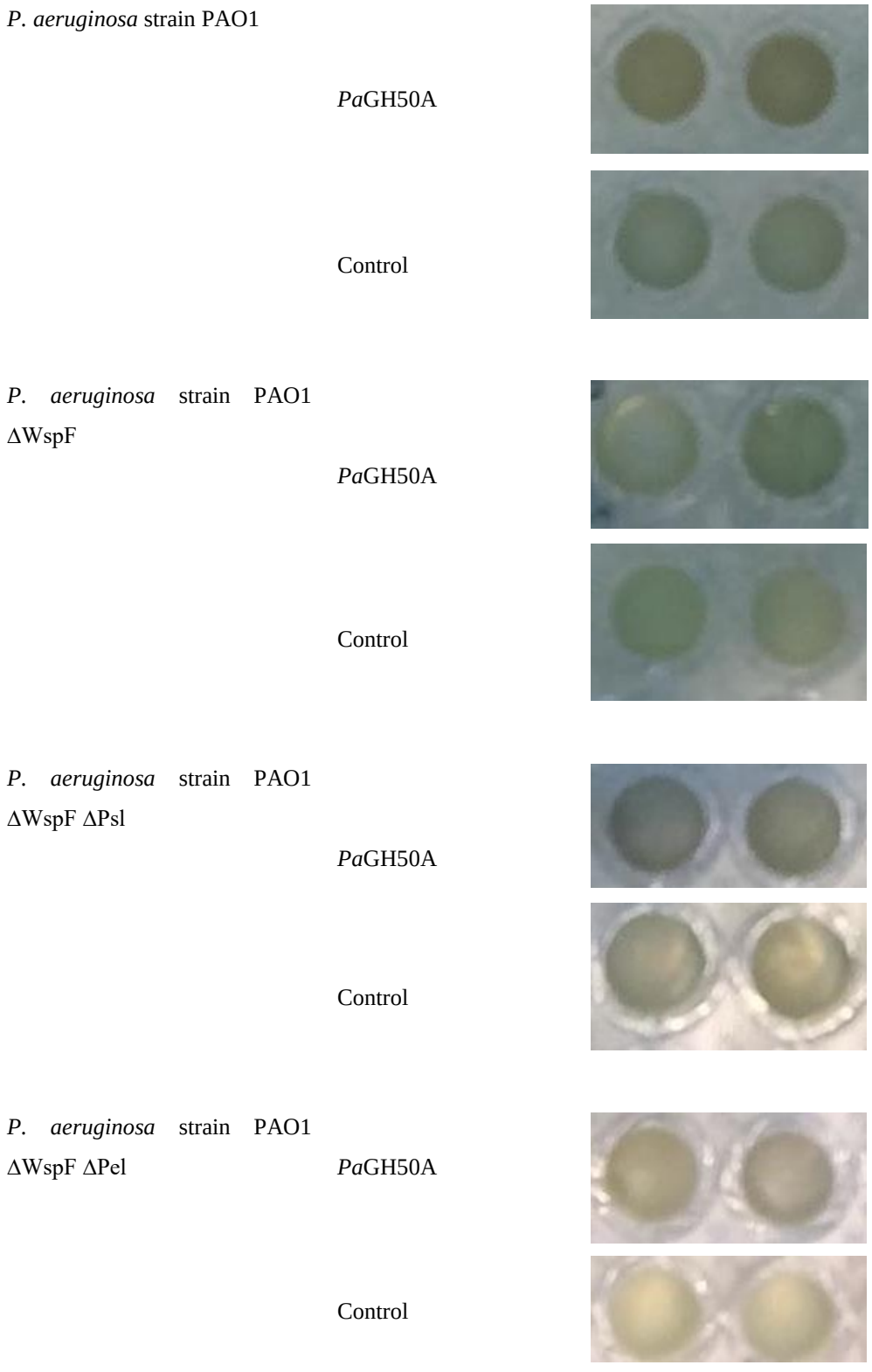

Figure 4-25 Color shifts in P. aeruginosa cultures in microtiter wells. P. aeruginosa suspensions were preincubated statically for 18 hours at 37 °C prior to adding 6 µM PaGH50A, followed by 24 hour incubation. A, B, C, D) shows samples with PaGH50A and controls for the following P. aeruginosa strains; PAO1, P A O 1 æ W s p F , P A O 1 æ W s p F æ P s l a n æ P eTwo parallels with PaGH50A and controls for each P. aeruginosa strain.

Quantification of adherent biofilm showed that *Pa*GH50A inhibits biofilm formation in *P. aeruginosa* PAO1, this is likely caused by *Pa*GH50A depolymerization of Psl in the biofilm matrix. However, the results also showed that biofilm formation was induced *P. aeruginosa* PAO1 ΔWspF ΔPsl (**Figure 4-29**). This could be due to a loss of Psl triggering overexpression of other exopolysaccharides such as cyclic-β-1,3-glucans in the biofilm matrix (Sadovskaya, et al., 2010).

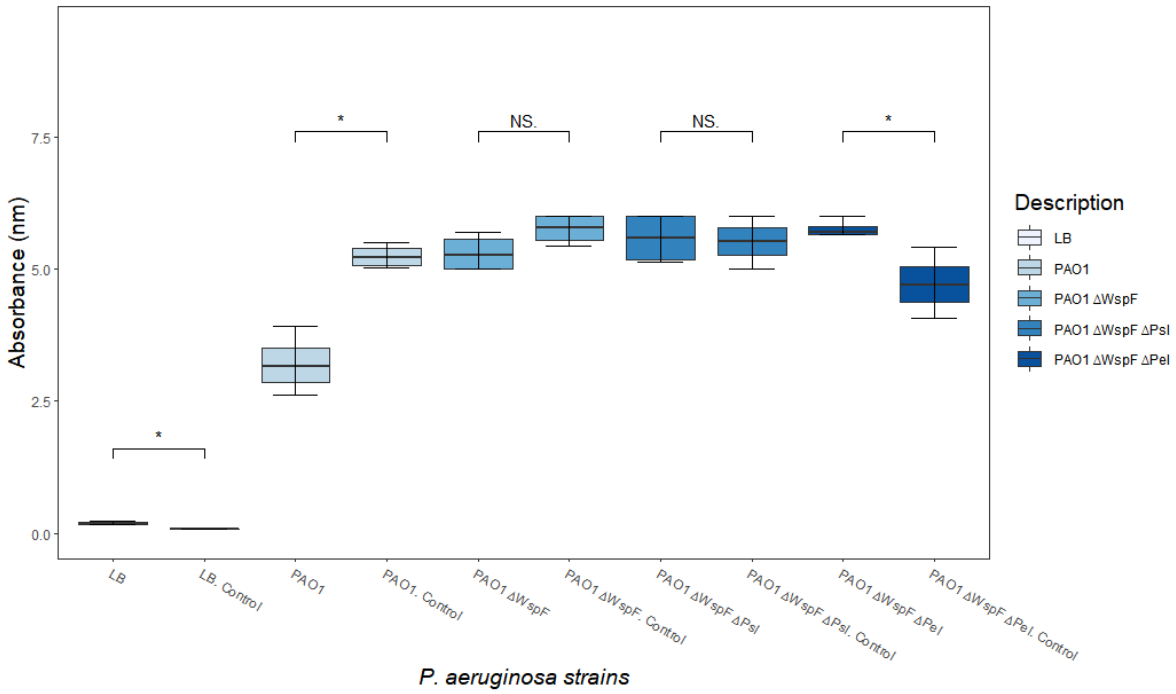

Figure 4-26. Analysis of adherent biofilm biomass after treatment with PaGH50A. P. aeruginosa suspensions were preincubated statically for 18 hours at 37 ºC prior to adding 6 µM PaGH50A, followed by 24 hour incubation. *The x-axis represents the P. aeruginosa strains; P A O 1 , P A O 1 æ W s p F , P A O 1 æ W s p F with applied PaGH50A and P A O 1 æ and controls while the y-axis represents the* OD_{595}*. Statical significance is marked with stars and NS. (Not significant).*

4.6.3.2 Analysis of P. aeruginosa biofilm formation when *Pa*GH50 is applied concurrently

Further investigation of the effect of *Pa*GH50A on biofilm formation and microbial attachment was performed. Similar to when *Pa*GH50A was applied to mature biofilm, a pigment shift was observed between samples with *Pa*GH50A and controls (**Figure 4-30**). Likely due to the same factors described for the colour change in section 4.6.3.1. However, the colour changed appeared more extreme when *Pa*GH50A when was applied concurrently with the *P. aeruginosa* cultures.

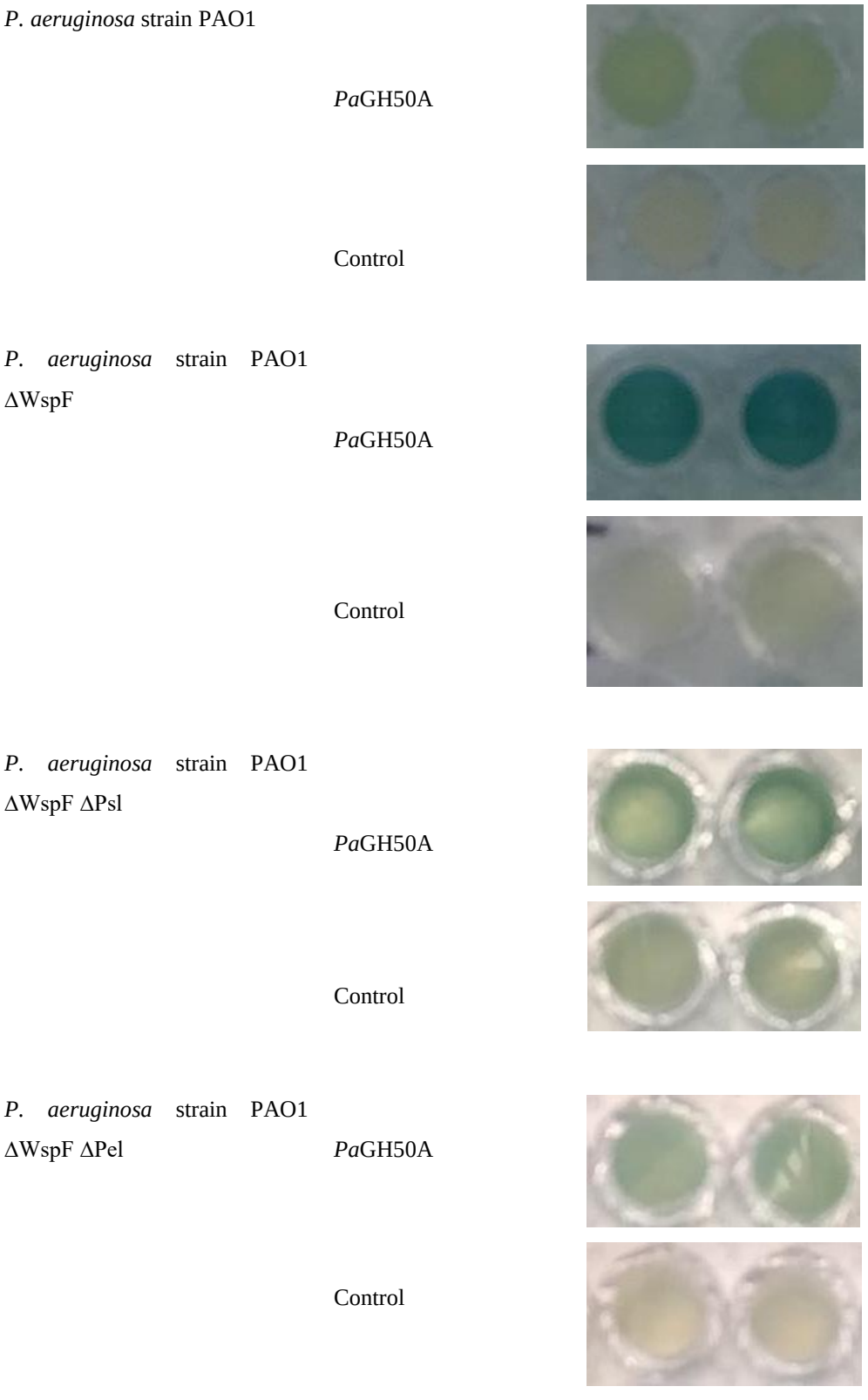

Figure 4-27. Color shifts in P. aeruginosa cultures in microtiter wells. P. aeruginosa suspensions were incubated concurrently with PaGH50A. A, B, C, D) shows samples with PaGH50A and controls for the following P. aeruginosa strains; PAO1, PAO1 æWspF, PAO1 æWspF æPsl and PAO1 æWspF æPel. Each P. aeruginosa strain alleles were incubated with PaGH50A and controls.

Quantification of adherent biofilm showed that *Pa*GH50A stimulates biofilm formation in all *P. aeruginosa* strains including the control strains PAO1 ΔWspF and PAO1 ΔWspF ΔPsl which produces little to no Psl (**Figure 4-31**). The reason for this occurrence is unknown without proteomics analysis. However, it is known that *P. aeruginosa* can develop biofilms under extreme conditions by secreting other exopolysaccharides such as cyclic-β-1,3-glucans (Sadovskaya, et al., 2010) in addition to producing more eDNA through cell lysis which strengths the biofilm architecture (Thi, Wibowo, & Rehm, 2020).

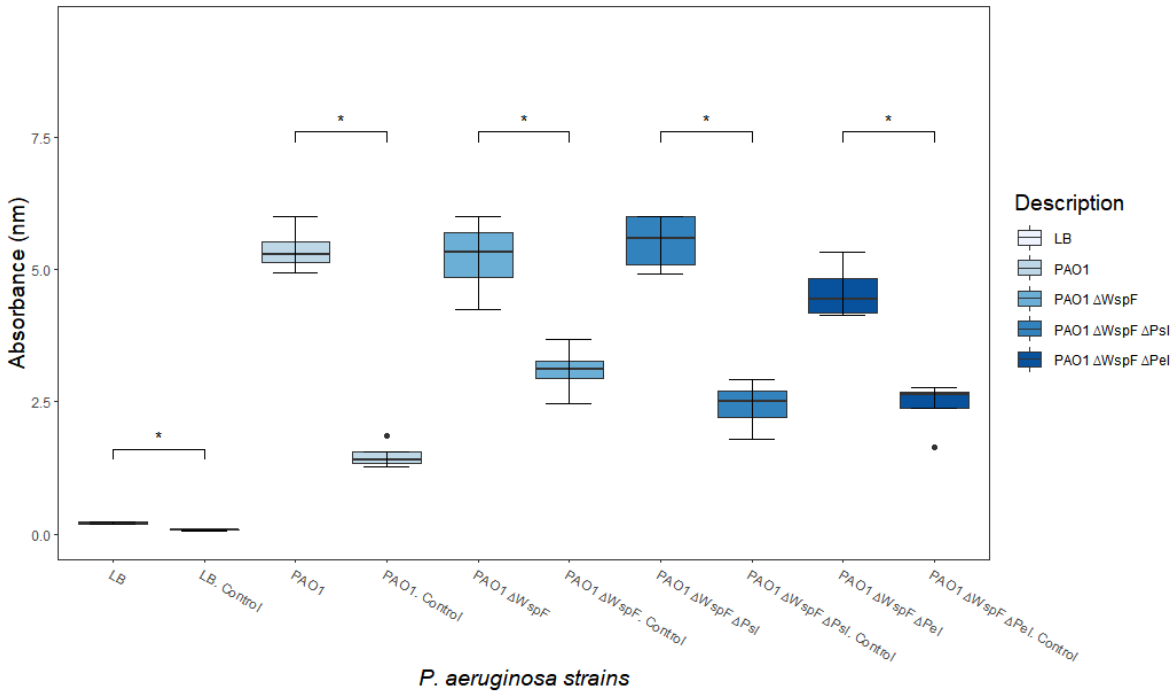

Figure 4-28. Analysis of adherent biofilm biomass after treatment with PaGH50A. P. aeruginosa suspensions were inoculated concurrently with 6 µM PaGH50A for 24 hours at 37 °C. The x-axis represents the P. aeruginosa strains PAO1 ΔWspF ΔPsl and PAO1 ΔWspF ΔPel while the y-axis represents the optical density of PaGH50A and measured at 595 nm. Statical significance is marked with stars and NS. (Not significant).

5. Discussion

In the present study, the aim was to provide a deeper biochemical characterization of *Pa*GH50A, a GH50 protein found in *P. aeruginosa* PA14 that previously has been shown to hydrolyze b-1,3 glycosidic bonds (Yi, yan, Jiang, & Wang, 2018). The secondary aim was to investigate its potential activity towards Psl and its potential in modulating the biofilm formation of *P. aeruginosa*.

5.1 Expression and purification

*Pa*GH50A was successfully cloned, expressed, and purified from the periplasm of *E. coli* BL21, however the production organism provided an inefficient protein yield. Initially, protein expression was investigated through optimization of parameters such as temperature, growth medium, incubation time and IPTG concentration. This did not lead to effective protein expression therefore cultivation in Lex-48 bioreactor in conjunction with extraction from periplasm was attempted. This method was more effective, and the elution fraction yielded 0.945 mg protein /L of *Pa*GH50A when *E. coli* BL21 was grown in Lex-48 bioreactor in comparison to 0.663 mg protein /L when using a shaker incubator. Increasing the number of cells did lead to higher protein expression, however the persistence of the low yield problem indicated that the enzyme was difficult to express. A phenomenon observed during IMAC purification and shown in the SDS-PAGE gels were that an almost equal amount of *Pa*GH50A was found in the wash fraction as in the elution fraction (**Figure 4-10**). The excessive presence of target protein in the wash fraction could have been due to the protein incorrectly folding such that the hexa histidine tag was unable to bind to the ligand in the column. Additionally, it was observed a large mass of protein at approximately 80 kDa in the cell pellet when cultivating in the Lex-48 bioreactor. This could be due to the formation of inclusion bodies leading the target protein to aggregate (Marisch, Bayer, Cserjan-Puschmann, Luchner, & Striedner, 2013). This may therefore also explain why the wash fraction contained enzymatically active misfolded target proteins. The problem occurring with low protein yields, where that samples with relative high concentration of imidazole to enzyme ratio could influence photometric measurements and potentially enzyme activity by interacting with the catalytic residues inducing conformational changes (Caramia, Gatius, Piaz, Gaja, & Hochkeppler, 2017). Therefore, it is

common to further purify target protein using a size exclusion chromatography, however due to the low protein yield further reduction of imidazole happened exclusively with buffer exchange.

5.2 Biochemical properties

An initial study of *Pa*GH50A already existed where activity towards lichenan and curdlan was shown using PaBglu50A. In the current study we set out to repeat these findings, but also characterize other properties of enzyme activity like product profile characterization by MALDI-TOF MS. Firstly the enzyme activity was investigated towards lichenan and curdlan using DNSA, a reducing end assay. The results verified that the enzyme called PaBglu50A by Yi et al, re-named *Pa*GH50A in this study, was indeed able to hydrolyze β-1,3 glycosidic linkages of lichenan and curdlan. The product formation were slightly different as most experiments in this study showed a 60-minute lag before activity accelerated. Non-linearity in product formation is often related to substrate depletion (Robinson, 2015), however this was accounted for, yet this phenomenon was recurrent in all experiments (**Figure 4-14**). It was showed that at curdlan concentration of 61.7 mM, the OD measurement remained lower than at 18.5 and 33.3 mM curdlan indicating that low enzyme activity was not caused by substrate depletion. A different problem which was encountered while performing enzyme activity assays were low enzyme activity levels relative to enzyme concentration. High productivity enzymes typically require low concentration of enzyme for substrate hydrolysis, however *Pa*GH50A required a concentration of 5.9 µM to average an OD of 1 Au (**Figures 4-12, 4-13**). Therefore, this problem may be more likely related to substrate specificity even though Yi, et al. determined that PaBglu50A was most active towards curdlan out of all tested substrates (Yi, yan, Jiang, & Wang, 2018).

For characterization of optimal conditions for subsequent experiments, optimum pH range was assessed. Results showed that the optimum pH for enzyme activity were within the range of 6.5-8.5, optimally at 8.5 (**Figure 4-15**). This contrasted from the results for PaBglu50A which showed that the enzyme was most active in acidic environments similar to most enzymes with endo-β-glucanase activity (Yi, yan, Jiang, & Wang, 2018). While pH optimum of AgWH50C, a homologous GH50 protein was determined at pH 6.0 with loss of activity at pH 5.0, 8.0 and 9.0 (Liu, Mao, Yang, Mu, & Wei, 2014) Thus a possible reason for *Pa*GH50A being most active

in alkaline environments could be suggested to be caused by when and where the enzyme is expressed in *P. aeruginosa* rather than what optimal pH is common for members of the GH50 family.

In an attempt to increase enzyme activity, *Pa*GH50A was incubated with divalent metal ions which could function as external electron donors. The results showed that the enzyme activity was weakly inhibited by the metal ions (**Figure 4-16**). Metal ions associating with *Pa*GH50A acted as an activity reducing agent by binding to the enzyme's catalytic residues, thus seizing space from substrates binding (Kilipin & Dyson, 2013). A similar phenomenon was seen with Sco3487, a GH50 protein found in S*teptomyces Coelicolor* A3. Here the Ca^{2+} and Zn^{2+} also weakly inhibit enzyme activity, Zn^{2+} more so than Ca^{2+} (Temuujin , Chi, Chang, & Hong, 2012).

MALDI-TOF was used to analyze hydrolysis products of curdlan and confirmed that *Pa*GH50A hydrolyzes curdlan by an endo-mechanism into β-1,3-oligosaccharides with different degrees of polymerization (**Figure 4-17**). The major products were disaccharides to pentasaccharide, however the hydrolysis products ranged from disaccharides to heptasaccaride when enzyme activity was at its optimal. The products ranged from disaccharide to nonasaccharide under non favorable conditions. Varying external conditions such as substrate concentrations, pH, temperature, and addition of inert salts did not alter the product profile, only increased or decreased signal intensities. In comparison major hydrolysis products (analyzed by Thin-Layer chromatography) by PaBglu50A ranged from glucose to tetrasaccharide. AgaB found in *Vibrio* sp., member of the GH50 family and hydrolyzes agarose to yield major hydrolysis products neoagarotetraose and neoagarhexaose (Matsumoto, Norna, & Sugano, 1994) . Moreover, AgWH50A found in *Agarivorans gilvus* WH801 generates mainly neoagarotetraose (Liu, Mao, Du, Mu, & Wei, 2014)B. The predominant product generated by *Pa*GH50A being a tetramer resonates well with findings for other members of the GH50 family. Psl was unable to be analyzed using MALDI-TOF. One of reason for the inadequacy of the method for analysis of Psl may be that the sizes of the hydrolysis products were outside the range of the MALDI-TOF MS analysis since the repeating unit of Psl is a pentasaccharide (**Figure 1-4**). Thus, if *Pa*GH50A is only specific for one bond in the backbone of Psl, the smallest product is predicted to be 669 Da, the second smallest 1337.3 Da. If these are produced in smaller amounts than detectable while the larger oligosaccharides are generated in higher amounts, could be a factor in why MALDI-TOF analysis was unsuccessful. Moreover, analysis of oligosaccharides was attempted with HPLC-Rezex-RI and with HPLC-PGC-CAD. However, analysis of hydrolysis products were unsuccessful with both methods. Neither method could separate the

oligosaccharides of curdlan, lichenan and Psl, leading all the analytes to elute simultaneously. Possible causes for terrible separation in the column could be that too low amounts of hydrolysis products were generated, that the oligosaccharides had low retention in the column or that the methods had low sensitivity. It would be interesting to develop a method specific for analysis hydrolysis products for PaGH50A, it would allow for analysis of product profiles for lichenan and Psl as well, which was unsuccessful with MALDI-TOF.

STRING analysis showed that *Pa*GH50A was associated with PslG, a GH39 protein involved in the Psl biosynthetic process. PslG is directly involved in Psl synthesis in *P. aeruginosa*, however when applied exogenously or overexpressed disrupts the Psl matrix to disperse sessile cells from the biofilm (Yu , et al., 2015). This suggested that in combination with *Pa*GH50A β-1,3-hydrolase activity also could degrade the Psl polymer. The results showed that *Pa*GH50A could in fact hydrolyse the β-1,3-glycosidic linkages in purified Psl (**Figure 4-25**). Enzyme activity in Psl degradation was similar to curdlan and lichenan degradation, indicating that *Pa*GH50A can react with multiple substrates equally and perhaps due to the low enzyme activity with all the substrates that the specific substrate for *Pa*GH50A is unknown.

The melting curve of *Pa*GH50A showed that the enzyme had melting temperatures of 28 and 51 ^{o}C (**Figure 4-11**). This suggested that the enzyme consisted of more than the GH50 domain, diverging from what was previously predicted (**Figure 4-2**). MALDI-TOF analysis of hydrolysis products at 23 ^{o}C generated a similar specter as at 50 ^{o}C (**Figure 4-19**). Though nothing definitive can be said it seems that the smaller domain does not play a direct role in enzyme activity but could play an indirect role by lowering temperature stability and structural integrity.

5.3 Targeting *P. aeruginosa* biofilms

Biofilm structures are consortium of sessile cells encapsulated in a self-generated matrix. Eradication of *P. aeruginosa* cells in planktonic state is without much difficulty, however problem arises when *P. aeruginosa* forms biofilms. Biofilms allows for *P. aeruginosa* in sessile state to be resistant to antimicrobial agents. Prevention strategies are imperative for effective disruption of biofilms followed by suppression of biofilm formation with antimicrobial agents. Biofilm formation and disassembly involves hydrolases that target exopolysaccharides in the ECM (Thi, Wibowo, & Rehm, 2020). Based on the promising results in the present study

showing Psl depolymerization by *Pa*GH50A (**Figure 4-25**), the ability of the enzyme to modulate or disrupt biofilm formation by *P. aeruginosa* was investigated. Similar approaches targeting *P. aeruginosa* Pel and alginate have shown promising results for biofilm disruption (Kovach, Fleming, Wells, Rumbaugh, & Gordon, 2020).

90 % of the biofilm biomass is composed of EPS. This feature of biofilms was exploited with agar-based biofilm assay. Despite *Pa*GH50A being applied exogenously to LB agar plates with *P. aeruginosa* strains PAO1 and its mutants PAO1 ΔWspF, PAO1 ΔWspF ΔPsl and PAO1 ΔWspF ΔPel, no halos that indicate biofilm degradation, were observed in the enzyme application zone (**Figure 4-26 and 4-27**). In the absence of a positive control, it was not possible to make any concrete conclusion about the biofilm degrading abilities of *Pa*GH50A, but the lack of halo formation indicate that this enzyme alone is not enough to prevent *P. aeruginosa* form forming a Psl containing biofilm.

Since agar-based biofilm assay has many limitations, a better suited method was applied, using plastic microtiter plates for biofilm development and crystal violet for biofilm staining and quantification. In the first assay, the *P. aeruginosa* biofilms were formed prior to addition of *Pa*GH50A in order to determine if the enzyme could disintegrate the biofilm structure. The results showed that it indeed seemed that *Pa*GH50A could partly degrade the biofilm of *P. aeruginosa* strain PAO1, but interestingly not in the Psl overexpression mutant PAO1 ΔWspF and PAO1 ΔWspF ΔPel (**Figure 4-29**). The reason for this may be that *Pa*GH50A triggered overexpression of other exopolysaccharides than psl and pel in *P. aeruginosa* biofilm such as cyclic-β-1,3-glucans which is localized in the biofilm pellicle and gives biofilm an increased resistance to antibiotics through physical interactions (Sadovskaya, et al., 2010), Pel when expressed is also found in the pellicle region. Additionally, a higher production of pyocyanin recognized by its characteristic blue color (**Figure 4-30**, **P A O 1 æ Y**, **p** cell lysis and release of eDNA which also promotes biofilm maturation and integrity (Thi, Wibowo, & Rehm, 2020). *P. aeruginosa* adapted to CF lungs by overexpressing alginate instead of Psl and pel, alginate may add support to the biofilm integrity, however alginate adhesion is very weak to abiotic surfaces (Nivens, Ohman, Williams, & Franklin, 2001) and would not explain the increased adherent biomass which was quantified. A different reason for higher adherent biomass may be due to Psl expression being up regulated by c-di-GMP signaling (Valentini & Filloux, 2016) to a degree in where it out competes *Pa*GH50A. It was previously shown that at higher curdlan concentration, that the enzyme activity fell significantly (**Figure 4-14**), something similar may be occurring here.

The experiment was repeated, but instead of adding *Pa*GH50A after biofilm had matured, the enzyme was added concurrently with *P. aeruginosa* suspensions to determine if biofilm deposition could be prevented or delayed. Surprisingly, the results showed that the complete opposite occurred. *Pa*GH50A appeared to have biofilm stimulating properties in all of the *P. aeruginosa* strains including the control strains PAO1 ΔWspF and PAO1 ΔWspF ΔPsl which were not expected to have an increase in biomass due to (low or) lack of Psl expression (**Figure 4-31**). Why and how *Pa*GH50A mediate the biofilm formation to this capacity is unknown, however it can be speculated that for the same reasons given for increased biofilm biomass in PAO1 ΔWspF ΔPel (**Figure 4-29**) affects the biofilm in the early stages of development. Additionally, components of early biofilm vary from the components in mature biofilm, therefore *Pa*GH50A may be thought to interact with different proteins and substrates at different points during the biofilm formation, leading to up or down regulation of genes by QS system involved in virulence (Thi, Wibowo, & Rehm, 2020). This may be the case for PAO1 ΔWspF and PAO1 ΔWspF ΔPsl which showed no significant difference between mature biofilm with *Pa*GH50A and the controls (**Figure 4-29**), but showed the opposite when the cultures were incubated concurrently with *Pa*GH50A (**Figure 4-31**). To be able to say anything conclusive about the reason for why and how *Pa*GH50A is able to both inhibit and stimulate biofilm formation depending on time of application more experimentation is required along with creating mutants of *Pa*GH50A.

Another interesting observation made was how *Pa*GH50A effected the pigmentation of *P. aeruginosa* cultures in the microtiter wells depending on when the enzyme was applied (**Figure 4-28 and 4-30**). Possible explanations may depend on pigment compounds pyocyanin, pyorubin, pyomelanin and pyoverdine which gives the *P. aeruginosa* colonies the following distinct colors blue, red, brown, and yellow-green (Debritto, et al., 2020). During a *P. aeruginosa* infection, a bluish green pigment is observed which is typical for *P. aeruginosa* strains, however the brown pigment was hypothesized to be caused by spontaneous mutants with altered characteristics such as increased resistance to virulent bacteriophages and growth advantages in the presence of sulfathiazole (Howarth & Dedman, 1964). Pyoverdine is essential for *P. aeruginosa* pathogenesis and crucial for iron scavenging while pyocyanin is a cytotoxic antioxidant that causes cell lysis through generation of reactive oxygen intermediates (Hassett, Charniga, Bean, Ohman, & Cohen, 1996). The results indicate that when *P. aeruginosa* was inoculated concurrently with *Pa*GH50A the bacteria became more virulent thus stimulating

biofilm formation. The direct interactions between *Pa*GH50A and *P. aeruginosa* which caused the pigment change was not further studied due to lack of time.

6. Concluding remarks and future perspectives

The focus of this study was biochemical characterization of *Pa*GH50A, a GH50 protein found *P. aeruginosa* PA14 that previously had been shown to hydrolyze b-1,3 glycosidic linkages. *Pa*GH50A was successfully cloned, expressed, and purified from *E. coli* BL21. Biochemical properties such as enzyme activity under various conditions and melting temperature were assessed to develop an understanding of the biological function of *Pa*GH50A. Analysis of *Pa*GH50A confirmed that the enzyme does indeed catalyzes the hydrolysis of β-1,3 glycosidic linkages in curdlan, lichenin and Psl. MALDI-TOF analysis showed that the mayor hydrolysis products of curdlan ranged from disaccharide to pentasaccharide.

Furthermore, the potential of *Pa*GH50A in modulating biofilm formation of *P. aeruginosa* was investigated. Analysis showed that *Pa*GH50A could act as a biofilm inducer and inhibitor depending on whether the enzyme was applied to mature biofilm or concurrently with *P. aeruginosa* cultures. Interesting results were shown, however with the lack of research on a single enzyme with such properties, it can only be speculated that *Pa*GH50A interacts with various systems triggering different cellular responses. Future research on *Pa*GH50A should be directed at the biofilm stimulating properties by investigating which proteins *Pa*GH50A up or down regulates through proteomics analysis. Additionally, methods for quantifying and identifying the hydrolysis products of Psl should be established.

7. References

Allen, L., Dockrell, D. H., Pattery, T., Lee, D. G., Cornelis, P., Hellewell, P. G., & Whyte, M. K. (2005, March 15). *Pyocyanin Production by Pseudomonas aeruginosa Induces Neutrophil Apoptosis and Impairs Neutrophil-Mediated Host Defenses In Vivo*. Retrieved from The Journal of Immunology, Vol. 174, Issue 6: https://doi.org/10.4049/jimmunol.174.6.3643

Allen, P., Borick, J., & Borick , J. (2020, Janurary 29). *Acute and Chronic Infection Management in CF*. Retrieved from Cystic Fibrosis in Primary Care pp 69–87: https://dx.doi.org/10.1007%2F978-3-030-25909-9_8

Almeling, S., IIko, D., & Holzgrabe, U. (2012, March 21). *Charged aerosol detection in pharmaceutical analysis*. Retrieved from Journal of Pharmaceutical and Biomedical Analysis 69:50-63: http://dx.doi.org/10.1016/j.jpba.2012.03.019

Anthis, N. J., & Clore, M. G. (2013). *Sequence-specific determination of protein and peptide concentrations by absorbance at 205 nm*. Retrieved from Protein Science: https://dx.doi.org/10.1002%2Fpro.2253

Anthon, G. E., & Barrett, D. M. (2002). *Determination of Reducing Sugars with 3-Methyl-2-benzothiazolinonehydrazone*. Retrieved from Analytical Biochemistry Volume 305, Issue 2, pages 287-289: https://doi.org/10.1006/abio.2002.5644

Armbruster, C. R., & Matthew, P. R. (2018, April 9). *New insight into the early stages of biofilm formation*. Retrieved from The Proceedings of the National Academy of Sciences, 115 (17), pages 4317-4319: https://doi.org/10.1073/pnas.1804084115

Armenteros, J. J., Tsirigos, K. D., Sønderby, C. K., Petersen, T. N., Winther, O., Brunak, S., . . . Nielsen, H. (2019). *SignalP 5.0 improves signal peptide predictions using deep neural networks*. Retrieved from Nature Biotechnology volume 37, pages: 420–423 : https://doi.org/10.1038/s41587-019-0036-z

Asif, A., Mohsin, H., Tanvir, R., & Rehman, Y. (2017). *Revisiting the Mechanisms Involved in Calcium Chloride Induced Bacterial Transformation*. Retrieved from Frontiers in Microbiology: https://doi.org/10.3389/fmicb.2017.02169

Ati, J., Lafite, P., & Daniellou, R. (2017, May 2). *Enzymatic synthesis of glycosides: from natural O- and N-glycosides to rare C- and S-glycosides*. Retrieved from Beilstein Journal of Organic Chemistry: 13, pages 1857–1865.: https://dx.doi.org/10.3762%2Fbjoc.13.180

Bachta, K. E., Allen, J. P., Cheung, B. H., Chiu, C.-H., & Hauser, A. R. (2020, Janurary 28). *Systemic infection facilitates transmission of Pseudomonas aeruginosa in mice*. Retrieved from Nature Communications, Issue 11, page 543: https://dx.doi.org/10.1038%2Fs41467-020-14363-4

Bapiro, T. E., Frances, R. M., & Jodrell, D. I. (2016, May 26). *Understanding the Complexity of Porous Graphitic Carbon (PGC) Chromatography: Modulation of Mobile-Stationary Phase Interactions Overcomes Loss of Retention and Reduces Variability*. Retrieved from Analytical Chemistry: 88(12): pages: 6190–6194: https://dx.doi.org/10.1021%2Facs.analchem.6b01167

Bashir, K. M., & Choi, J.-S. (2017, September 5). *Clinical and Physiological Perspectives of β-Glucans: The Past, Present, and Future*. Retrieved from International Journal of Molecular Sciences: 18(9), page 1906: https://dx.doi.org/10.3390%2Fijms18091906

Benedetti, S. D., Leogrande, C., Castagna, F., Heinzl, G. C., Pasquali, M., Heinzl, A. L., . . . Scaeafoni, A. (2022, January 3). *Thermal Shift Assay as a Tool to Evaluate the Release of Breakdown Products during Seed Germination in Vigna unguiculata L. Walp. and Cowpea*. Retrieved from Monecules: Chemical and Functional Properties of Food Proteins, page, 277: https://doi.org/10.3390/molecules27010277

Blum, M., & et. al. (2021, Janurary 8). *The InterPro protein families and domains database: 20 years on* . Retrieved from Nucleic Acids Research, Volume 49, Issue D1, Pages D344–D354: https://doi.org/10.1093/nar/gkaa977

Brady, P. N., & Macnaughtan, M. A. (2015). *Evaluation of Colorimetric Assays for Analyzing Reductively Methylated Proteins: Biases and Mechanistic Insights*. Retrieved from Analytical Biochemistry, Volume 491, pages: 43-51: https://dx.doi.org/10.1016%2Fj.ab.2015.08.027

Briand, L., Marcion, G., Kriznik, A., Heydel, J. M., Artur, Y., Garrido, C., . . . Neiers, F. (2016). *A self-inducible heterologous protein expression system in Escherichia coli*. Retrieved from Sceintific Reports: https://dx.doi.org/10.1038%2Fsrep33037

Byrd, M. S., Sadovskaya, I., Vinogradov, E., Haiping, L., Sprinkle, A. B., & et, al. (2009, August 7). *Genetic and Biochemical Analyses of the Pseudomonas aeruginosa Psl Exopolysaccharide Reveal Overlapping Roles for Polysaccharide Synthesis Enzymes in Psl and LPS Production*. Retrieved from Molecular Microbiology, Volume 73, Issue 4, pages 622-638: https://dx.doi.org/10.1111%2Fj.1365-2958.2009.06795.x

Campoccia, D., Montanaro, L., & Arciola, C. R. (2021, August 23). *Extracellular DNA (eDNA). A Major Ubiquitous Element of the Bacterial Biofilm Architecture*. Retrieved from International Journal of Molecular Sciences; 22(16): 9100: https://dx.doi.org/10.3390%2Fijms22169100

Caramia, S., Gatius, A. G., Piaz, F. D., Gaja, D., & Hochkeppler, A. (2017). *Dual role of imidazole as activator/inhi-glucosidase. of sweet* Retrieved from Biochemistry and Biophysics Reports, Volume 10, Pages 137-144: https://doi.org/10.1016/j.bbrep.2017.03.007

Casares, D., Escriba, P. V., & Rossello, C. A. (2019, May 20). *Membrane Lipid Composition: Effect on Membrane and Organelle Structure, Function and Compartmentalization and Therapeutic Avenues*. Retrieved from International Journal of Molecular Sciences : https://dx.doi.org/10.3390%2Fijms20092167

Castro-Chavez, F. (2012). *Escaping the Cut by Restriction Enzymes Through Single-Strand Self-Annealing of Host-Edited 12-bp and Longer Synthetic Palindromes*. Retrieved from DNA Cell Biol; 31(2): 151–163. : https://doi.org/10.1089%2Fdna.2011.1339

Cerquerira, N., Bras, N., Ramos, M. J., & Fernandes, P. A. (2011, November 29). *Glycosidases ï A Mechanistic Overview In (Ed.), Carbohydrates - Comprehensive Studies on Glycobiology and Glycotechnology.* Retrieved from IntechOpen: https://doi.org/10.5772/52019

Chaudhari, V., Buttar, H. S., Bagwe-Parab, S., Tuli, H. S., Vora, A., & Kaur, G. (2021, June 28). *Therapeutic and Industrial Applications of Curdlan With Overview on Its Recent Patents*. Retrieved from Frontiers in Nutrition: 8: 646988. : https://dx.doi.org/10.3389%2Ffnut.2021.646988

Colvin, K. M., Irie, Y., Tart, C. S., Urbano, R., Whitney, J. C., Ryder, C., . . . Parsek, M. R. (2011). *The Pel and Psl polysaccharides provide Pseudomonas aeruginosa structural redundancy within the biofilm matrix*. Retrieved from Environmental Microbiology,

Volume 14, Issue 8, pages 1913-1928: https://dx.doi.org/10.1111%2Fj.1462-2920.2011.02657.x

Darling, S., Burge, R., Manley, G., Sami, S., & Tummalai, S. (2016, January 15). *The Ongoing Evolution of Buffer Exchange*. Retrieved from Genetic Engineering & Biotechnology News Vol. 36, No. 2: http://dx.doi.org/10.1089/gen.36.02.13

Debritto, S., Gajbar, T., Satapute, P., Sundaram, L., Lakshimikantha, R. Y., Jogaiah, S., & Ito, S.-i. (2020). *Isolation and characterization of nutrient dependent pyocyanin from Pseudomonas aeruginosa and its dye and agrochemical properties*. Retrieved from Scientific Reports volume 10, Article number: 1542 : https://doi.org/10.1038/s41598-020-58335-6

Diggle, S. P., & Whiteley, M. (2020, January 16). *Microbe Profile: Pseudomonas aeruginosa: opportunistic pathogen and lab rat*. Retrieved from Microbiology, Volume 166, Issue 1: https://dx.doi.org/10.1099%2Fmic.0.000860

Donlan, R. M. (2001, October 15). *Biofilm Formation: A Clinically Relevant Microbiological Process*. Retrieved from Clinical Infectious Diseases, Volume 33, Issue 8, Pages 1387–1392,: https://doi.org/10.1086/322972

Drula, E., Garron, M.-L., Dogan, S., Lombard, V., Henrissat, B., & Terrapon, N. (2022, Janurary 7). *The carbohydrate-active enzyme database: functions and literature*. Retrieved from Nucleic Acids Research, Volume 50, Issue D1, Pages: D571–D577: https://doi.org/10.1093/nar/gkab1045

Elias, S., & Banin, E. (2012, September 1). *Multi-species biofilms: living with friendly neighbors*. Retrieved from FEMS Microbiology Reviews, Volume 36, Issue 5, Pages 990–1004: https://doi.org/10.1111/j.1574-6976.2012.00325.x

Fasciano, J. M., Mansour, F. R., & Danielson, N. D. (2016, July). *Ion-Exclusion High-Performance Liquid Chromatography of Aliphatic Organic Acids Using a Surfactant-Modified C18 Column*. Retrieved from Journal of Chromatographic Science, Volume 54, Issue 6, July 2016, Pages 958–970: https://doi.org/10.1093/chromsci/bmw028

Ferriol-Gonzalez, C., & Domingo-Calep, P. (2020, May 21). *Phages for Biofilm Removal*. Retrieved from Antibiotics 2020, 9(5), page 268: https://doi.org/10.3390/antibiotics9050268

Franklin , M. J., Nivens, D. E., Weadge, J. T., & Howell, P. L. (2011, August 22). *Biosynthesis of the Pseudomonas aeruginosa extracellular polysaccharides, alginate, Pel, and Psl*. Retrieved from Frontiers in Microbiology: https://doi.org/10.3389/fmicb.2011.00167

Gasteiger, E., Hoogland, C., Gattiker, A., Duvaud, S., Wilkins, M. R., Appel, R. D., & Bairoch, A. (2005). *Protein Identification and Analysis Tools on the ExPASy Server*. Retrieved from John M. Walker (ed): The Proteomics Protocols Handbook, Humana Press, Pages: 571-607: https://web.expasy.org/docs/expasy_tools05.pdf

Gaudino, S. J., & Kumar, P. (2019, March 6). *Cross-Talk Between Antigen Presenting Cells and T Cells Impacts Intestinal Homeostasis, Bacterial Infections, and Tumorigenesis*. Retrieved from Frotiers in Immunology: https://dx.doi.org/10.3389%2Ffimmu.2019.00360

Gellatly, S. L., & Hancock, R. E. (2013, April 1). *Pseudomonas aeruginosa : new insights into pathogenesis and host defenses*. Retrieved from Pathogens and Disease, Volume 67, Issue 3, Pages 159–173: https://doi.org/10.1111/2049-632X.12033

Gessard, C. (1882). *On the Blue and Green Coloration that Appears on Bandages*. Retrieved from CLASSICS IN INFECTIOUS DISEASES: http://citeseerx.ist.psu.edu/viewdoc/download?doi=10.1.1.965.8365&rep=rep1&type=pdf

Golovkine, G., Faudry, E., Bouillot, S., Voulhoux, R., Attree, I., & Huber, P. (2014, March 13). *VE-Cadherin Cleavage by LasB Protease from Pseudomonas aeruginosa Facilitates Type III Secretion System Toxicity in Endothelial Cells*. Retrieved from Journal Plos Pathogens: https://doi.org/10.1371/journal.ppat.1003939

Golovkine, G., Reboud, E., & Huber, P. (2019, Janurary 11). *Pseudomonas aeruginosa Takes a Multi-Target Approach to Achieve Junction Breach*. Retrieved from Frontiers in Cellular and Infection Microbiology: https://doi.org/10.3389/fcimb.2017.00532

Gomila, M., Pena, A., Mulet, M., Lalucat, J., & Garcia-Valdes, E. (2015, March 18). *Phylogenomics and systematics in Pseudomonas*. Retrieved from Frontiers in Microbiology: https://doi.org/10.3389/fmicb.2015.00214

Gupta, N. (2019). *DNA Extraction and Polymerase Chain Reaction*. Retrieved from Journal of cytology 36(2): 116–117: https://doi.org/10.4103%2FJOC.JOC_110_18

Gusakov, A. V., Kondratyeva, E. G., & Sinitsyn, A. P. (2011). *Comparison of Two Methods for Assaying Reducing Sugars in the Determination of Carbohydrase Activities*. Retrieved from International Journal of Analytical Chemistry, vol. 2011, Article ID 283658, 4 pages: https://dx.doi.org/10.1155%2F2011%2F283658

Hashim, H. O. (2018, January 10). *chromatography and HPLC principles, 1-15*. Retrieved from http://dx.doi.org/10.13140/RG.2.2.33635.25126

Hassett, D. J., Charniga, L., Bean, K., Ohman, D. E., & Cohen, M. S. (1996, February). *Response of Pseudomonas aeruginosa to pyocyanin: mechanisms of resistance, antioxidant defenses, and demonstration of a manganese-cofactored superoxide dismutase*. Retrieved from Infection Immunity; 60 (2), pages 328–336. : https://dx.doi.org/10.1128%2Fiai.60.2.328-336.1992

Ho, C., Lam, K., Chan, M. H., & et, al. (2003, February 24). *Electrospray Ionisation Mass Spectrometry: Principles and Clinical Applications*. Retrieved from The Clinical Biochemist Reviews 2003: 3–12. : https://www.ncbi.nlm.nih.gov/pubmed/18568044

Horn, S. J., & Eijsink, V. G. (2003). *A reliable reducing end assay for chito-oligosaccharides*. Retrieved from Elsevier Ltd. Carbohydrate Polymers 56 (2004) 35–39: https://doi:10.1016/j.carbpol.2003.11.011

Hotterbeekx, A., Kumar-Singh, S., Goossens, H., & Malhotra-Kumar, S. (2017, April 3). *In vivo and In vitro Interactions between Pseudomonas aeruginosa and Staphylococcus spp.* Retrieved from Frontiers in Cellular and Infection Microbiology; 7: 106. : https://dx.doi.org/10.3389%2Ffcimb.2017.00106

Howarth, S., & Dedman, M. D. (1964, August). *PIGMENTATION VARIANTS OF PSEUDOMONAS AERUGINOSA*. Retrieved from JOURNAL OF BACrERIOLOGY Vol. 88, No. 2, pages 273-278: https://dx.doi.org/10.1128%2Fjb.88.2.273-278.1964

Huffnagle, G. B., Dickson, R. P., & Lukacs, N. W. (2016, December 14). *The respiratory tract microbiome and lung inflammation: a two-way street*. Retrieved from Mucosal Immunology volume 10, pages 299–306 : https://doi.org/10.1038/mi.2016.108

Huszcynski, S. M., Lam, J. S., & Khursigara, C. M. (2019, December 19). *The Role of Pseudomonas aeruginosa Lipopolysaccharide in Bacterial Pathogenesis and Physiology*. Retrieved from Pathogens 9(1), 6: https://doi.org/10.3390%2Fpathogens9010006

Irie, Y., Borlee, B. R., O'Connor, J. R., Hill, P. J., Harwood, C. S., Wozniak, D. J., & Parsek, M. (2012, November 21). *Self-produced exopolysaccharide is a signal that stimulates biofilm formation in Pseudomonas aeruginosa*. Retrieved from The Proceedings of the National Academy of Sciences, 109(50): 20632–20636: https://doi.org/10.1073/pnas.1217993109

Isopencu, G., Tanase, A., Joseceanu, A., & Lavric, V. (2014, December). Influence of the Operating Parameters on the E. Coli BL21 (DE3) Growth in Fedbatch Bioreactor. *Revista de Chimie -Bucharest- Original Edition, 65(12)*, pages; 1511-1516. Retrieved from Revista de Chimie -Bucharest- Original Edition, 65(12), pages :1511-1516.

Jamal, M. A., Sharma, S. P., Chung, H.-J., Kim, H.-J., Hong, S.-T., & Lee, S. (2017, August 17). *Ultra-High Efficient Colony PCR for High Throughput Screening of Bacterial Genes*. Retrieved from Indian Journal of Microbiology volume : https://dx.doi.org/10.1007%2Fs12088-017-0665-1

Jamal-Livani, N., Nikokar, E., & Safdari, Y. (2020). *In-Situ Gel-Free Plasmid Reassembling for Rapid Gene*. Retrieved from Brazilian Archives of Biology and Technology. 63 (4): http://dx.doi.org/10.1590/1678-4324-2020190223

James, Z. F. (2017, February 17). *Mechanisms of Microbial Infections*. Retrieved from Pathologic Basis of Veterinary Disease (Sixth Edition), Pages 132-241: https://dx.doi.org/10.1016%2FB978-0-323-35775-3.00004-7

Jefferson, K. K. (2004, July). *What drives bacteria to produce a biofilm?* Retrieved from FEMS Microbiology Letters, Volume 236, Issue 2, Pages 163–173: https://doi.org/10.1111/j.1574-6968.2004.tb09643.x

Jennings, L. K., Storek, K. M., Ledvina, H. E., Coulon, C., & et. al. (2015, September 8). *Pel is a cationic exopolysaccharide that cross-links extracellular DNA in the Pseudomonas aeruginosa biofilm matrix*. Retrieved from The Proceedings of the National Academy of Sciences; 112(36), pages 11353–11358: https://dx.doi.org/10.1073%2Fpnas.1503058112

Jensen, L. J., & et. al. (2009, Januray). *STRING 8ð a global view on proteins and their functional interactions in 630 organisms*. Retrieved from Nucleic Acids Research, 37, D412–D416: https://dx.doi.org/10.1093%2Fnar%2Fgkn760

Kadri, K. (2019, June 7). *Polymerase Chain Reaction (PCR): Principle and Applications*. Retrieved from IntechOpen: https://www.intechopen.com/chapters/67558

Kang, D., Revtovich, A. V., Chen, Q., Shah, K. N., Cannon, C. L., & Kirienko, N. V. (2019, September 6). *Pyoverdine-Dependent Virulence of Pseudomonas aeruginosa Isolates From Cystic Fibrosis Patients*. Retrieved from Frintiers in Microbiology: https://doi.org/10.3389/fmicb.2019.02048

Karthikesh, M. S., & Yang, X. (2021). *The effect of ultrasound cavitation on endothelial cells*. Retrieved from Experimental Biology and Medicine: https://dx.doi.org/10.1177%2F1535370220982301

Kaur, J., & Reinhardt, D. P. (2012). *Immobilized Metal Affinity Chromatography Co-Purifies TGF-β 1 with His-Tagged Recombinant Extracellular Proteins*. Retrieved from Plos One: https://doi.org/10.1371/journal.pone.0048629

Kelley, L. A., Mezulis, S., Yates, C. M., Wass, M. N., & Sternberg, M. J. (2015, May 7). *The Phyre2 web portal for protein modeling, prediction and analysis*. Retrieved from Nature Protocols volume 10, pages 845–858 : https://doi.org/10.1038/nprot.2015.053

Kerem, B.-S., Zielenski, J., Markiewich, D., Bozon, D., Gazit, E., Yahav, J., . . . Tsui, L.-C. (1990, November). *Identification of mutations in regions corresponding to the two putative nucleotide (ATP)-binding folds of the cystic fibrosis gene*. Retrieved from The Proceedings of the National Academy of Sciences, Vol. 87, pp. 8447-8451: https://doi.org/10.1073/pnas.87.21.8447

Kilipin, K. J., & Dyson, P. J. (2013). *Enzyme inhibition by metal complexes: concepts, strategies and applications*. Retrieved from Chemical Science, 4, 1410-1419: https://doi.org/10.1039/C3SC22349C

Kipnis, E., Sawa, T., & Wiener-Kronish, J. (2006, February 3). *Targeting mechanisms of Pseudomonas aeruginosa pathogenesis*. Retrieved from Médecine et Maladies Infectieuses, pages 78-91. : https://doi.org/10.1016/j.medmal.2005.10.007

Klein, S., Lorenzo, C., Hoffmann, S., Waltger, J. M., StorBeck, S., & et. al. (2008, December 15). *Adaptation of Pseudomonas aeruginosa to various conditions includes tRNA-dependent formation of alanyl-phosphatidylglycerol*. Retrieved from Molecular Microbiology, Volume 71, Issue 3 p. 551-565: https://doi.org/10.1111/j.1365-2958.2008.06562.x

Kovach, K. N., Fleming, D., Wells, M. J., Rumbaugh, K. P., & Gordon, V. D. (2020, Janurary 28). *Specific Disruption of Established P. aeruginosa Biofilms Using Polymer-Attacking Enzymes*. Retrieved from Langmuir 2020, 36, 6, pages 1585–1595: https://dx.doi.org/10.1021%2Facs.langmuir.9b02188

Kralik, P., & Ricchi, M. (2017). *A Basic Guide to Real Time PCR in Microbial Diagnostics: Definitions, Parameters, and Everything*. Retrieved from Frontiers In Microbiology: https://doi.org/10.3389/fmicb.2017.00108

Kunzelmann, K., Schreiber, R., & Hadorn, H. B. (2017, November). *Bicarbonate in cystic fibrosis*. Retrieved from Journal of Cystic Fibrosis: Volume 16, Issue 6, Pages 653-662: https://doi.org/10.1016/j.jcf.2017.06.005

LaBauve, A. E., & Wargo, M. J. (2021, May 6). *Growth and Laboratory Maintenance of Pseudomonas aeruginosa*. Retrieved from Current Protocols in Microbiology, Volume 25, Issue 1 p. 6E.1.1-6E.1.8: https://dx.doi.org/10.1002%2F9780471729259.mc06e01s25

Lahiri, K. K. (1998, January 5). *EVALUATION OF HOSPITAL ACQUIRED PSEUDOMONAS INFECTION IN PARAPLEGIC AND ORTHOPAEDIC CASES*. Retrieved from Medical Journal Armed Forces India, Volume 54, Issue 1, January 1998, Pages 23-26: https://dx.doi.org/10.1016%2FS0377-1237(17)30401-X

Lai, Y.-H., & Wang, Y.-S. (2017, September 22). *Matrix-Assisted Laser Desorption/Ionization Mass Spectrometry: Mechanistic Studies and Methods for Improving the Structural Identification of Carbohydrates*. Retrieved from Mechanistic Studies and Methods for Improving the Structural Identification of Carbohydrates, Mass Spectrometry, 2017, Volume 6, Issue 3, Pages S0072: https://dx.doi.org/10.5702%2Fmassspectrometry.S0072

Lamppa, J. W., & Griswold, K. E. (2013, December 28). *Alginate Lyase Exhibits Catalysis-Independent Biofilm Dispersion and Antibiotic Synergy*. Retrieved from ASM Journals: Antimicrobial Agents and Chemotherapy, Volume. 57, No. 1: https://dx.doi.org/10.1128%2FAAC.01789-12

Latifi, A. M., Khajeh, K., Farnoosh, G., Hassanpour, K., & Khodi, S. (2015). *The Cytoplasmic and Periplasmic Expression Levels and Folding of Organophosphorus*

Hydrolase Enzyme in Escherichia coli. Retrieved from Jundishapur Journal of Microbiololgy: ;8(12): e17790: https://doi.org/10.5812%2Fjjm.17790

Lee, P. Y., Costumbrado, J., Hsu, C.-Y., & Kim, Y. (2009). *Agarose Gel Electrophoresis for the Separation of DNA Fragments*. Retrieved from Electrophoresis, 30(Suppl 1): S188–S195. : https://doi.org/10.1002%2Felps.200900052

Li, X., Wu , Y., Zhang, L., Cao, Y., Li, Y., Li, J., . . . Wu, G. (2014). *Comparison of three common DNA concentration measurement*. Retrieved from Analytical Biochemistry, Volume 451, Pages 18-24: https://doi.org/10.1016/j.ab.2014.01.016

Liu, J., Gerken, H., & Li, Y. (2014). *Single-tube colony PCR for DNA amplification and transformant screening of oleaginous microalgae*. Retrieved from Journal of Applied Phycology volume 26, pages: 1719–1726 : http://dx.doi.org/10.1007/s10811-013-0220-3

Liu, N., Mao, X., Du, Z., Mu, B., & Wei, D. (2014). *Cloning and characterisation of a novel neoagarotetraose-forming-β-agarase, AgWH50A from Agarivorans gilvus WH0801*. Retrieved from Carbohydrate Research Volume 388, 31, Pages 147-151: https://doi.org/10.1016/j.carres.2014.02.019

Liu, N., Mao, X., Yang, M., Mu, B., & Wei, D. (2014). *Gene cloning, expression and characterisation of agarase, AgWH50C, producing neoagarobiose from Agarivorans gilvus WH0801*. Retrieved from World Journal of Microbiology and Biotechnology volume 30, pages1691–1698 : https://doi.org/10.1007/s11274-013-1591-y

Liu, T., Zhang, L., Joo, D., & Sun, S.-C. (2017, July 14). *NF-κB signaling in inf*. Retrieved from Signal Transduction and Targeted Therapy volume 2 17023: https://doi.org/10.1038/sigtrans.2017.23

Loewe, D., Dieken, H., Grein, T. A., Salzig, D., & Czermak, P. (2018). *A Combined Ultrafiltration/Diafiltration Process for the Purification of Oncolytic Measles Virus*. Retrieved from Membranes: State-of-the-Art Membrane Science and Technology in Germany: https://doi.org/10.3390/membranes12020105

Lorenz, T. C. (2012). *Polymerase Chain Reaction: Basic Protocol Plus Troubleshooting and Optimization Strategies*. Retrieved from JOVE Journal: https://doi.org/10.3791%2F3998

Lucena-Aguilar, G., Sanchez-Lopez, A. M., Barberan-Aceituno, C., Charillo-Avila, J. A., Lopez-Guerrero, J. A., & Aguilar-Quesada, R. (2016). *DNA Source Selection for Downstream Applications Based on DNA Quality Indicators Analysis*. Retrieved from Biopreservation Biobanking, 14(4): 264–270.: https://doi.org/10.1089%2Fbio.2015.0064

Lukacs, G. L., & Verkman, A. S. (2012, February 1). *CFTR: folding, misfolding and correcting the ΔF508 conformational defect*. Retrieved from Trends in Molecular Medicine: Volume 18, Issue 2, pages 81-91: https://dx.doi.org/10.1016%2Fj.molmed.2011.10.003

Lyczak, J. B., Cannon, C. L., & Pier, G. B. (2002, April 15). *Lung Infections Associated with Cystic Fibrosis*. Retrieved from Clinical Microbiology Reviews, volume 2, pages 194–222: https://dx.doi.org/10.1128%2FCMR.15.2.194-222.2002

Malthouse, J. P. (2020). *Kinetic Studies of the Effect of pH on the Trypsin-Catalyzed Hydrolysis of N-Ŭ-benzyloxycarbonyl-l-lysine-p-nitroanilide: Mechanism of Trypsin Catalysis*. Retrieved from ACS Omega, 5, 10, 4915–492: https://doi.org/10.1021/acsomega.9b03750

Mamouei, M., Budidha, K., Baishya, N., Qassem, M., & Kyriacou, P. A. (2021). *An empirical investigation of deviations from the Beerï Lambert law in optical estimation of lactate*. Retrieved from Scientific Reports volume 11, Article number: 13734 : https://doi.org/10.1038/s41598-021-92850-4

Marisch, K., Bayer, K., Cserjan-Puschmann, M., Luchner, M., & Striedner, G. (2013). *Evaluation of three industrial Escherichia coli strains in fed-batch cultivations during high-level SOD protein production*. Retrieved from Microbial Cell Factories volume 12, Article number: 58 : https://doi.org/10.1186/1475-2859-12-58

Matsumoto, T., Norna, M., & Sugano, Y. (1994). *Sequence analysis of the agaB gene encoding agarase from Vibrio sp. strain JT0107*. Retrieved from Biochimica et Biophysica Acta (BBA) - Gene Structure and Expression, Volume 1218, Issue 1, Pages 105-108: https://doi.org/10.1016/0167-4781(94)90109-0

Maurice, N. M., Bedi, B., & Sadikot, R. (2018, Janurary 25). *Pseudomonas aeruginosa Biofilms: Host Response and Clinical Implications in Lung Infections*. Retrieved from

American Journal of Respiratory Cell and Molecular Biology, Volume 58, Issue 4: https://dx.doi.org/10.1165%2Frcmb.2017-0321TR

Merritt, J. H., Kadouri, D. E., & O'Toole, G. A. (2005, July 15). *Growing and Analyzing Static Biofilms*. Retrieved from Current Protocols in Microbiolog: Volume 00, Issue 1 p. 1B.1.1-1B.1.17: https://dx.doi.org/10.1002%2F9780471729259.mc01b01s00

Miles, J. S., & Wolf, R. C. (1989). *Principles of DNA cloning*. Retrieved from Scientific Tools in Medicine: https://doi.org/10.1136%2Fbmj.299.6706.1019

Molitor, R., Bollinger , A., Kubicki, S., Loeschcke, A., Jaeger, K.-E., & Thies, S. (2019, April 23). *Agar plate-based screening methods for the identification of polyester hydrolysis by Pseudomonas species*. Retrieved from Microbial Biotechnolog: Volume 13, Issue 1 p. 274-284: https://doi.org/10.1111/1751-7915.13418

Moore, N. M., & Flaws, M. L. (2011, Janurary 24). *Epidemiology and Pathogenesis of Pseudomonas aeruginosa Infections*. Retrieved from American Society for Clinical Laboratory Science, pages 43-46: https://doi.org/10.29074/ascls.24.1.43

Moore, N. M., & Flaws, M. L. (2011, Desember). *Introduction: Pseudomonas aeruginosa*. Retrieved from Clinical laboratory science: journal of the American Society for Medical Technology: http://dx.doi.org/10.29074/ascls.24.1.41

Moradali, M. F., Ghods, S., & Rehm, B. H. (2017, February 15). *Pseudomonas aeruginosa Lifestyle: A Paradigm for Adaptation, Survival, and Persistence*. Retrieved from Frontiers In Cellular and Infection Microbiology: https://doi.org/10.3389/fcimb.2017.00039

Nivens, D. E., Ohman, D. E., Williams, J., & Franklin, M. J. (2001, February 1). *Role of Alginate and Its O Acetylation in Formation of Pseudomonas aeruginosa Microcolonies and Biofilms*. Retrieved from ASM Journals, Journal of Bacteriology, Vol. 183, No. 3: https://dx.doi.org/10.1128%2FJB.183.3.1047-1057.2001

Nowakowski, A. B., Wobig, W. J., & Petering, D. H. (2014, May 6). *Native SDS-PAGE: High Resolution Electrophoretic Separation of Proteins With Retention of Native Properties Including Bound Metal Ions*. Retrieved from Metallomics (5): https://doi.org/10.1039/c4mt00033a

Obrador-Sanchez, A. J., Tzec-Sima, M., Higuera-Ciapara, I., & Canto-Canche, B. (2017). *A quick and effective in-house method of DNA purification from agarose gel, suitable for sequencing*. Retrieved from 3 Biotech; 7(3): 180: https://doi.org/10.1007%2Fs13205-017-0851-1

Pang, Z., Raudonis, R., Glick, B. R., Lin, T.-J., & Cheng, Z. (2019, January–February). *Antibiotic resistance in Pseudomonas aeruginosa: mechanisms and alternative therapeutic strategies*. Retrieved from Biotechnology Advances: Volume 37, Issue 1, Pages 177-192: https://doi.org/10.1016/j.biotechadv.2018.11.013

Perlin, A. S., & Suzuki, S. (1961, September 13). *THE STRUCTURE OF LICHENIN: SELECTIVE ENZYMOLYSIS STUDIES*. Retrieved from Canadian Journal of Chemistry; 40(1), pages 50-56: http://dx.doi.org/10.1139/v62-009

Pesingi, P. V., Singh, B. R., Pesingi, P. K., Bhardwaj, M., Singh, S. V., Kumawat, M., . . . Gandham, R. K. (2019, November 19). *MexAB-OprM Efflux Pump of Pseudomonas aeruginosa Offers Resistance to Carvacrol: A Herbal Antimicrobial Agent*. Retrieved from Frontiers in Microbiology: https://doi.org/10.3389/fmicb.2019.02664

Phillips, A. T. (1995, May). *Desalting, Concentration, and Buffer Exchange by Dialysis and Ultrafiltration*. Retrieved from Current protocols in protein science: http://dx.doi.org/10.1002/0471140864.ps0404s02

Powlegde, T. M. (2004). *The polymerase chain reaction*. Retrieved from American Physiological Society, Volume 28, issue 2, Pages 44-50: https://doi.org/10.1152/advan.00002.2004

Qiu, X., Kulasekara, B. R., & Lory, S. (2009, August 19). *Role of Horizontal Gene Transfer in the Evolution of Pseudomonas aeruginosa Virulence*. Retrieved from Genome dynamics: Volume 6, pages 126-139: https://doi.org/10.1159/000235767

Reddy, P. R., & Raju, N. (2012). Gel electrophorisis and Its Application . In S. Magdelin, *Gel Electrophorisis - Principles and Basics* (pp. 15-16). IntechOpen.

Rempel, B. P., & Withers, S. G. (2008, August). *Covalent inhibitors of glycosidases and their applications in biochemistry and biology* . Retrieved from Glycobiology, Volume 18, Issue 8, Pages 570–586: https://doi.org/10.1093/glycob/cwn041

Riguero , V., Clifford, R., Dawley, M., Dickson, M., Gastfriend, B., Thompson, C., . . . O'Connor, E. (2020). *Immobilized metal affinity chromatography optimization for poly-histidine tagged proteins*. Retrieved from Journal of Chromatography A: https://doi.org/10.1016/j.chroma.2020.461505

Roberts, M. A. (2019). *Recombinant DNA technology and DNA sequencing*. Retrieved from Essays in Biochemistry, 63 (4): 457–468.: https://doi.org/10.1042/EBC20180039

Robinson, P. K. (2015). *Enzymes: principles and biotechnological applications*. Retrieved from Essays In Biochemistry 59: 1–41: https://doi.org/10.1042%2Fbse0590001

Rocha, A. J., Barsottini, M. R., Rocha, R. R., Laurindo, M. V., Moraes, F. L., & Rocha, S. L. (2019, May 16). *Pseudomonas Aeruginosa: Virulence Factors and Antibiotic Resistance Genes*. Retrieved from Brazilian Archives of Biology and Technology: Review - Human and Animal Health : http://dx.doi.org/10.1590/1678-4324-2019180503

Rollet, C., Gal, L., & Guzzo, J. (2009, Janurary 1). *Biofilm-detached cells, a transition from a sessile to a planktonic phenotype: a comparative study of adhesion and physiological characteristics in Pseudomonas aeruginosa*. Retrieved from FEMS Microbiology Letters, Volume 290, Issue 2, Pages 135–142: https://doi.org/10.1111/j.1574-6968.2008.01415.x

Rosano, G. L., & Ceccarelli, E. A. (2014). *Recombinant protein expression in Escherichia coli: advances and challenges*. Retrieved from Frontiers in Microbiology: https://doi.org/10.3389/fmicb.2014.00172

Rutherford, S. T., & Bassier, B. L. (2012, November 2). *Bacterial Quorum Sensing: Its Role in Virulence and Possibilities for Its Control*. Retrieved from Cold Spring Harbor Perspectives in Medicine: issue 11: https://doi.org/10.1101/cshperspect.a012427

Sadovskaya, I., Vinogradov, E., Li, J., Hachani, A., Kowalska, K., & Filioux, A. (2010). *High-level antibiotic resistance in Pseudomonas aeruginosa biofilm: the ndvB gene is involved in the production of highly glycerol-phospho r y l a(t1eŸd3lu)dcans, which bind aminoglycosides* . Retrieved from Glycobiology, Volume 20, Issue 7, Pages 895–904: https://doi.org/10.1093/glycob/cwq047

Samuels, S. D., Drecktrah, D., & Hall, L. S. (2017). *Genetic Transformation and Complementation*. Retrieved from Methods in Molecular Biology: https://dx.doi.org/10.1007%2F978-1-4939-7383-5_15

Sanger, F., Nicklen, S., & Coulson, A. R. (1977). *DNA sequencing with chain-terminating inhibitors*. Retrieved from Medical Research Council Laboratory of Molecular Biology, Cambridge CB2 2QH, England: https://dx.doi.org/10.1073%2Fpnas.74.12.5463

Sasagawa, N. (2018, November 5). *Plasmid Purification*. Retrieved from IntechOpen: https://www.intechopen.com/chapters/60894

Schafer, J., Griese, M., Chandrasekaran, R., Chotirmall, S. H., & Harti, D. (2018, May 22). *Pathogenesis, imaging and clinical characteristics of CF and non-CF bronchiectasis*. Retrieved from BMC Pulmonary Medicine volume 18, Article number: 79 : https://dx.doi.org/10.1186%2Fs12890-018-0630-8

Schimek, C., Egger, E., Tauer, C., Striedner, G., Brocard, C., Cserjan-Puschmann , M., & Hahn, R. (2020). *Extraction of recombinant periplasmic proteins under industrially relevant process conditions: Selectivity and yield strongly depend on protein titer and methodology*. Retrieved from Biotechnology Progress: https://doi.org/10.1002/btpr.2999

Schmid , M., Prinz, T. K., Stabler, A., & Sangerlaub, S. (2016). *Effect of Sodium Sulfite, Sodium Dodecyl Sulfate, and Urea on the Molecular Interactions and Properties of Whey Protein Isolate-Based Films*. Retrieved from Frontiers in Chemistry: https://doi.org/10.3389%2Ffchem.2016.00049

Schoch CL, et al. . (2020). *NCBI Taxonomy: a comprehensive update on curation, resources and tools*. Retrieved from Database (Oxford): https://www.ncbi.nlm.nih.gov/Taxonomy/Browser/wwwtax.cgi?mode=info&id=287

Shei, R.-J., Peabody, J. E., Kaza, N., & Rowe, S. M. (2018, December). *The Epithelial Sodium Channel (ENaC) as a Therapeutic Target for Cystic Fibrosis*. Retrieved from Current Opinion in Pharmacology: Volume 43, Pages 152-165: https://dx.doi.org/10.1016%2Fj.coph.2018.09.007

Silby, M. W., Winstanley, C., Godfrey, S. A., Levy, S. B., & Jackson, R. W. (2011, July 01). *Pseudomonas genomes: diverse and adaptable*. Retrieved from FEMS Microbiology

Reviews, Volume 35, Issue 4, July 2011, Pages 652–680: https://doi.org/10.1111/j.1574-6976.2011.00269.x

Singhal, N., Kumar, M., Kanaujia, P. K., & Virdi, J. S. (2015). *MALDI-TOF mass spectrometry: an emerging technology for microbial identification and diagnosis*. Retrieved from Frontiers In Microbiology: https://doi.org/10.3389/fmicb.2015.00791

Structural Genomics Consortium, et al. (2008). *Protein production and purification*. Retrieved from Nature methods: https://dx.doi.org/10.1038%2Fnmeth.f.202

Temuujin , U., Chi, W.-J., Chang, Y.-K., & Hong, S.-K. (2012). *Identification and Biochemical Characterization of Sco3487 from Streptomyces coelicolor A3(2), an Exo- and Endo-Type -Agarase-Producing Neoagarobiose*. Retrieved from Journal of Bacteriology 194(1):142-9: http://dx.doi.org/10.1128/JB.05978-11

Thi, M. T., Wibowo, D., & Rehm, B. H. (2020, November 17). *Pseudomonas aeruginosa Biofilms*. Retrieved from International Journal of Molecular Science, page: 8671: https://dx.doi.org/10.3390%2Fijms21228671

Throop, A. L., & LaBaer, J. (2015). *Recombinational Cloning Using Gateway and In-Fusion Cloning Schemes*. Retrieved from Current Protocols in Molecular BiologyVolume 110, Issue 1 p. 3.20.1-3.20.23: https://dx.doi.org/10.1002%2F0471142727.mb0320s110

Trabbic-Carlson, K., Liu, L., Kim, B., & Chilkoti, A. (2004). *Expression and purification of recombinant proteins from Escherichia coli: Comparison of an elastin-like polypeptide fusion with an oligohistidine fusion*. Retrieved from Protein Science: https://dx.doi.org/10.1110%2Fps.04931604

Tuon, F. F., Dantas, L. R., Suss, P. H., & Riberiro, V. S. (2022, February 27). *Pathogenesis of the Pseudomonas aeruginosa Biofilm: A Review*. Retrieved from Pathogens 2022, 11(3), page 300: https://doi.org/10.3390/pathogens11030300

Valentini, M., & Filloux, A. (2016, June 10). *Biofilms and Cyclic di-GMP (c-di-GMP) Signaling: Lessons from Pseudomonas aeruginosa and Other Bacteria*. Retrieved from Journal of Biological Chemistry; Volume 291, Issue 24, Pages 12547-12555: https://doi.org/10.1074/jbc.R115.711507

Valot, B., Guyeux, C., Rolland, J. Y., Mazouzi, K., Bertrand, X., & Hocquet, D. (2015, May 11). *What It Takes to Be a Pseudomonas aeruginosa? The Core Genome of the Opportunistic Pathogen Updated*. Retrieved from Journals: Plos One: https://doi.org/10.1371/journal.pone.0126468

Vandeventer, P. E., Mejia, J., Nadim, A., Johal, M. S., & Niemz, A. (2013). *DNA Adsorption to and Elution from Silica Surfaces: Influence of Amino Acid Buffers*. Retrieved from J. Phys. Chem. B, 117, 37, 10742–10749: https://doi.org/10.1021%2Fjp405753m

Verchere, A., Dezi, M., Adrien, V., Broutin, I., & Picard, M. (2015, April 22). *In vitro transport activity of the fully assembled MexAB-OprM efflux pump from Pseudomonas aeruginosa*. Retrieved from Nature Communications volume 6, Article number: 6890 : https://doi.org/10.1038/ncomms7890

Wade, J. H., & Bailey, R. C. (2013, December 12). *Refractive Index-Based Detection of Gradient Elution Liquid Chromatography using Chip-Integrated Microring Resonator Arrays*. Retrieved from Analytical Chemistry 2014, 86, 1, 913–919: https://dx.doi.org/10.1021%2Fac4035828

Walpole, G. F., & et. al. (2020, June 2). *Inactivation of Rho GTPases by Burkholderia cenocepacia Induces a WASH-Mediated Actin Polymerization that Delays Phagosome Maturation*. Retrieved from Cell Reports: Volume 31, Issue 9, 107721: https://doi.org/10.1016/j.celrep.2020.107721

Waterhouse, A. M., Procter, J. B., Martin, D. M., Clamp, M., & Barton, G. J. (2009, May 1). *Jalview Version 2ð a multiple sequence alignment editor and analysis workbench* . Retrieved from Bioinformatics, Volume 25, Issue 9, Pages: 1189–1191: https://doi.org/10.1093/bioinformatics/btp033

Watford, M., & Wu, G. (2018, July 27). *Protein*. Retrieved from Advances in Nutrition: https://dx.doi.org/10.1093%2Fadvances%2Fnmy027

Whaley, D., Damyar, K., Witek, R. P., Mendoza, A., Alexander, M., & Lakey, J. R. (2021). *Cryopreservation: An Overview of Principles and Cell-Specific Considerations*. Retrieved from Cell Transplantation: https://doi.org/10.1177%2F0963689721999617

Yan, X. (2014, October). *HPLC for Carbohydrate Analysis*. Retrieved from HPLC Principle, Practices and Procedures pp.22:

https://www.researchgate.net/publication/301698343_HPLC_for_Carbohydrate_Analysis

Yang, L., Haagensen, J. A., Jelsbak, L., Johansen, H. K., Sternberg, C., Høiby, N., & Molin, S. (2007, Desember 21). *In Situ Growth Rates and Biofilm Development of Pseudomonas aeruginosa Populations in Chronic Lung Infections*. Retrieved from Journal of Bacteriology: https://dx.doi.org/10.1128%2FJB.01581-07

Yi, P., yan, Q., Jiang, Z., & Wang, L. (2018, Janurary). *A first glycoside hydrolase family 50 endo-ß-1,3-D-glucanase from Pseudomonas aeruginosa*. Retrieved from Enzyme and Microbial Technology Volume 108, Pages 34-41: https://doi.org/10.1016/j.enzmictec.2017.09.002

Yu , S., Su, T., Wu, H., Liu, S., Wang, D., Zhao, T., . . . Ma, L. Z. (2015, November 27). *PslG, a self-produced glycosyl hydrolase, triggers biofilm disassembly by disrupting exopolysaccharide matrix.* Retrieved from Cell Reseach 25, pages 1352–1367: https://doi.org/10.1038/cr.2015.129

Yuan, S., Le Roy, K., Venken, T., Lammens, W., Den Ende, W. V., & De Maeyer, M. (2012, May 25). *pKa Modulation of the Acid/Base Catalyst within GH32 and GH68: A Role in Substrate/Inhibitor Specificity?* Retrieved from Plos One: 7(5), e37453: https://dx.doi.org/10.1371%2Fjournal.pone.0037453

Zhu, Z., & Lu, J. J. (2012). *Protein Separation by Capillary Gel Electrophoresis: A Review*. Retrieved from Analytica Chimica Acta, Volume 709, Pages 21-31: https://doi.org/10.1016%2Fj.aca.2011.10.022

8. Appendices

8.1 Appendix A

The recombinant DNA was constructed by inserting *Pa*GH50A into high copy pNIC-CH plasmid. pNIC-CH cloning and expression vector with a hexa His-tag was used to express and purify *Pa*GH50A for characterization studies during this thesis project (**Figure 8-1**).

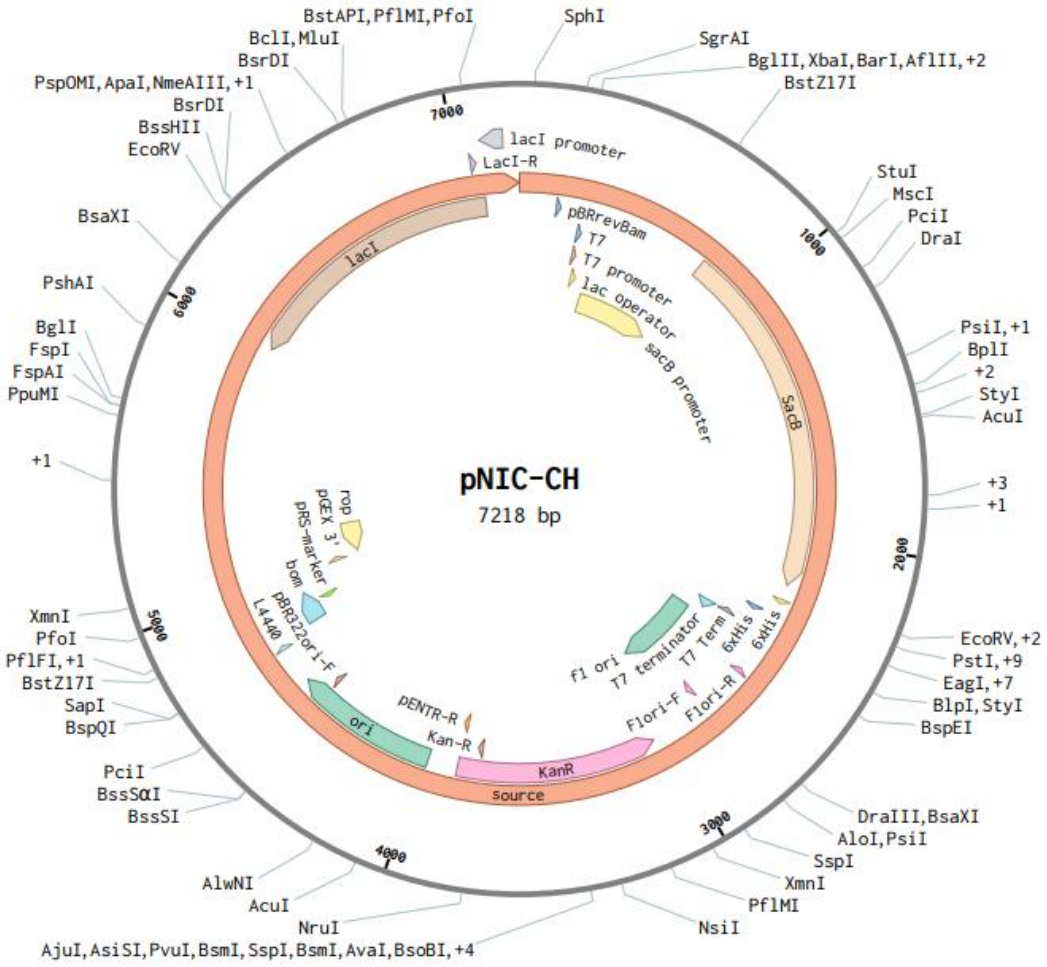

Figure 8-1. Vector map of pNIC-CH vector for cloning and expression of PaGH50A. The figure gives an overview of different sites in the pNIC-CH vector necessary for protein expression. The T7 promoter is inducible with Isopropyl ß-D-1-thiogalactopyranoside (IPTG) and regulates transcription of PaGH50A. For linearization of pNIC-CH plasmid restriction sites AfIii and PstI-HF were utilized. KanR encodes for kanamycin monosulfate resistance. Downstream the SacB gene is the

hexa histidine tag which allows for purification of PaGH50A. Figure obtained from Opher Gileadi Lab via Addgene provided by co-supervisor Per Kristian Thorén Edvardsen.

8.2 Appendix B

Amino acid sequence with SP for *Pa*GH50A found in *P. aeruginosa* PA14. The gene *Pa*GH50A encoding the amino acid sequence was isolated from a pCC1 plasmid. The enzyme was expressed in *E. coli* BL21 (**Figure 8-2**).

.

MELRKTGFMIRSRWHLPLLLGLLAVAAPLAANDTQQVLFNFVKPMAVVGITLEDADLPSVTAEATPE
GDILRRVTFSPAQRPTLRMSPAQGRWDWSAADYVSLRIQNAMSWDMTLEVAIEGEQGAPGLQASIE
LPAGPPQTLLVPLRAVSPEALGMRAGPPMPQMVEGQRMLLAPRVEGSLDRARVGALSLSLRSPQAP
QSILLGRFGIRAGRAVERSILTGLIDRYGQYSRADWPEKIRSDEQLRSAYAAEAAQLRDGERQTPARD
RFGGLLGGPVFEASGFFRTEKRGGRWWLVTPEGHPFWSLGVNAVTADGGRTYVEGREPMFAELPAE
GEPLAAFFGEGDDRRGVAAQAGRRFGHGRWFDFLGANRQRIAPQASADQLAGEWRQRTLERLSAW
GFNSLGNWSDPALAAQARMPYSLPLSIAGDYATVSSGFDWWGAMPDPFDPRFAMAAERVIAIAARD
HRDDPWLFGYYADNELAWAGRDGSAQARYGLAFGALRLSMDSPAKRAFVKQLKAKYLRHEALAQ
AWGIELAAWEALEAPGYAAPLPGEGHPAIAEDYSAFLRLYADAYFKTLRDALQWHAPNHLLLGGRF
AVSTPEAITSCARYCDLLSFNLYTPLPGQGLDDSLLARLDKPVLISEFHFGSRDRGPFWGGVSEAANE
RARGDSYRTFLEAALKSPYIVGAHWFQYLDQPASGRLLDGENGHIGLVGITGLPFAGFVDTVRRSNL
AALSRLSAMASSMPAVEPPPPREDSAGS

Figure 8-2. Amino acid sequence of the full-length PaGH50A with signal peptide (SP, shown in red). PA14_50830 gene for PaGH50A is encoded in the genome of P. aeruginosa PA14.

8.3 Appendix C

Representative chromatograms for IMAC purifications. IMAC purification of cytoplasmic extract incubated in a shaker for 24 hours at 37 ^{o}C with 220 rpm agitation (**Figure 8-3**) while IMAC purification of periplasmic extract with identical parameters (**Figure 8-4**). IMAC purification of periplasmic extract incubated in a Lex-48 bioreactor for 24 hours at 37 ^{o}C with moderate aeration (**Figure 8-5**).

All purifications were performed with *E. coli* BL21 cultivated in 500 mL TB medium. 35 mL of flowthrough and 20 mL of wash and elution fractions were collected from purifications. Enzymatically active *Pa*GH50A was isolated from wash and elution fractions.

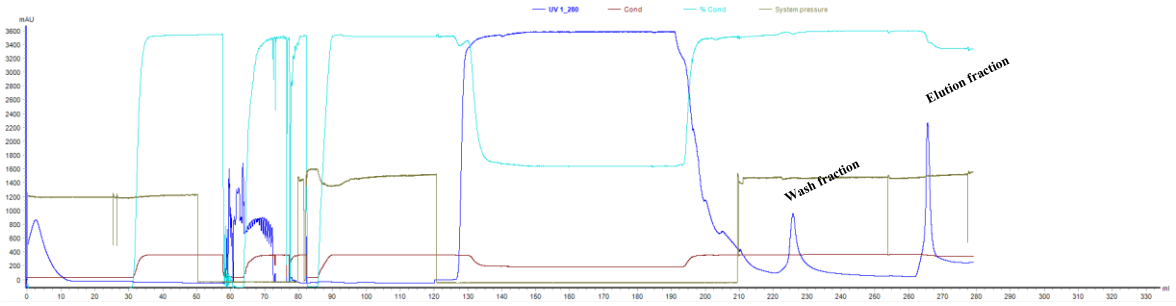

Figure 8-3. Chromatogram from IMAC purification of cytoplasmic extract cultivated in a shaker incubator. During IMAC purification fractionation was done manual and fractions were collected in three steps: flowthrough, wash, and elution. The y-axys represents the mili absorbance units (mAU) for the UV signal while the x-axis represents buffer volume given in mL. The peaks were marked depending on the IMAC buffer utilized.

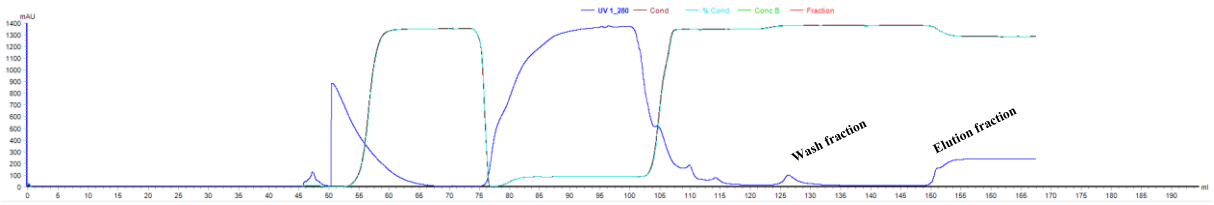

Figure8-4. Chromatogram from IMAC purification of periplasmic extract cultivated in a shaker incubator. During IMAC purification fractionation was done manual and fractions were collected in three steps: flowthrough, wash, and elution. The y-axys represents the mili absorbance units (mAU) for the UV signal while the x-axis represents buffer volume given in mL. The peaks were marked depending on the IMAC buffer utilized.

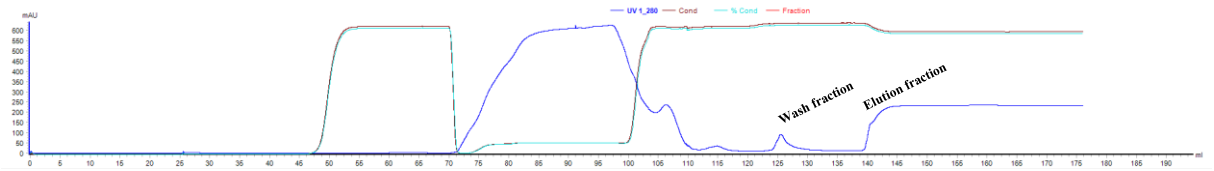

Figure8-5. Chromatogram from IMAC purification of periplasmic extract cultivated in Lex-48 bioreactor. During IMAC purification fractionation was done manual and fractions were collected in three steps: flowthrough, wash, and elution. The y-axys represents the mili absorbance units (mAU) for the UV signal while the x-axis represents buffer volume given in mL. The peaks were marked depending on the IMAC buffer utilized.

Norges miljø- og biovitenskapelige universitet
Noregs miljø- og biovitskapelege universitet
Norwegian University of Life Sciences

Postboks 5003
NO-1432 Ås
Norway